DESIGN, SYNTHESIS, AND EVALUATION OF BIODEGRADABLE HYDROGELS AND NOVEL POLYMERIC NANOCARRIERS FOR THE TREATMENT OF COLORECTAL CANCER

by

Padmanabh Chivukula

A dissertation submitted to the faculty of
The University of Utah
in partial fulfillment of the requirements for the degree of

Doctor of Philosophy

Department of Pharmaceutics and Pharmaceutical Chemistry

The University of Utah

December 2012

The University of Utah Graduate School

STATEMENT OF DISSERTATION APPROVAL

The dissertation of **Padmanabh Chivukula**

has been approved by the following supervisory committee members:

Jindřich Kopeček	, Chair	**May 19, 2008** Date Approved
You Han Bae	, Member	**May 11, 2008** Date Approved
Thomas Cheatham	, Member	**May 19, 2008** Date Approved
Pavla Kopečková	, Member	**May 19, 2008** Date Approved
Patrick Kiser	, Member	**May 19, 2008** Date Approved

and by **David Grainger** , Chair of

the Department of **Pharmaceutics and Pharmaceutical Chemistry**

and by Charles A. Wight, Dean of The Graduate School.

ABSTRACT

Colorectal cancer (CRC) is one of the most lethal malignancies, ranking second to lung cancer in males and breasts cancer in females. Its death rate has not significantly changed over the past 20 years in spite of surgical procedures that have vastly improved in the same period. This is likely due to the late stage at which CRC is diagnosed, and the intrinsically high, nonspecific toxicity that conventional chemotherapeutic treatments suffer from.

Novel drug delivery strategies can be implemented to reduce the nonspecific toxicities of conventional chemotherapeutics. In such a strategy, a two-pronged approach to deliver therapeutic agents both locally and systemically may lead to a shift in the paradigm on the current treatment of CRC. For the first approach, a colon-specific drug delivery system based on biodegradable hydrogels and novel linear polymeric carriers was designed. The second approach exploits the benefits of systemic delivery by utilizing a targeted polymeric carrier.

For colon-specific drug delivery, interpenetrating network (IPN) hydrogels composed of pH-sensitive, aromatic azo group-containing hydrogels as one of its components, and a hydrolyzable network as the other were synthesized. The properties of IPNs were investigated with the aim of identification of structures suitable as colon-specific drug delivery systems. The swelling kinetics for hydrogels with different compositions were determined at conditions mimicking the gastrointestinal tract. Also,

physical properties of degradability and the modulus of elasticity in compression were used to characterize the properties of the IPN hydrogels.

In the second study, three derivatives of the cyclic constrained nonapeptide specific to CRC, namely YW-KPIEDRPME (RPM1), methacryloylglycylglycine-6-aminohexanoyl-8-amino-3,6-dioxaoctanoyl-8-amino-3,6-dioxaoctanoyl-8-amino-3,6-dioxaoctanoyl-YW-KPIEDRPME (RPM2), and K(fluorescein)-KPIEDRPME (RPM3), were synthesized. RPM1 and RPM2 were incorporated into the water-soluble N-(2-hydroxypropyl)methacrylamide (HPMA) copolymer.

For the final study, two novel, linear polymeric systems were designed, one for systemic and the other for local delivery. The former system was a carrier composed of N-(2-hydroxypropyl)methacrylamide (HPMA) copolymer, 9-aminocamptothecin (9-AC), and biorecognizable cyclic nonapeptide. In the latter system, a copolymer of HPMA and 9-aminocamptothecin bound via an aromatic azo bond and a self-elimination spacer was synthesized. Therapeutic efficiency of a systemic versus local approach was evaluated *in vivo* using a noninvasive orthotopic tumor model.

TABLE OF CONTENTS

LIST OF TABLES

LIST OF FIGURES

LIST OF SCHEMES

ACKNOWLEDGMENTS

I would like to thank Dr. Jindřich Kopeĉek for teaching by example and for instilling the importance of the broad picture in me. The way he practiced science has been a source of inspiration and has qualitatively changed my outlook on science. His enthusiasm to understand the essential content of the problem has been infectious. He raised the bar by giving me the freedom to pursue a wide variety of problems and at the same time always served as a guiding light in my pursuits. Not only has he been a great mentor but also a wonderful person.

I would also like to thank my parents, Ramakrishna Murty Chivukula and Shyamala Chivukula, for their wisdom passed on to me over the years. I would like to dedicate this dissertation to my parents, as a small symbol to graduate for their countless sacrifices made over the years to educate us.

CHAPTER 1

BACKGROUND AND SIGNIFICANCE

1.1. Colorectal Cancer

Colorectal cancer (CRC) is one of the most lethal malignancies (*1, 2*), ranking second to lung cancer in males and breast cancer in females. The term colorectal cancer includes cancer of the colon, rectum, appendix, and anus. It has been shown that both genetic and environmental factors are leading causes implicated in the disease morphology (*3*). There were approximately 500,000 new cases diagnosed and 250,000 deaths recorded worldwide in 2000 (*4*). Factors that affect prognosis include the stage of the cancer, the blood levels of carcinoembryonic antigens (CEA), and the patient's general health (*5*). The lifetime probability of developing colorectal cancer was estimated at 6.0 % for women, and 6.2 % for men (*6*).

The pathologic stage is the most important determinant of prognosis. After diagnosis, five stages (0-IV) are used to assess the spreading of colon cancer cells within the colon or other parts of the body. In stage 0, the cancer cells have not spread to nearby tissues and there is no regional lymph node or distal metastasis. Treatment including local excision of the tumor with adjuvant therapy is given at this stage. In stage I, tumor has invaded submucosa but there is no regional lymph node or distal metastasis. Here, treatments include resection/anastomosis (removal of diseased tissue followed by the connection of healthy sections) of the diseased area. In stage II, tumor invades through

muscular layer into subserosa but there is again no regional lymph node or distal metastasis. Treatment includes resection/anastomosis followed by systemic treatment by chemo, radiation or biological therapy. In stage III, tumor cells have spread to organs and lymph nodes near the colon/rectum. The treatment is similar to that of stage II. Stage IV includes the spread of tumors cells to other parts of the body, such as liver or lungs. Here, treatment could include surgery for the removal of parts of the organ (like lung, liver, or ovaries) where the cancer may have spread, followed by the standard drug treatments (*7*).

1.1.1. Current Screening Modalities

Early diagnosis of colorectal cancer through screening can prevent most deaths (*8, 9*) since the prognosis is heavily dependent on the stage of the disease. Screening involves the identification of neoplasms (which are cancerous precursor adenomatous polyps) in asymptomatic individuals (*9*). Identification and removal of such polyps (growth in the colon that projects from the lining of the intestine or rectum) can decrease cancer incidence and death (*10, 11*). It is well established that it is essential to screen for CRC in certain high-risk populations such as families with a history of familial adenomatous polyposis (FAP), and hereditary nonpolyposis colorectal cancer (HNPCC) (*8*). There are currently four predominant methods for the screening of colorectal cancer (*12*), Fecal Occult Blood Test (FOBT) (*13-15*), Flexible Sigmoidoscopy (*16, 17*), Double Contrast Barium Enema (DCBE) (*18-20*), and Colonoscopy (*21*).

Fecal Occult Blood Testing (FOBT) is the most common screening modality used in the United States (*22*). This test is based on detecting the level of hemoglobin in the stool. It is conducted with a guaiac-impregnated card (a paper surface that has a phenolic compound, alpha-guaiaconic acid) that turns blue in the presence of peroxidase-like

substances, such as heme (*23*). The hemoccult test can detect about 20 ml of blood loss per day in 80-90% of patients and 10 ml of blood loss per day in 67 % (*15*). For a single test, three separate stool samples collected on consecutive days are tested. However, this technique has a major disadvantage in its low sensitivity (more than 40 % of cancers will be missed by this technique) (*24*). Sigmodoscopy has high sensitivity and specificity in CRC detection for the distal colon. This method can reduce mortality caused by rectal cancer and distal colon tumors in patients who have undergone the test (*25*). The technique is limited by its low sensitivity for lesions beyond the reach of the instruments, which constitutes about half of all colorectal neoplasms (*22*). Colonoscopy, on the other hand, allows direct visualization of the entire colon and the detection of adenomas with high sensitivity. This technique provides the opportunity for direct removal of adenomas and samples for biopsies of suspicious lesions can be removed. This procedure can decrease mortality by up to 70%, and is currently the most sensitive method for detecting CRC. Finally, Double Contrast Barium Enema (DCBE) allows examination of the entire colon and is relatively inexpensive (*26*). This technique is inferior to colonoscopy for the detection of polyps. When comparing DCBE against colonoscopy examination, DCBE detected only 39 % of all adenomas. This uncomfortable procedure also renders it not patient compliant. On a positive test, DCBE has to be also followed by colonoscopy, which has reduced the utility of DCBE for CRC screening.

1.1.2. Current Treatment Options

The treatment of CRC predominantly involves the surgical removal of the right or left side of the colon (hemicolectomy). This is the principal treatment for colorectal cancer and the only treatment that can cure the patient. The cure rate of patients

undergoing hemicolectomy for adenocarcinoma removal is only 50%, depending on the tumor grade, stage, and the presence of vascular or lymphatic invasion (*27, 28*). Local recurrence rates vary from 4% to 54%, which are directly correlated with rates of survival. Newer surgical procedures such as laparoscopic resection are being evaluated for colorectal tumor removal. These techniques significantly improve the quality of life of patients by reducing postoperative morbidity. Recurrence after colon cancer surgery, predominantly involves the liver, which is the sole metastatic site in 30 % of patients (*29*). These relapsed tumors are treated with systemic low molecular weight chemotherapeutics. These therapies are effective in prolonging time to disease progression, but the percentage of overall survival is still quite low (*30*). The major hurdle for adjuvant chemotherapy is its indiscriminate uptake into normal tissues, which can result in severe toxicities, including nausea, vomiting, diarrhea, mucositis, myelosuppression, and cardiac and neurologic effects, thereby limiting its therapeutic efficacy. Hence, novel strategies are being developed to optimize drug delivery to the site of action.

1.1.3. Chemotherapeutics of Colorectal Cancer Treatment

Surgery is an integral part in the treatment of CRC and the extent of surgery for treatment has undergone constant modification (*31*). Only 50% of patients undergoing treatment for rectal adenocarcinoma can be cured and surgery remains the principal tool. While a large number of patients with colon cancer will have potentially curative resection after surgery, a significant number will develop recurrence. Without surgery, the median survival in patients with hepatic metastatic disease is 4.5 months. Chemotherapy is thus used as supportive care for treatment of disease. It has been

demonstrated that chemotherapy is effective in prolonging time to disease progression and overall survival (*32*). For tumors at distant sites like lungs and bone, systemic chemotherapy is used whereas for local relapse, local radiotherapy is more appropriate.

5-Fluorouracil (5-FU) is a prodrug which inhibits thymidylate synthase. 5-FU has been used for the treatment of colorectal cancer for the past 40 years. The plasma half-life of 5-FU is very short (about 8-14 min); for this reason, prolonged infusional therapy is preferred to a bolus therapy. It has been demonstrated that 5-FU alone as a single agent has a response rate of about 11% and a median survival of 11 months in those with advanced disease (*33*). Traditionally, chemotherapy has been given intravenously as this route has more predictable plasma concentration. Comparable efficacy and median survival by the use of intravenous 5-FU and an oral formulation have been shown (*34, 35*). The toxicity profiles were similar, with greater hand-foot syndrome and less mucositis, neutropenia, and alopecia in the oral treatment. New chemotherapeutic agents with mechanistically novel modes of action are also being developed. Irinotecan® is a topoisomerase I inhibitor that blocks cell division by inducing single-strand DNA breaks. This drug has been shown to have a response rate of 11-23 % in patients with 5-FU resistance and advanced CRC (*36, 37*). Oxaliplatin® is a third-generation platinum analogue that produces DNA cross-linkages and apoptotic cell death. Studies have shown response rates of 46 % of 5-FU plus oxaliplatin versus 10% with oxaliplatin alone (*38*). Clearly, with novel approaches enhanced, response rates can be achieved.

1.1.4. Camptothecins

Camptothecin (CPT) is a specific topoisomerase I inhibitor discovered in the 1960s is a naturally occurring alkaloid (*39*). It was first extracted from the stem wood of

the Chinese tree *Camptotheca acuminata* while screening thousands of plants in search of steroids. The tree extract showed significant antitumor activity in standard in vivo cell culture and preliminary animal model (induced with tumors). During Phase I and Phase II clinical trials, it showed strong antitumor activity among patients with gastrointestinal cancers, though it caused severe side effects, with the most severe being myelosupression and haemorrhagic cystitis. These side effects eventually resulted in the suspension of Phase II trials in 1972.

The early mechanism of action of camptothecin suggested that cytotoxicity might result from inhibition for DNA and RNA synthesis, and it was concentration dependent (*40-43*).

Another mechanism of action was discovered in the late 1980s. It was identified as an unequivocal inhibitor of topoisomerase I (*44, 45*). This sparked a new wave of interest in developing novel derivatives which could be given as combination chemotherapeutic, as it presented a novel mode of action. During its early revival, it was observed that the open lactone ring of camptothecin is a much less potent antitumor agent with severe adverse effects (*46*). Hence, several camptothecin derivatives with an intact lactone ring were synthesized. Within these series of compounds, two CPT analogs (Fig. 1.1) have been approved and are used in cancer chemotherapy today, topotecan® and irinotecan® (*47-49*).

Significant improvement of survival was demonstrated with CPT analogs topotecan and irinotecan; however, patients still suffer from myelosupression, neutropenia, anemia and diarrhea and these appear to be dose-limiting factors for these

compounds. There is great interest in the design of a new generation of camptothecins that exert strong topoisomerase I inhibitory activity with a good toxicity profile.

1.2. Biodegradable Hydrogels as Drug Delivery System

Hydrogels are three-dimensional networks of hydrophilic polymer chains that are water-insoluble. Due to the presence of physical or chemical crosslinks they can absorb large amounts of water without dissolving, hydrogels (*50*) have been extremely useful as biomaterials. Their uses have been proposed for a wide range of biomedical and pharmaceutical applications. Applications, including drug delivery (*51-53*), tissue engineering (*54-56*) and contact lens design (*57, 58*), have widely adapted the use of these gels. Hydrogels used as drug delivery systems are typically polymers or copolymers from among poly[N-(2-hydroxypropyl)methacrylamide] (PHPMA) (*59*), poly(hydroxyethyl methacrylate) (PHEMA), poly(vinyl alcohol) (PVA), polyurethane (PU), and poly(ethylene oxide) (PEO) (*60*). One of the most widely used hydrogels as novel material is based on poly(hydroxyethyl metacrylate) (PHEMA) (*61, 62*). Copolymer of (2-hydroxyethyl) methacrylate (HEMA) and ethyleneglycol dimethacrylate (EGDMA) (Fig. 1.2.) results in a crosslinked hydrogel structure which has been used for the production of soft contact lenses and as reservoirs for drug delivery (*63*). Hydrogels have been synthesized by three main synthetic processes, namely, a) crosslinking polymerization, b) formation of crosslinks with existing polymer chains and c) joining of active chain ends into crosslinks (end-linked networks). The typical parameters used to characterize hydrogels networks include polymer volume fraction in the swollen state ($\nu_{2,s}$), the molecular weight of the polymer chain between two neighboring crosslinking points (M_c), and the corresponding mesh size (ξ). The amount of fluid embedded and

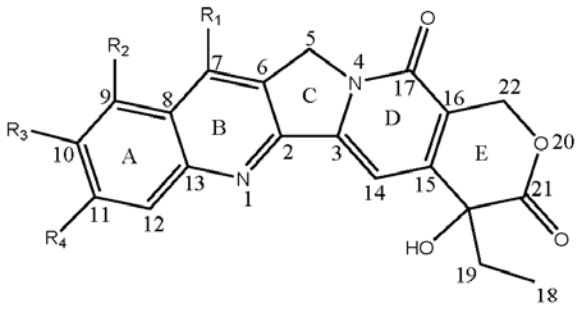

Analog	R1	R2	R3	R4
Camptothecin	H	H	H	H
Topotecan	H	$CH_2NH(CH_3)_2$	OH	H
Irinotecan	C_2H_5	H	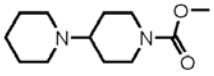	H
DB-67		H	OH	H
BNP-1350	$CH_2CH_2Si(CH_3)_3$	H	H	H
SN-38	C_2H_5	H	OH	H
Exatecan	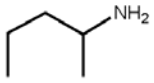		CH_3	F
IDEC-132	H	NH_2	H	H
Rubitecan	H	NO_2	H	H
Lutotecan	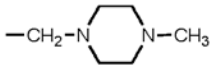	H	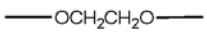	
GI-149893	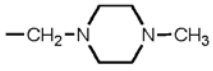	H	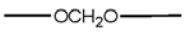	
ST-1481	$H_2C{=}NOC(CH_3)_3$	H	H	H
CKD-602	$CH_2CH_2NHCH(CH_3)_2$	H	H	H

Figure 1.1. Chemical structure of camptothecin and camptothecin analogues that are currently under development (adapted from (*64*)).

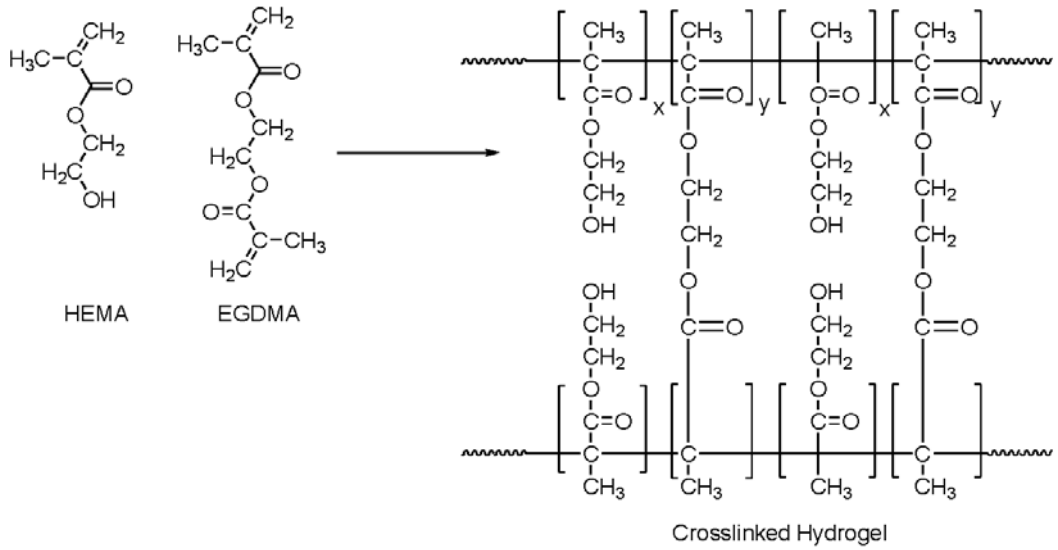

Figure 1.2. Synthesis of a three-dimensional network.

retained by the hydrogel in the swollen state is a measure of the polymer volume fraction. The degree of crosslinking of a polymer network can be characterized by the molecular weight between two consecutive crosslinks (which can be formed physically or chemically). Finally, the mesh size provides a measure of space available between the macromolecular chains. These parameters can be determined theoretically or through the use of a variety of experimental techniques. Two techniques which are utilized to elucidate the structure of hydrogels are equilibrium-swelling theory (*65*) and statistical branching theory (*66*).

The equilibrium swelling of polymer gels is often described in terms of the Flory-Rehner theory, which describes the forces at play when a crosslinked network is immersed in a fluid and allowing the system to reach equilibrium. This force can be written in terms of Gibbs free energy Eq. (1), the thermodynamic force of mixing and the retractive force of the polymer chains.

$$\Delta G_{Total} = \Delta G_{elastic} + \Delta G_{mixing} \quad (1)$$

Here, the ΔG_{mixing} is a measure of the Gibbs free energy change due to the mixing of a polymer with a solvent, and $\Delta G_{elastic}$ is the contribution of the forces involved in the deformation of the crosslinked network elastically.

The statistical branching theory, as described by Dušek et al. (*66-69*), is a Markov process that models a polymer structure in which each individual in generation *n* produces some random number of individuals in generation *n* + 1, according to a fixed probability distribution that does not vary from individual to individual. Statistical theories have been used frequently in crosslinking studies due to their ability to explain

complex chemical systems in a simpler manner. Analysis of a statistical network using the 1st-order Markov process is described below (adapted from (*70*)). The probability of bond formation of a given type depends only on the states of units the bond connects. The probability that the selected unit A in state i extends a bond to unit B in state j by reaction of groups p and r, respectively, is written as

$$p_{Aip\rightarrow rBj} \equiv p_{AiprBj;}$$

$$\sum_{j}\sum_{r} p_{AiprBj} = 1 \quad (2)$$

Very often, less precise specifications of transition probabilities are used and the states of units A and B are disregarded

$$p_{Ap\rightarrow rB} \equiv p_{AprB\ and}$$

$$\sum_{r} p_{aprB} = 1 \quad (3)$$

In a number of instances, units A bear groups a and units B bear groups b. Then, relation (3) is simplified to

$$p_{Aa\rightarrow bX} \equiv p_{AabB\ \equiv P_{AB} and p_{AA}+P_{AB}=1}$$

$$P_{BA} + p_{BB} = 1$$

For only A and B units having, respectively, groups a and b, when only bonds a-b are

$$p_{Aa\rightarrow bB} \equiv p_{AabB\ \equiv P_{AB}=1}$$

$$P_{AB} = 1 \quad (5)$$

In this simplest case, the fraction of reacted groups engaged in bonds a-b is equal to $\alpha_A p_{AB} = \alpha_A$. The nature of statistical generation of a branched structure can also be further analyzed using branching theories (*71-74*).

1.2.1. Stimuli Responsive Materials

Stimuli responsive hydrogels that exhibit swelling behavior dependent on the external environment are of great interest in the biomedical field. These gels can be tailored to dynamic change their swelling ratio depending on the stimuli. Various stimuli can be used to modulate the swelling ratio like external pH (*75, 76*), temperature (*77, 78*), and ionic strength of the local environment. pH-responsive materials are of great importance because they can be customized to exploit their physical property.

Hydrogels which exhibit pH-dependent swelling behavior contain a pendant ionizable group (either acidic or basic pendant groups). In aqueous media of appropriate pH and ionic strength, the pendent groups can ionize, developing fixed charges on the gel. Hence, these materials attract the most interest as they hold great potential in drug delivery applications. One example of pH-sensitive systems used in drug delivery is a system developed by Ishihara et al. (*79*). They combined a pH-sensitive hydrogel with glucose oxidase enzyme to regulate insulin release. This system was based on the fact that when glucose entered the hydrogel, glucose oxidase enzyme would convert glucose to gluconic acid, thereby reducing the pH and ionizing the pendent side chains. The ionization would cause charge repulsion, thereby expanding the gel and releasing the insulin.

Currently, hydrogels suitable for colon-specific delivery have received considerable interest as they afford the release of therapeutics locally (*80*). While one

approach, pioneered by Saffran (*81*), relies on hydrogels containing aromatic azobonds in the crosslinks (*82-84*), another approach is based on polysaccharide drug delivery systems (*85*). The colon-specificity in both designs relies on the specificity of bacterial enzymatic systems and on the physicochemical properties of the hydrogels. The degradability of hydrogels depends strongly on the equilibrium degree of swelling (*86, 87*). The high degree of swelling of colon-specific hydrogels is usually based on an ionizable comonomer-containing COOH group (*88*). The ionizable COOH groups deprotonate immediately after they reach the small intestine, followed by a rapid increase in the degree of swelling due to an increase in osmotic pressure, which modulates the expansion of the polymer chains. To achieve high rates of degradation, hydrogels with a large equilibrium degree of swelling have to be used.

Brøndsted et al. (*89, 90*) designed a novel hydrogel that contained both acidic comonomer and degradable azoaromatic cross-links. Radical polymerization of acrylic acid, n-tert-butylacrylamide, and N-methacrylamide crosslinked with 4,4'-di-(methacryloylamino)-azobenzene was used for synthesis. They found that the crosslinks were degradable by microbial azoreductase present predominantly in the colon, but the degradability in vitro was found to be related to the degree of swelling, and the structure and length of the crosslinking agent.

The structure of the azoaromatic crosslinks was further modified by Yeh et al. (*87*). Here, N,N-dimethylacrylamide copolymers precursors were crosslinked with N,N'-ε-aminocaproyl)-4,4'-diaminoazobenzene (Fig. 1.3). The degradability of hydrogels synthesized by two different methods, crosslinking of polymeric precursors and crosslinking copolymerization, were compared. They observed azo bond cleavage rate of

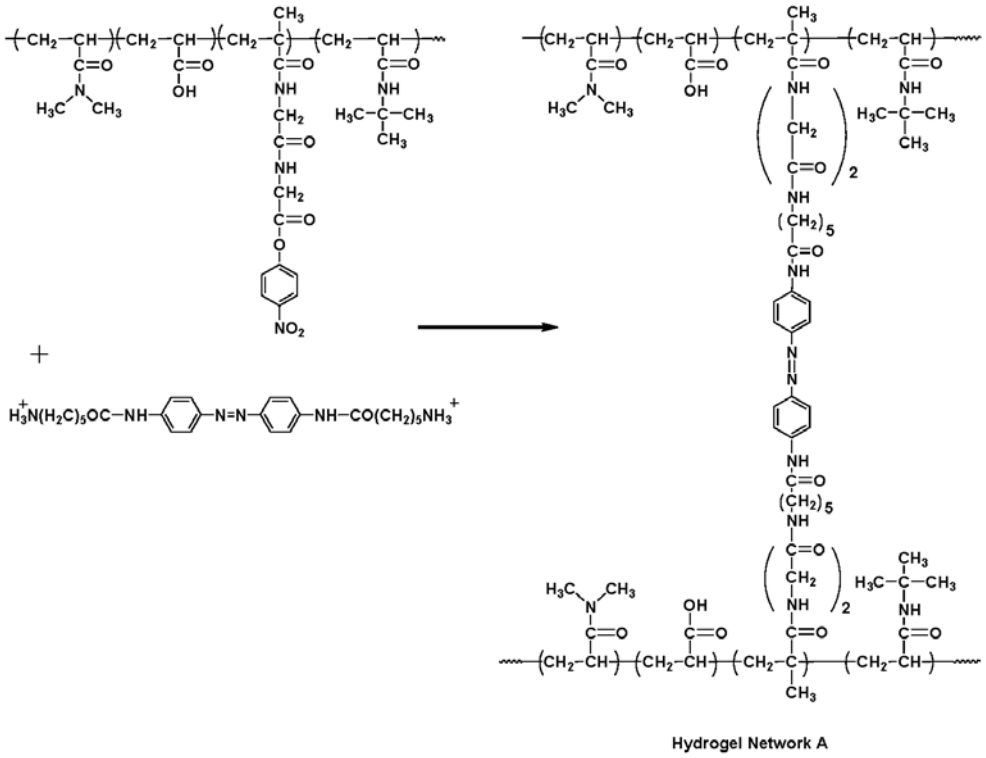

Figure 1.3. Colon-specific hydrogel synthesized by crosslinking of polymeric precursors.

hydrogels prepared by crosslinking of polymeric precursors was faster than that of hydrogels prepared by crosslinking copolymerization. The differences in the gel degradation pattern and the cleavage rate of azo bonds were attributed to the differences in the structure of the hydrogel network, i.e., the molecular weight of primary chains and the formation of chain entanglements.

To further control the kinetics of swelling of pH sensitive azoaromatic crosslinked hydrogels, Akala et al. (*76*) introduced a hydrolyzable comonomer in the network structure. Hence, the hydrogels contained two types of crosslinking agents, one hydrolyzable, the other enzymatically degradable. The hydrolyzable crosslinking agent was based on N-alkanoyl, O-acylhydroxylamine moieties. They studied the dependence on the length of the alkyl chain of the hydrolyzable comonomer on the rate of hydrolysis. Their studies indicated that the introduction of N,O-disubstituted hydroxylamine moieties into crosslinks of hydrogels produced structures whose kinetics of swelling at neutral pH can be controlled.

1.2.2. Interpenetrating Polymer Networks

Interpenetrating networks (IPNs) are binary systems composed of two mixed polymers, each of which is individually crosslinked (Fig. 1.4) (*91*). Adjustable swelling kinetics can be achieved with these systems. By combining two different systems, unique properties can be achieved with these biomaterials (*92*). For example, combinations of pH- and temperature-sensitive polymers (*93*) and polymers forming polyelectrolyte complexes (*94*) have been investigated. Compared to the individual

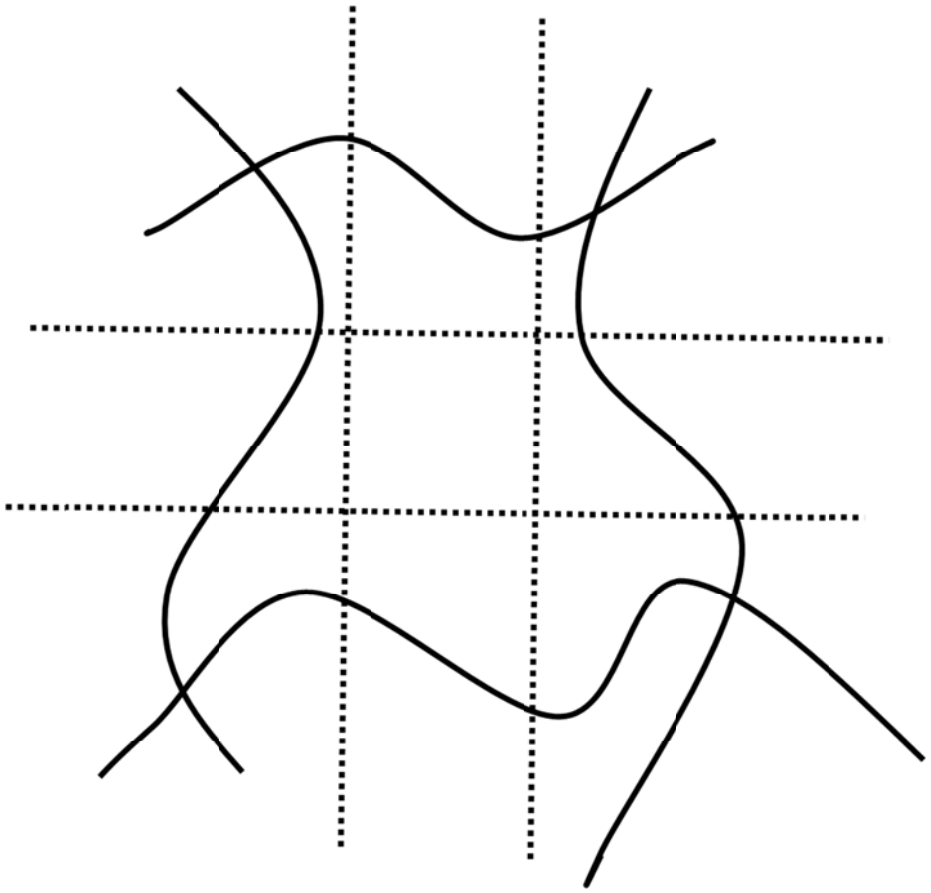

Figure 1.4. Illustrates an IPN composed of two crosslinked polymers.

networks, IPN hydrogels may have stronger mechanical properties due to the physical entanglements and network interactions.

There are two main synthetic processes to synthesize IPNs. The former is prepared by sequential IPN synthesis technique and the latter by a simultaneous interpenetrating networks (SINs) formation. Sequential IPNs are formed by polymerizing the first network (which contains monomer, crosslinking agent, and initiator), which is then swollen with the second combination of monomers and crosslinking agent, and then polymerized to form an IPN structure (Fig. 1.5). The latter technique involves the synthesis of IPN by two different polymerization techniques (for example, free radical and condensation reaction). Hence, IPN can be formed from two different monomer and crosslinking agent pairs together in one step. IPNs can be further classified by their structure, which can be full-IPNs or semi-IPNs. These two distinctions come from the fact that full IPNs are completely interlocked, thus generating a lot of entanglements and interaction between the networks. In the case of full IPNs, one network cannot be removed from another without chemical linkages being broken. Semi-IPNs involve a network where only one component is three-dimensional, and the other has a linear structure. The linear component can interact with the first network and change its physical properties. These sorts of systems are unique in that the linear component of the IPN can be removed from the network if the material is swollen in the appropriate solvent.

1.3. Polymeric Carriers for Systemic Delivery

The use of hydrophilic polymers as drug delivery vehicles is well accepted and might dramatically change the way patients are diagnosed and treated. Drugs that are

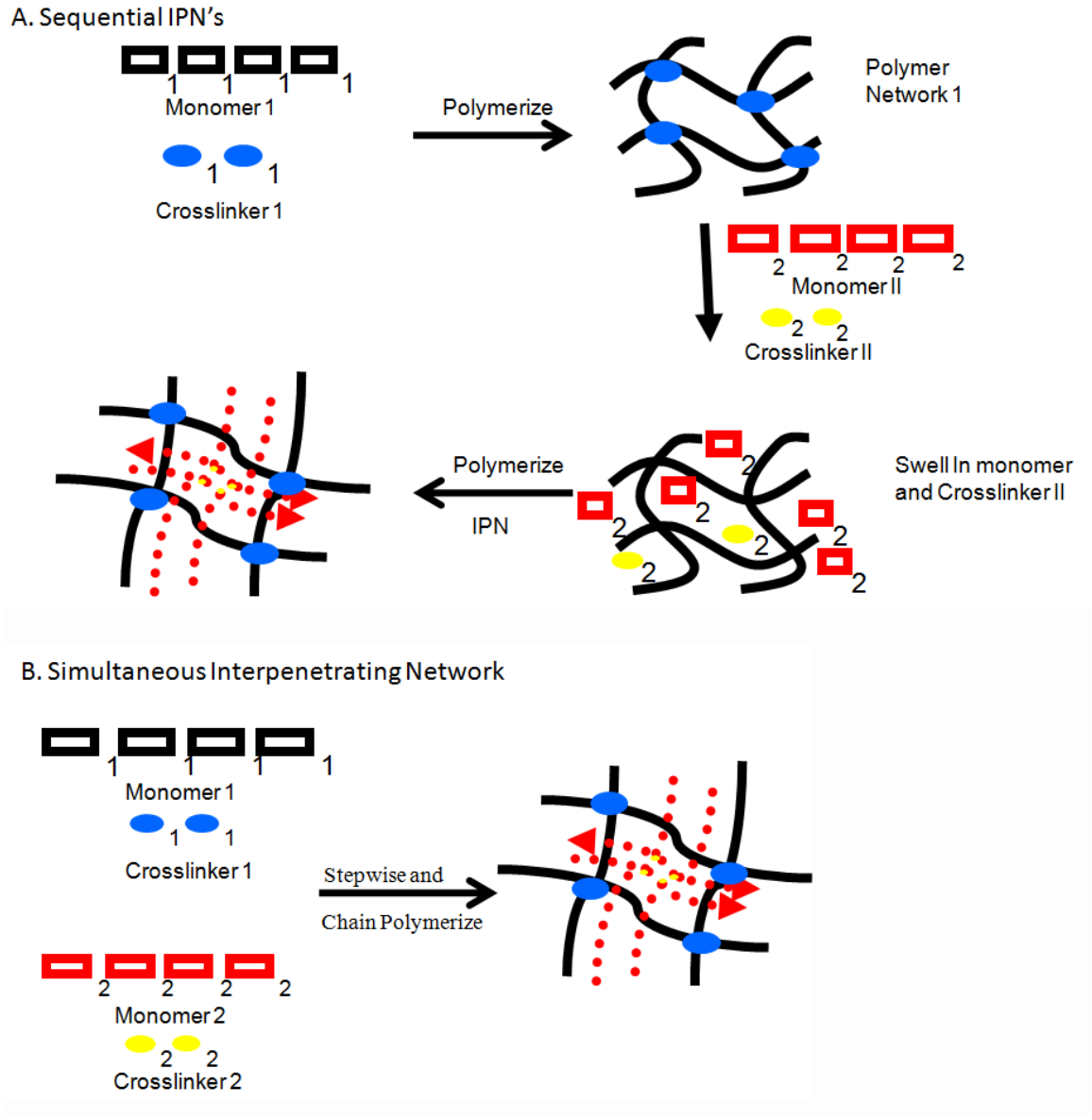

Figure 1.5. Methods of preparing interpenetrating polymer networks (adapted from (*95*)).

incorporated in polymeric carriers have various advantages (when compared to low-molecular weight drugs), including long-lasting circulation in the bloodstream, decreased nonspecific toxicity of the conjugated drug, increased solubility of hydrophobic compounds, decreased immunogenicity of the targeting moiety (*96, 97*), and the modulation of the cell signaling and apoptotic pathways (*98, 99*). An assortment of polymeric carriers are currently being developed, including liposomes (*100, 101*), polymeric nanoparticles (*102*), micelles (*103, 104*), and dendrimers (*105*).

Macromolecules afford the advantage of nonspecific accumulation inside solid tumors (Fig. 1.6). This phenomenon is due to the so-called Enhanced Permeability and Retention (EPR) effect (*106*). This effect is based on the fact that vasculature of normal and diseased tissue is vastly different; the latter have leaky vasculature which increases their permeability and, coupled with their poor lymphatic drainage, leads to the preferential extravasation and retention of macromolecules.

After the localization of macromolecules into a solid tumor, they have to be internalized and then release their cargo. The entry of macromolecules into the cell is through endocytosis. After internalization of particles, the contents are trapped in the endosome. Then, in a subsequent step, the endosome is fused with lysosome. The lysosome contains hydrolytic enzymes which are encompassed in an acidic environment. All endocytosed nanoparticles will be finally localized in this compartment (*107*). The lysosomal compartment is permeable only to small hydrophobic molecules. Hence, any drug attached to the polymeric carrier must be released before it is therapeutically efficacious. Various approaches have been used by researchers to achieve this goal.

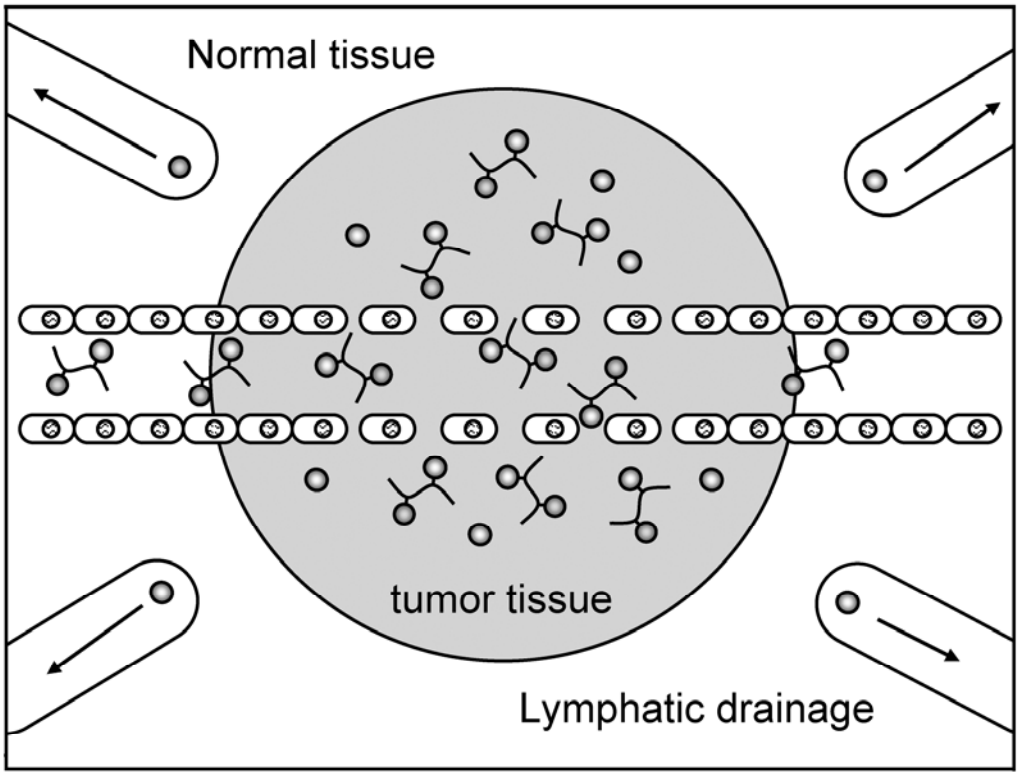

Figure 1.6. The enhanced permeability and retention (EPR) effect of macromolecules (adapted from (*116*)).

Oligopeptides spacers with the sequence glycylphenylalanylleucylglycyl (GFLG) have been extensively used for this purpose (*108, 109*). Other spacers which are acid sensitive can also be employed, like acetals, cis-aconityl, and hydrazone (*110, 111*).

Various strategies are being developed for the delivery of camptothecins, including conjugation to polymers to improve solubility and reduce nonspecific toxicity (*112-114*). Berrada et al. (*115*) designed a novel biodegradable and biocompatible injectable thermogelling drug delivery system based on chitosan polymers. The addition of glycerol-2-phosphate (β-GP) to the polymer solution induces a sol-gel transition at physiological temperature. When injected, this vehicle flows to fill voids within a cavity and becomes a solid at physiological temperature. The chitosan used in this study showed degradation in vivo in 6 months.

In their study (Berrada et al. (*115*)), they designed a system such that the anticancer drug camptothecin was homogenously dispersed within the chitosan hydrogel. Drug encapsulated within the gel is released due to the swelling, diffusion, and degradation of the matrix. This delivery system was then implanted intratumorally into a subcutaneous mouse tumor model. The effectiveness of this novel delivery system was measured in terms of tumor growth delay. The polymeric implant had delayed tumor growth over a long period of time (approximately 30 days), as compared to free drug given systemically (8 days) at the same dose. Controlled local delivery was also shown to have lower systemic toxicity as compared to the free drug. Finally, the increased therapeutic efficacy of their hydrogel system was attributed due to the extended controlled release of the therapeutics.

A different strategy proposed by Caiolfa et al. (*117*) involved the covalent attachment of camptothecin to a polymer carrier. In their study, N-(2-hydroxypropyl)methacrylamide (HPMA) copolymer was synthesized containing 5 and 10 wt % camptothecin (CPT). CPT was attached to the polymeric backbone via a Gly-Phe-Leu-Gly spacer. This spacer afforded the release of unmodified drug by esterolytic and proteolytic activity. The conjugated drug was fairly stable in buffer solution at neutral pH with a hydrolysis rate of 0.2-0.4 % free CPT/h. Attachment of CPT to the polymeric carrier changes the biodistribution of the parent compound with higher accumulation at the tumor site. A cumulative dose of 60 mg/kg had a 90 % tumor growth inhibition when incorporated in the polymeric construct without inducing any toxic side effects. On the other hand, free drug of a cumulative dose of 60 mg/kg administered i.v. as 12.5mg/kg/day had induced 5/7 toxic deaths. It was clearly shown that tumor accumulation and retention plays a key role in the pharmacology of the conjugates in terms of higher tolerability and enhanced potency.

1.3.1. Targeted Polymeric Carrier for Colorectal Cancer

Anticancer drugs intrinsically suffer from high toxicity, which limits their dosage and effectiveness in a clinic setting. Polymeric systems in general afford the advantage of improving drug solubility, increasing stability, enhanced tumor accumulation, and sustained release when compared to free drug. By implementing these strategies, the therapeutic window of potent and toxic drugs can be increased. A drawback of these delivery systems is that although enhanced tumor accumulation occurs, there is still a significant amount of drug not reaching the tumor.

Another drawback of conventional polymeric delivery systems relates to the slow rate of internalization after passive targeting to tumor tissue through the endocytic pathway. Hence, there is an immense interest in designing a new generation of molecularly targeted therapeutics through tumor-specific mAbs or ligands that bind to receptors present on tumor cells. Development of these systems can potentially lead to a higher local concentration and enhance tumor cytotoxicity as compared to its untargeted counterpart. Furthermore, targeted therapeutics may change the mechanism of cell entry from fluid phase pinocytosis to receptor-mediated endocytosis. The latter mode of entry results in a faster rate of internalization when compared to fluid phase (nontargeted systems) uptake (*118*) and is thus more efficient. Numerous antibodies (*119, 120*) and peptides (*121-124*) have been developed to target colon cancer. The most interesting targeting agent for colorectal cancers is based on peptide sequences. Combinatorial peptide library techniques have accelerated the identification of targeting peptides and stimulated their application due to their ease of synthesis, low immunogenicity, and desirable pharmacokinetic properties. Two of the most promising sequences found in the literature are the HEWSYLAPYPWF (*124*) sequence targeted to WiDr cells and the nonapeptide, CPIEDRPMC, derived from a disulfide constrained CX_7C library and shown to bind specifically to poorly differentiated colon carcinoma cells (HT-29) (*121*). Kelly et al. (*121*) used bacteriophage-derived libraries to select peptides binding to colon cancer cells. They used a subtraction method to distinguish between well-differentiated HCT116 and poorly differentiated HT29 colon carcinoma cells. Utilizing this method yielded peptides that displayed a consensus RPM sequence motif, which mediated preferential binding to HT29 cells. This peptide sequence was then further modified to

carry an imaging agent for real-time endoscopic tumor detection in a murine model (*125*). The modified peptide had a 24-min blood half-life, and the tumoral accumulation was 6.9% of injected dose/g, approximately 7-fold higher than a scrambled control peptide. They also observed that orthotopic colonic tumors (HT29) were readily detectable by fluorescence endoscopy even when tumors were submucosal.

1.4. Polymeric Carriers for Local Delivery

The oral route is the preferred manner of administration for most drugs. It is well known that there in an increased tight junction (TJ) permeability of macromolecules in epithelial cancers (*126*). This macromolecular permeability has been shown to be also present in polyps their TJs are leaky, allowing the uptake of high molecular weight dyes (*127, 128*). This serendipitous phenomenon (enhanced permeability of macromolecules) can be exploited by novel drug delivery design. Specific targeting of drugs to the colon is recognized to have several therapeutic advantages. Molecules that are susceptible to be destroyed by the acidic environment of the stomach or metabolized by pancreatic enzymes are only slightly affected in the colon. Treatment of colonic diseases such as colorectal cancer is more effective with the direct delivery of drugs to the colon (*80*). This sort of treatment will maximize the effectiveness of the drug. There is an increased interest in the design and synthesis of nanomedicine technology for colon-specific delivery.

Patients with relapsed CRC predominantly have disease confined to the liver, and their blood supply derived from the portal vein. A study performed with six randomized trials of hepatic arterial infusion demonstrated response rate of 41 % compared with 14%

for systemic therapy (*129*). Hence, targeting of drugs specifically to the colon using new and improved delivery strategies could provide significant clinical benefits.

One approach to target polymer-bound drug to the colon is by choosing the appropriate spacer. Spacers containing aromatic azobonds in the side chain are frequency employed for this purpose (*130-132*). After selectively targeting the macromolecule to the colon, the unmodified drug can be released at the site of action (*133*).

Local delivery of cyclosporin A can be effective in treatment of inflammatory bowel disease (IBD). Hence, Lu et al. (*134*) conjugated cyclosporin A to N-(2-hydroxypropyl)methacrylamide (HPMA) copolymer via an aromatic azo bond, which can be specifically cleaved by azoreductase activity in colon. The cleavage of the aromatic azo bond was monitored in vitro, results indicated that the free drug was released due to azoreductase activity and the conjugates were resistant to endopeptidase activity.

Sakuma et al. (*133*) synthesized N-(2-hydroxypropyl)methacrylamide (HPMA) copolymer conjugates containing 9-aminocamptothecin (9-AC) to the side chain. Here, 9-AC was bound via spacers containing amino acid residues (leucylalanine or alanine) and aromatic azo bonds. Their studies indicated that the azo bond was reduced first, generating a peptide-9-AC intermediate. In a subsequent step, cleavage of the peptide bond by peptidase activity released the unmodified 9-AC. They also found that the degradation of peptide bonds and release of unmodified 9-AC depended strongly on the chemical structure of the spacer between the drug and the azo residue. The researchers also found changing the peptide spacer from Ala to Leu-Ala resulted in a dramatic change in the degradation profile. The amino acid 9-AC conjugate was only negligible cleaved, whereas an oligopeptide spacer containing 9-AC showed complete release.

These data nevertheless did not translate to optimum in vivo results (*135*). The release rate from the conjugate was not fast enough to achieve high colon concentrations of free 9-AC when tested in rats. Hence, a second generation of 9-aminocamptothecin bound via an aromatic azo bond and a self-elimination spacer was synthesized by Gao et al. (*132*) (Fig. 1.7). Their results indicated a fast and highly efficient release of unmodified 9-AC from the polymer in the colon after azo bond cleavage. The novel aromatic azo bond spacers presented here have a potential for colon-specific drug delivery.

1.5. Statement of Objectives

The objective of this project is to design and synthesize novel drug delivery systems that can be implemented to reduce the nonspecific toxicities of conventional chemotherapeutics. To achieve this goal, we utilized a two-pronged approach to deliver therapeutic agents both locally and systemically. This may lead to a shift in the paradigm on the current treatment of CRC. For the first approach, a colon-specific drug delivery system based on biodegradable hydrogels and novel linear polymeric carriers was designed. The second approach exploits the benefits of systemic delivery by utilizing a targeted polymeric carrier.

Novel drug delivery strategies can be implemented to reduce the nonspecific toxicities of conventional chemotherapeutics. In such a strategy, a two-pronged approach to deliver therapeutic agent both locally and systemically may lead to a shift in the paradigm on the current treatment of CRC. To design such a system, three specific aims were proposed:

1) For colon-specific drug delivery, interpenetrating network (IPN) hydrogels composed of pH-sensitive, aromatic azo group-containing hydrogels as one of

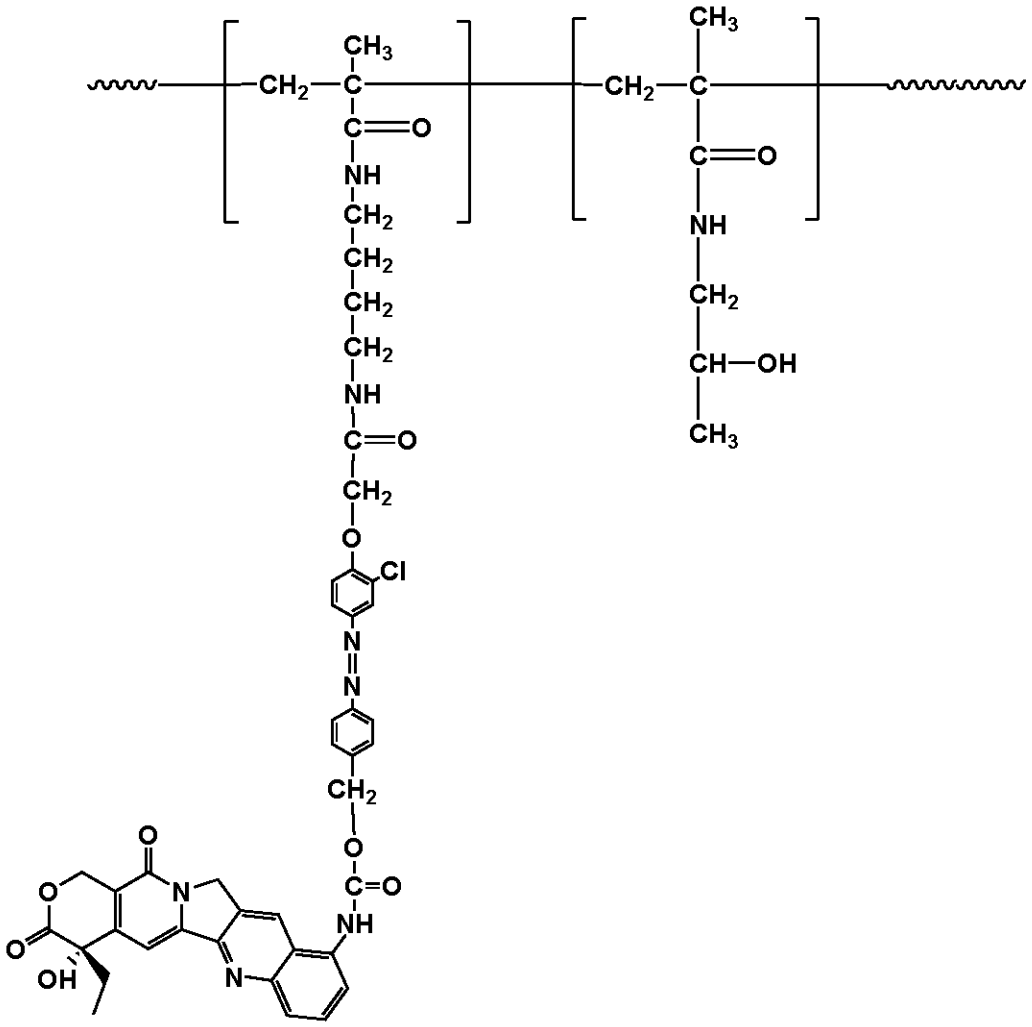

Figure 1.7. HPMA Copolymer-9AC conjugates containing an aromatic azo bond and a self-elimination spacer.

its components, and a hydrolyzable network as the other will be synthesized and the relationship between their structure and properties will be evaluated (addressed in Chapter 2).

2) Design a new generation of cellular targeted therapeutics that binds to receptors that are present on colonic tumor cells. The impact of the structure of the HPMA copolymer-peptide conjugates on the biorecognition by poorly differentiated HT-29 colon carcinoma cells will be investigated (addressed in Chapter 3).
3) Two linear polymeric-systems will be designed, one for systemic and the other for local delivery. Therapeutic efficiency of a systemic versus local approach will evaluated in vivo using a noninvasive bioluminescence imaging tumor model (addressed in Chapter 4).

1.6 References

(1) Chau, I., and Cunningham, D. (2002) Chemotherapy in colorectal cancer: new options and new challenges. *Br Med Bull 64*, 159-180.

(2) Gill, S., Thomas, R. R., and Goldberg, R. M. (2003) Review article: colorectal cancer chemotherapy. *Aliment Pharmacol Ther 18*, 683-692.

(3) Nicum, S., Midgley, R., and Kerr, D. J. (2003) Colorectal cancer. *Acta Oncol 42*, 263-275.

(4) Ferlay, J., Bray, F. Pisani, P. Parkin, D.M. (2001) *GLOBOCAN 2000: Cancer Incidence, Mortality and Prevalence Worldwide*, IARCPress.

(5) Cohen, A. M., and Winawer, S. J. (1995) *Cancer of the colon, rectum, and anus*, McGraw-Hill, New York.

(6) Ries, L. E., MP. Kosary, CL. Hankey, BF. Miller, BA. Clegg, L. Mariotto, A. Fay, MP. Feuer, EJ. and Edwards, BK. Eds. (2000) *SEER Cancer Statistics Review*, Bethesda, MD.

(7) Greene, F., and Page, D. (2002) Colon and Rectum, in *AJCC Cancer Staging Manual* (Haller, D., and Morrow D., Eds.) pp 113-124, Springer, New York, NY.

(8) Kahi, C. J., and Rex, D. K. (2004) Current and future trends in colorectal cancer screening. *Cancer Metastasis Rev 23*, 137-144.

(9) Rex, D. K., Johnson, D. A., Lieberman, D. A., Burt, R. W., and Sonnenberg, A. (2000) Colorectal cancer prevention 2000: screening recommendations of the American College of Gastroenterology. American College of Gastroenterology. *Am J Gastroenterol 95*, 868-877.

(10) Jorgensen, O. D., Kronborg, O., and Fenger, C. (1993) The Funen Adenoma Follow-up Study. Incidence and death from colorectal carcinoma in an adenoma surveillance program. *Scand J Gastroenterol 28*, 869-874.

(11) Winawer, S. J., Zauber, A. G., Ho, M. N., O'Brien, M. J., Gottlieb, L. S., Sternberg, S. S., Stewart, E. T., Bond, J. H., Schapiro, M., Panish, J. F., and et al. (1993) The National Polyp Study. *Eur J Cancer Prev 2 Suppl 2*, 83-87.

(12) Nicum, S., Midgley, R., and Kerr, D. J. (2003) Colorectal cancer. *Acta Oncol 42*, 263-275.

(13) Mandel, J. S., Bond, J. H., Church, T. R., Snover, D. C., Bradley, G. M., Schuman, L. M., and Ederer, F. (1993) Reducing mortality from colorectal cancer

by screening for fecal occult blood. Minnesota Colon Cancer Control Study. *N Engl J Med 328*, 1365-1371.

(14) Mandel, J. S., Church, T. R., Ederer, F., and Bond, J. H. (1999) Colorectal cancer mortality: effectiveness of biennial screening for fecal occult blood. *J Natl Cancer Inst 91*, 434-437.

(15) Doran, J., and Hardcastle, J. D. (1982) Bleeding patterns in colorectal cancer: the effect of aspirin and the implications for faecal occult blood testing. *Br J Surg 69*, 711-713.

(16) Selby, J. V., Friedman, G. D., Quesenberry, C. P., Jr., and Weiss, N. S. (1992) A case-control study of screening sigmoidoscopy and mortality from colorectal cancer. *N Engl J Med 326*, 653-657.

(17) Barry, M. J. (2002) Fecal occult blood testing for colorectal cancer: a perspective. *Ann Oncol 13*, 61-64.

(18) Petty, D. R., and Mannion, R. A. (2003) A case of multiple linseeds mimicking polyposis coli on double contrast barium enema. *Clin Radiol 58*, 87-88.

(19) Chong, A., Shah, J. N., Levine, M. S., Rubesin, S. E., Laufer, I., Ginsberg, G. G., Long, W. B., and Kochman, M. L. (2002) Diagnostic yield of barium enema examination after incomplete colonoscopy. *Radiology 223*, 620-624.

(20) Elmas, N., Killi, R. M., and Sever, A. (2002) Colorectal carcinoma: radiological diagnosis and staging. *Eur J Radiol 42*, 206-223.

(21) Bennett, D. H., and Hardcastle, J. D. (1994) Screening for colorectal cancer. *Postgrad Med J 70*, 469-474.

(22) Ransohoff, D. F., and Sandler, R. S. (2002) Clinical practice. Screening for colorectal cancer. *N Engl J Med 346*, 40-44.

(23) Rockey, D. C. (1999) Occult gastrointestinal bleeding. *N Engl J Med 341*, 38-46.

(24) Hobbs, F. D. (2000) ABC of colorectal cancer: the role of primary care. *Bmj 321*, 1068-1070.

(25) Newcomb, P. A., Norfleet, R. G., Storer, B. E., Surawicz, T. S., and Marcus, P. M. (1992) Screening sigmoidoscopy and colorectal cancer mortality. *J Natl Cancer Inst 84*, 1572-1575.

(26) Rex, D. K. (2002) Barium studies/virtual colonoscopy: the gastroenterologist's perspective. *Gastrointest Endosc 55*, S33-36; discussion S36.

(27) Hohenberger, W., Altendorf-Hofmann, A., and Haas, C. (1996) Curative interventions for recurrence of gastrointestinal carcinomas--incidence and prognosis. *Langenbecks Arch Chir Suppl Kongressbd 113*, 218-221.

(28) Hohenberger, W. (1997) The surgeon and surgical procedure as prognostic factor. *European Journal of Cancer 33*, 310-310.

(29) Scheele, J., Stang, R., Altendorf-Hofmann, A., and Paul, M. (1995) Resection of colorectal liver metastases. *World J Surg 19*, 59-71.

(30) Group, C. c. c. (2000) Palliative chemotherapy for advanced or metastatic colorectal cancer. Colorectal Meta-analysis Collaboration. *Cochrane Database Syst Rev*, CD001545.

(31) McArdle, C. S., and Hole, D. (1991) Impact of variability among surgeons on postoperative morbidity and mortality and ultimate survival. *Bmj 302*, 1501-1505.

(32) Simmonds, P. C. (2000) Palliative chemotherapy for advanced colorectal cancer: systematic review and meta-analysis. Colorectal Cancer Collaborative Group. *Bmj 321*, 531-535.

(33) Anonymous. (1994) Meta-analysis of randomized trials testing the biochemical modulation of fluorouracil by methotrexate in metastatic colorectal cancer. Advanced Colorectal Cancer Meta-Analysis Project. *J Clin Oncol 12*, 960-969.

(34) Carmichael, J., Popiela, T., Radstone, D., Falk, S., Borner, M., Oza, A., Skovsgaard, T., Munier, S., and Martin, C. (2002) Randomized comparative study of tegafur/uracil and oral leucovorin versus parenteral fluorouracil and leucovorin in patients with previously untreated metastatic colorectal cancer. *J Clin Oncol 20*, 3617-3627.

(35) Douillard, J. Y., Hoff, P. M., Skillings, J. R., Eisenberg, P., Davidson, N., Harper, P., Vincent, M. D., Lembersky, B. C., Thompson, S., Maniero, A., and Benner, S. E. (2002) Multicenter phase III study of uracil/tegafur and oral leucovorin versus fluorouracil and leucovorin in patients with previously untreated metastatic colorectal cancer. *J Clin Oncol 20*, 3605-3616.

(36) Pitot, H. C., Wender, D. B., O'Connell, M. J., Schroeder, G., Goldberg, R. M., Rubin, J., Mailliard, J. A., Knost, J. A., Ghosh, C., Kirschling, R. J., Levitt, R., and Windschitl, H. E. (1997) Phase II trial of irinotecan in patients with metastatic colorectal carcinoma. *J Clin Oncol 15*, 2910-2919.

(37) Rougier, P., Bugat, R., Douillard, J. Y., Culine, S., Suc, E., Brunet, P., Becouarn, Y., Ychou, M., Marty, M., Extra, J. M., Bonneterre, J., Adenis, A., Seitz, J. F., Ganem, G., Namer, M., Conroy, T., Negrier, S., Merrouche, Y., Burki, F., Mousseau, M., Herait, P., and Mahjoubi, M. (1997) Phase II study of irinotecan in

the treatment of advanced colorectal cancer in chemotherapy-naive patients and patients pretreated with fluorouracil-based chemotherapy. *J Clin Oncol 15*, 251-260.

(38) de Gramont, A., Tournigand, C., Louvet, C., Andre, T., Molitor, J. L., Raymond, E., Moreau, S., Vignoud, J., Le Bail, N., and Krulik, M. (1997) [Oxaliplatin, folinic acid and 5-fluorouracil (folfox) in pretreated patients with metastatic advanced cancer. The GERCOD]. *Rev Med Interne 18*, 769-775.

(39) Wall, M. E. W., M.C. Cook, C.E. Palmer, K.H. McPhail, A.I. Sim, G.A. (1966) Plant antitumor agents. I. The isolation and structure of camptothecin, a novel alkaloidal leukemia and tumor inhibitor from camptotheca acuminate. *J. Am. Chem. Soc 88*, 3888-3890.

(40) Abelson, H. T., and Penman, S. (1972) Selective interruption of high molecular weight RNA synthesis in HeLa cells by camptothecin. *Nat New Biol 237*, 144-146.

(41) Horwitz, S. B., Chang, C. K., and Grollman, A. P. (1971) Studies on camptothecin. I. Effects of nucleic acid and protein synthesis. *Mol Pharmacol 7*, 632-644.

(42) Kessel, D. (1971) Effects of camptothecin on RNA synthesis in leukemia L1210 cells. *Biochim Biophys Acta 246*, 225-232.

(43) Kessel, D., Bosmann, H. B., and Lohr, K. (1972) Camptothecin effects on DNA synthesis in murine leukemia cells. *Biochim Biophys Acta 269*, 210-216.

(44) Hsiang, Y. H., Hertzberg, R., Hecht, S., and Liu, L. F. (1985) Camptothecin induces protein-linked DNA breaks via mammalian DNA topoisomerase I. *J Biol Chem 260*, 14873-14878.

(45) Hsiang, Y. H., and Liu, L. F. (1988) Identification of mammalian DNA topoisomerase I as an intracellular target of the anticancer drug camptothecin. *Cancer Res 48*, 1722-1726.

(46) Gottlieb, J. A., Guarino, A. M., Call, J. B., Oliverio, V. T., and Block, J. B. (1970) Preliminary pharmacologic and clinical evaluation of camptothecin sodium (NSC-100880). *Cancer Chemother Rep 54*, 461-470.

(47) Negoro, S., Fukuoka, M., Masuda, N., Takada, M., Kusunoki, Y., Matsui, K., Takifuji, N., Kudoh, S., Niitani, H., and Taguchi, T. (1991) Phase I study of weekly intravenous infusions of CPT-11, a new derivative of camptothecin, in the treatment of advanced non-small-cell lung cancer. *J Natl Cancer Inst 83*, 1164-1168.

(48) Negoro, S., Fukuoka, M., Niitani, H., Suzuki, A., Nakabayashi, T., Kimura, M., Motomiya, M., Kurita, Y., Hasegawa, K., Kuriyama, T., and et al. (1991) [A phase II study of CPT-11, a camptothecin derivative, in patients with primary lung cancer. CPT-11 Cooperative Study Group]. *Gan To Kagaku Ryoho 18*, 1013-1019.

(49) Rowinsky, E. K., Grochow, L. B., Hendricks, C. B., Ettinger, D. S., Forastiere, A. A., Hurowitz, L. A., McGuire, W. P., Sartorius, S. E., Lubejko, B. G., Kaufmann, S. H., and et al. (1992) Phase I and pharmacologic study of topotecan: a novel topoisomerase I inhibitor. *J Clin Oncol 10*, 647-656.

(50) Peppas, N. A., Bures, P., Leobandung, W., and Ichikawa, H. (2000) Hydrogels in pharmaceutical formulations. *Eur J Pharm Biopharm 50*, 27-46.

(51) Davis, K. A., and Anseth, K. S. (2002) Controlled release from crosslinked degradable networks. *Crit Rev Ther Drug Carrier Syst 19*, 385-423.

(52) Woerly, S., Pinet, E., de Robertis, L., Van Diep, D., and Bousmina, M. (2001) Spinal cord repair with PHPMA hydrogel containing RGD peptides (NeuroGel). *Biomaterials 22*, 1095-1111.

(53) Gayet, J. C., and Fortier, G. (1995) Drug release from new bioartificial hydrogel. *Artif Cells Blood Substit Immobil Biotechnol 23*, 605-611.

(54) Cao, Y., Rodriguez, A., Vacanti, M., Ibarra, C., Arevalo, C., and Vacanti, C. A. (1998) Comparative study of the use of poly(glycolic acid), calcium alginate and pluronics in the engineering of autologous porcine cartilage. *J Biomater Sci Polym Ed 9*, 475-487.

(55) Elisseeff, J., Anseth, K., Sims, D., McIntosh, W., Randolph, M., and Langer, R. (1999) Transdermal photopolymerization for minimally invasive implantation. *Proc Natl Acad Sci U S A 96*, 3104-3107.

(56) Awad, H. A., Butler, D. L., Boivin, G. P., Smith, F. N., Malaviya, P., Huibregtse, B., and Caplan, A. I. (1999) Autologous mesenchymal stem cell-mediated repair of tendon. *Tissue Eng 5*, 267-277.

(57) Otsuka, J., Amano, J., and Tanaka, K. (1968) Presentation of newly-made hydrogel contact lenses. *Kaiin Dayori Nippon Kontakuto Renzu Gakkai 10*, 15-17.

(58) Hyon, S. H., Cha, W. I., Ikada, Y., Kita, M., Ogura, Y., and Honda, Y. (1994) Poly(vinyl alcohol) hydrogels as soft contact lens material. *J Biomater Sci Polym Ed 5*, 397-406.

(59) Říhová, B., Šrogl, J., Jelínková, M., Hovorka, O., Buresova, M., Šubr, V., and Ulbrich, K. (1997) HPMA-based biodegradable hydrogels containing different

forms of doxorubicin. Antitumor effects and biocompatibility. *Ann N Y Acad Sci 831*, 57-71.

(60) Peppas, N. A., Hilt, J. Z., Khademhosseini, A., and Langer, R. (2006) Hydrogels in biology and medicine: From molecular principles to bionanotechnology. *Advanced Materials 18*, 1345-1360.

(61) Michalek, J., Přádný, M., Artyukhov, A., Slouf, M., and Smetana, K., Jr. (2005) Macroporous hydrogels based on 2-hydroxyethyl methacrylate. Part III. Hydrogels as carriers for immobilization of proteins. *J Mater Sci Mater Med 16*, 783-786.

(62) Přádný, M., Lesny, P., Smetana, K., Jr., Vacik, J., Slouf, M., Michalek, J., and Sykova, E. (2005) Macroporous hydrogels based on 2-hydroxyethyl methacrylate. Part II. Copolymers with positive and negative charges, polyelectrolyte complexes. *J Mater Sci Mater Med 16*, 767-773.

(63) Wichterle, O., and Lim, D. (1960) Hydrophilic Gels for Biological Use. *Nature 185*, 117–118.

(64) Li, Q. Y., Zu, Y. G., Shi, R. Z., and Yao, L. P. (2006) Review camptothecin: current perspectives. *Curr Med Chem 13*, 2021-2039.

(65) Flory, P. J. (1953) *Principles of Polymer Chemistry*, Cornell University Press, Ithaca.

(66) Dušek, K., Dušková-Smrčková, M., Lewin, L. A., Huybrechts, J., and Barsotti, R. J. (2006) Branching theories and thermodynamics used to help designing precursor architectures and binder systems. *Surf Coat Int 89*, 123-131.

(67) Dušek, K. (1996) Diffusion control in the kinetics of cross-linking. *Polym Gels Networks 4*, 383-404.

(68) Dušek, K., Dušková-Smrčková, M., and Voit, B. (2005) Highly-branched off-stoichiometric functional polymers as polymer networks precursors. *Polymer 46*, 4265-4282.

(69) Dušek, K., and Dušková-Smrčková, M. (2000) Network structure formation during crosslinking of organic coating systems. *Progress in Polymer Science 25*, 1215-1260.

(70) Dušek, K. (2007) Applicability of statistical theories of network formation. *Macromol. Symp. 256*, 18-27.

(71) Dušek, K. (2007) My fifty years with polymer gels and networks and beyond. *Polym Bull 58*, 321-338.

(72) Chivukula, P., Dušek, K., Wang, D., Dušková-Smrčková, M., Kopeckova, P., and Kopeček, J. (2006) Synthesis and characterization of novel aromatic azo bond-containing pH-sensitive and hydrolytically cleavable IPN hydrogels. *Biomaterials 27*, 1140-1151.

(73) Dušek, K., and Dušková-Smrčková, M. (2003) Polymer networks from precursors of defined architecture. Activation of preexisting branch points. *Macromolecules 36*, 2915-2925.

(74) Wang, D., Dušek, K., Kopečková, P., Dušková-Smrčková, M., and Kopeček, J. (2002) Novel aromatic azo-containing pH-sensitive hydrogels: Synthesis and characterization. *Macromolecules 35*, 7791-7803.

(75) Risbud, M. V., Hardikar, A. A., Bhat, S. V., and Bhonde, R. R. (2000) pH-sensitive freeze-dried chitosan-polyvinyl pyrrolidone hydrogels as controlled release system for antibiotic delivery. *J Control Release 68*, 23-30.

(76) Akala, E. O., Kopečková, P., and Kopeček, J. (1998) Novel pH-sensitive hydrogels with adjustable swelling kinetics. *Biomaterials 19*, 1037-1047.

(77) Wang, B., Xu, X. D., Wang, Z. C., Cheng, S. X., Zhang, X. Z., and Zhuo, R. X. (2008) Synthesis and properties of pH and temperature sensitive P(NIPAAm-co-DMAEMA) hydrogels. *Colloids Surf B Biointerfaces*.

(78) Park, T. G. (1999) Temperature modulated protein release from pH/temperature-sensitive hydrogels. *Biomaterials 20*, 517-521.

(79) Ishihara, K. K., M. Ishimaru, N. Shinohara, I. (1984) Glucose Induced Permeation Control of Insulin through a Complex Membrane Consisting of Immobilized Glucose Oxidase and a Poly(amine). *Polym J 16*, 625–631.

(80) Shareef, M. A., Khar, R. K., Ahuja, A., Ahmad, F. J., and Raghava, S. (2003) Colonic drug delivery: an updated review. *AAPS PharmSci 5*, E17.

(81) Saffran, M., Kumar, G. S., Savariar, C., Burnham, J. C., Williams, F., and Neckers, D. C. (1986) A new approach to the oral administration of insulin and other peptide drugs. *Science 233*, 1081-1084.

(82) Van den Mooter, G., Maris, B., Samyn, C., Augustijns, P., and Kinget, R. (1997) Use of azo polymers for colon-specific drug delivery. *J Pharm Sci 86*, 1321-1327.

(83) Cheng, C. L., Gehrke, S. H., and Ritschel, W. A. (1994) Development of an azopolymer based colonic release capsule for delivering proteins/macromolecules. *Methods Find Exp Clin Pharmacol 16*, 271-278.

(84) Brøndsted, H., and Kopeček, J. (1991) Hydrogels for site-specific oral drug delivery: synthesis and characterization. *Biomaterials 12*, 584-592.

(85) Hovgaard, L., and Brøndsted, H. (1996) Current applications of polysaccharides in colon targeting. *Crit Rev Ther Drug Carrier Syst 13*, 185-223.

(86) Ulbrich, K., Strohalm, J., and Kopeček, J. (1982) Polymers containing enzymatically degradable bonds. VI. Hydrophilic gels cleavable by chymotrypsin. *Biomaterials 3*, 150-154.

(87) Yeh, P. Y., Kopečková, P., and Kopeček, J. (1995) Degradability of Hydrogels Containing Azoaromatic Crosslinks. *Macromol. Chem. Phys 196*, 2183-2202.

(88) Brøndsted, H., and Kopeček, J. (1992) pH Sensitive Hydrogels: Characteristics and Potential in Drug Delivery, in *Polyelectrolyte Gels* (Harland, R. S., and Prud'homme, R. K., Eds.) pp 285-304, American Chemical Society, Washington, DC.

(89) Brøndsted, H., and Kopeček, J. (1991) Hydrogels for site-specific oral drug delivery: synthesis and characterization. *Biomaterials 12*, 584-592.

(90) Brøndsted, H., and Kopeček, J. (1992) Hydrogels for site-specific drug delivery to the colon: in vitro and in vivo degradation. *Pharm Res 9*, 1540-1545.

(91) Klempner, D., Sperling, L. H., and Utracki, L. A. (1991) *Interpenetrating Polymer Networks*, American Chemical Society, New York.

(92) Diez-Pena, E., Quijada-Garido, I., Frutos, P., and Barrales-Rienda, J. M. (2002) Thermal Properties of Cross-Linked Poly(N-isopropylacrylamide) [P(N-iPAAm)], Poly(methacrylic acid) [P(MAA)], Their Random Copolymers [P(N-iPAAm-co-MAA)], and Sequential Interpenetrating Polymer Networks (IPNs). *Macromolecules 35*, 2667-2675.

(93) Zhang, J., and Peppas, N. A. (2002) Morphology of poly(methacrylic acid)/poly(N-isopropyl acrylamide) interpenetrating polymeric networks. *J Biomater Sci Polym Ed 13*, 511-525.

(94) Ilavský, M. M., G. Hanyková, L. Dušek, K. (2002) Phase transition in swollen gels 31. Swelling and mechanical behaviour of interpenetrating networks composed of poly(1-vinyl-2-pyrrolidone) and polyacrylamide in water/acetone mixtures. *Eur Polym J 38*, 875-883.

(95) Kim, S. C., and Sperling, L. H. (1997) *IPNs Around the World : Science and Engineering*, John Wiley, Chichester ; New York.

(96) Říhová, B., Ulbrich, K., Kopeček, J., and Mančal, P. (1983) Immunogenicity of N-(2-hydroxypropyl)-methacrylamide copolymers--potential hapten or drug carriers. *Folia Microbiol (Praha) 28*, 217-227.

(97) Říhová, B., Bilej, M., Větvička, V., Ulbrich, K., Strohalm, J., Kopeček, J., and Duncan, R. (1989) Biocompatibility of N-(2-hydroxypropyl) methacrylamide copolymers containing adriamycin. Immunogenicity, and effect on haematopoietic stem cells in bone marrow in vivo and mouse splenocytes and human peripheral blood lymphocytes in vitro. *Biomaterials 10*, 335-342.

(98) Duncan, R. (2003) The dawning era of polymer therapeutics. *Nat Rev Drug Discov 2*, 347-360.

(99) Kopeček, J., Kopečková, P., Minko, T., and Lu, Z. (2000) HPMA copolymer-anticancer drug conjugates: design, activity, and mechanism of action. *Eur J Pharm Biopharm 50*, 61-81.

(100) Fenske, D. B., Chonn, A., and Cullis, P. R. (2008) Liposomal nanomedicines: an emerging field. *Toxicol Pathol 36*, 21-29.

(101) Kale, A. A., and Torchilin, V. P. (2007) "Smart" drug carriers: PEGylated TATp-modified pH-sensitive liposomes. *J Liposome Res 17*, 197-203.

(102) Satchi-Fainaro, R., Puder, M., Davies, J. W., Tran, H. T., Sampson, D. A., Greene, A. K., Corfas, G., and Folkman, J. (2004) Targeting angiogenesis with a conjugate of HPMA copolymer and TNP-470. *Nat Med 10*, 255-261.

(103) Nishiyama, N., and Kataoka, K. (2006) Current state, achievements, and future prospects of polymeric micelles as nanocarriers for drug and gene delivery. *Pharmacol Ther 112*, 630-648.

(104) Nishiyama, N., Okazaki, S., Cabral, H., Miyamoto, M., Kato, Y., Sugiyama, Y., Nishio, K., Matsumura, Y., and Kataoka, K. (2003) Novel cisplatin-incorporated polymeric micelles can eradicate solid tumors in mice. *Cancer Res 63*, 8977-8983.

(105) Guillaudeu, S. J., Fox, M. E., Haidar, Y. M., Dy, E. E., Szoka, F. C., and Frechet, J. M. (2008) PEGylated dendrimers with core functionality for biological applications. *Bioconjug Chem 19*, 461-469.

(106) Matsumura, Y., and Maeda, H. (1986) A new concept for macromolecular therapeutics in cancer chemotherapy: mechanism of tumoritropic accumulation of proteins and the antitumor agent smancs. *Cancer Res 46*, 6387-6392.

(107) Krinick, N. L., and Kopeček, J. (1991) Soluble Polymers as Targetable Drug Carriers, in *Handbook of Experimental Pharmacology"Targeted Drug Delivery"* (Juliano, R. L., Ed.) pp 105-179, Springer.

(108) Duncan, R., Rejmanova, P., Kopeček, J., and Lloyd, J. B. (1981) Pinocytic uptake and intracellular degradation of N-(2-hydroxypropyl)methacrylamide copolymers. A potential drug delivery system. *Biochimica et Biophysica Acta 678*, 143-150.

(109) Rejmanova, P., Pohl, J., Baudys, M., Kostka, V., and Kopeček, J. (1983) Polymers Containing Enzymatically Degradable Bonds. 8. Degradation of Oligopeptide Sequences in N-(2-Hydroxypropyl)methacrylamide Copolymers by Bovine Spleen Cathepsin B. *Makromol Chem 184*, 2009-2020.

(110) Gillies, E. R., Goodwin, A. P., and Frechet, J. M. (2004) Acetals as pH-sensitive linkages for drug delivery. *Bioconjug Chem 15*, 1254-1263.

(111) Christie, R. J., and Grainger, D. W. (2003) Design strategies to improve soluble macromolecular delivery constructs. *Adv Drug Deliv Rev 55*, 421-437.

(112) Greenwald, R. B., Pendri, A., Conover, C., Gilbert, C., Yang, R., and Xia, J. (1996) Drug delivery systems. 2. Camptothecin 20-O-poly(ethylene glycol) ester transport forms. *J Med Chem 39*, 1938-1940.

(113) Greenwald, R. B., Pendri, A., Conover, C. D., Lee, C., Choe, Y. H., Gilbert, C., Martinez, A., Xia, J., Wu, D., and Hsue, M. (1998) Camptothecin-20-PEG ester transport forms: the effect of spacer groups on antitumor activity. *Bioorg Med Chem 6*, 551-562.

(114) Conover, C. D., Pendri, A., Lee, C., Gilbert, C. W., Shum, K. L., and Greenwald, R. B. (1997) Camptothecin delivery systems: the antitumor activity of a camptothecin-20-0-polyethylene glycol ester transport form. *Anticancer Res 17*, 3361-3368.

(115) Berrada, M., Serreqi, A., Dabbarh, F., Owusu, A., Gupta, A., and Lehnert, S. (2005) A novel non-toxic camptothecin formulation for cancer chemotherapy. *Biomaterials 26*, 2115-2120.

(116) Pan, H., and Kopeček, J. (2008) *Multifunctional Water-Soluble Polymers for Drug Delivery*, Vol. 4, Springer, New York.

(117) Caiolfa, V. R., Zamai, M., Fiorino, A., Frigerio, E., Pellizzoni, C., d'Argy, R., Ghiglieri, A., Castelli, M. G., Farao, M., Pesenti, E., Gigli, M., Angelucci, F., and Suarato, A. (2000) Polymer-bound camptothecin: initial biodistribution and antitumour activity studies. *J Control Release 65*, 105-119.

(118) Omelyanenko, V., Kopečková, P., Gentry, C., and Kopeček, J. (1998) Targetable HPMA copolymer-adriamycin conjugates. Recognition, internalization, and subcellular fate. *J Control Release 53*, 25-37.

(119) Roovers, R. C., van der Linden, E., de Bruine, A. P., Arends, J. W., and Hoogenboom, H. R. (2001) Identification of colon tumor-associated antigens by phage antibody selections on primary colorectal carcinoma. *Eur J Cancer 37*, 542-549.

(120) Welt, S., Divgi, C. R., Scott, A. M., Garin-Chesa, P., Finn, R. D., Graham, M., Carswell, E. A., Cohen, A., Larson, S. M., and Old, L. J. (1994) Antibody targeting in metastatic colon cancer: a phase I study of monoclonal antibody F19 against a cell-surface protein of reactive tumor stromal fibroblasts. *J Clin Oncol 12*, 1193-1203.

(121) Kelly, K. A., and Jones, D. A. (2003) Isolation of a colon tumor specific binding peptide using phage display selection. *Neoplasia 5*, 437-444.

(122) Laburthe, M., Rousset, M., Chevalier, G., Boissard, C., Dupont, C., Zweibaum, A., and Rosselin, G. (1980) Vasoactive intestinal peptide control of cyclic adenosine 3':5'-monophosphate levels in seven human colorectal adenocarcinoma cell lines in culture. *Cancer Res 40*, 2529-2533.

(123) Pallela, V. R., Thakur, M. L., Chakder, S., and Rattan, S. (1999) 99mTc-labeled vasoactive intestinal peptide receptor agonist: functional studies. *J Nucl Med 40*, 352-360.

(124) Rasmussen, U. B., Schreiber, V., Schultz, H., Mischler, F., and Schughart, K. (2002) Tumor cell-targeting by phage-displayed peptides. *Cancer Gene Ther 9*, 606-612.

(125) Kelly, K., Alencar, H., Funovics, M., Mahmood, U., and Weissleder, R. (2004) Detection of invasive colon cancer using a novel, targeted, library-derived fluorescent peptide. *Cancer Res 64*, 6247-6251.

(126) Mullin, J. M., Laughlin, K. V., Ginanni, N., Marano, C. W., Clarke, H. M., and Peralta Soler, A. (2000) Increased tight junction permeability can result from protein kinase C activation/translocation and act as a tumor promotional event in epithelial cancers. *Ann N Y Acad Sci 915*, 231-236.

(127) Mullin, J. M., and O'Brien, T. G. (1986) Effects of tumor promoters on LLC-PK1 renal epithelial tight junctions and transepithelial fluxes. *Am J Physiol 251*, C597-602.

(128) Mullin, J. M., Soler, A. P., Laughlin, K. V., Kampherstein, J. A., Russo, L. M., Saladik, D. T., George, K., Shurina, R. D., and O'Brien, T. G. (1996) Chronic

exposure of LLC-PK1 epithelia to the phorbol ester TPA produces polyp-like foci with leaky tight junctions and altered protein kinase C-alpha expression and localization. *Exp Cell Res 227*, 12-22.

(129) (1996) Reappraisal of hepatic arterial infusion in the treatment of nonresectable liver metastases from colorectal cancer. Meta-Analysis Group in Cancer. *J Natl Cancer Inst 88*, 252-258.

(130) Gao, S. Q., Sun, Y., Kopečková, P., Peterson, C. M., and Kopeček, J. (2008) Pharmacokinetic modeling of absorption behavior of 9-aminocamptothecin (9-AC) released from colon-specific HPMA copolymer-9-AC conjugate in rats. *Pharm Res 25*, 218-226.

(131) Gao, S. Q., Lu, Z. R., Kopečková, P., and Kopeček, J. (2007) Biodistribution and pharmacokinetics of colon-specific HPMA copolymer--9-aminocamptothecin conjugate in mice. *J Control Release 117*, 179-185.

(132) Gao, S. Q., Lu, Z. R., Petri, B., Kopečková, P., and Kopeček, J. (2006) Colon-specific 9-aminocamptothecin-HPMA copolymer conjugates containing a 1,6-elimination spacer. *J Control Release 110*, 323-331.

(133) Sakuma, S., Lu, Z. R., Kopečková, P., and Kopeček, J. (2001) Biorecognizable HPMA copolymer-drug conjugates for colon-specific delivery of 9-aminocamptothecin. *J Control Release 75*, 365-379.

(134) Lu, Z. R., Gao, S. Q., Kopeckova, P., and Kopeček, J. (2000) Synthesis of bioadhesive lectin-HPMA copolymer-cyclosporin conjugates. *Bioconjug Chem 11*, 3-7.

(135) Sakuma, S., Lu, Z. R., Pecharova, B., Kopeckova, P., and Kopeček, J. (2002) N-(2-hydroxypropyl)-methacrylamide copolymer-9-aminocamptothecin conjugate: Colon-specific drug delivery in rats. *J Bioact Compat Polym 17*, 305-319.

CHAPTER 2

SYNTHESIS AND CHARACTERIZATION OF NOVEL AROMATIC AZO BOND-CONTAINING PH-SENSITIVE AND HYDROLYTICALLY CLEAVABLE IPN HYDROGELS

2.1 Abstract

Novel interpenetrating network (IPN) hydrogels, composed of a pH-sensitive, aromatic azo group-containing network as one component (Network A), and a hydrolyzable network as the other (Network B) were prepared by a sequential process. The first network was formed by crosslinking of a reactive polymer precursor (copolymer of *N*,*N*-dimethylacrylamide, acrylic acid, N-tert.butylacrylamide, and *N*-methacryloyl-glycylglycine p-nitrophenyl ester) with an aromatic azo group containing diamine ((*N*,*N'*-ε-aminocaproyl)-4,4'-diaminoazobenzene). The second network was formed by radical crosslinking copolymerization of *N*-(2-hydroxypropyl)methacrylamide with *N*,*O*-dimethacryloylhydroxylamine. Hydrogels synthesized in this manner were homogeneous and showed no evidence of phase separation. The composition of the hydrogels was manipulated to determine the influence of hydrogel composition on the equilibrium degree of swelling, modulus of elasticity in compression, and on the rate of degradation of Network B. To mimic the conditions in the gastrointestinal tract, properties of the hydrogels were evaluated after abrupt change of pH from pH 2.0 to pH 7.4. The analysis

of IPN structure revealed that crosslinking efficiency of radically polymerized Network B (10-30%) was lower than that of step polyaddition Network A. In the IPN gels, the crosslinking efficiency was even lower and was close to 10%. Factors contributing to the low crosslinking efficiency of IPN include higher dilution at network formation and possible negative effect of the components of Network A on radical polymerization of Network B. The major advantage of IPN hydrogels, when compared to traditional pH-sensitive networks, is the linear swelling profile following abrupt change of pH from 2 to 7.4. This indicates the suitability of IPN as carriers for oral drug delivery.

2.2 Introduction

Oral delivery of peptides and proteins is an attractive therapeutic modality for chronic dosage in non-life-threatening disorders (1). The major problem associated with oral delivery of proteins and peptides is their degradation in the stomach and small intestine due to the high proteolytic activity present at these sites (2). To circumvent this problem, delivery of proteins and peptides to the colon is very desirable (3). The colon has low enzymatic activity and is a less hostile environment for protein delivery. Many attempts have been made by various groups to take advantage of colon-specific delivery using elaborate techniques such as nano-particulate carriers for the colonic mucosa (4), pressure-controlled colon delivery devices (5), and employing of enteric coatings (6). However, the major obstacle with all these techniques is associated with the colonic variation among different individuals and the transient variation of the local colonic region.

Aromatic azo bond-containing pH-sensitive hydrogels have been extensively studied as carriers for colon-specific delivery (7, 8). Due to the presence of carboxylic

groups in their structure, such hydrogels are compact at lower pH but swell as pH increases. Once inside the colon, highly swollen aromatic azo bond-containing hydrogels become accessible to azoreductase activities; this results in the reduction of the azo bond and degradation of the hydrogel matrix. The major drawbacks of these hydrogels are their swelling properties; a large burst effect occurs when the pH is changed from below to above its pKa and the swelling equilibrium is rapidly reached. This burst can cause the cargo present within the gel to be prematurely released in the small intestine. Many structural modifications have been attempted, for example the incorporation of hydrolyzable side-chains, with modest success (9).

Interpenetrating network hydrogels (IPN) consist of two independently crosslinked networks that are interlocked (10). Unique properties can be achieved with these biomaterials (11). For example, combinations of pH- and temperature-sensitive polymers (12) and polymers forming polyelectrolyte complexes (13) have been investigated. IPN hydrogels may have more favorable mechanical properties due to the physical entanglements and network interactions, when compared to individual crosslinked networks.

A novel approach to form IPN hydrogels, presented here, is the combination of a pH-sensitive network and a hydrolyzable network. IPN hydrogels that contained pH-sensitive subunits (acrylic acid) which were crosslinked with an aromatic azo bond were synthesized. Such hydrogels would be in a contracted state at the low pH of the stomach and they would start swelling at a higher pH in the intestine. It is well accepted that the equilibrium degree of swelling influences the degradation rate of the gel network (14, 15). If one assumes that the transit time to the colon from the stomach is approximately 6

h, then the hydrogel should be in the fully swollen state after this time period to provide degradability in the colon. To manipulate the swelling kinetics of the pH-sensitive network, we introduced a biodegradable crosslinking agent, (*N,O*-dimethacryloylhydroxylamine (DMHA) into one of the networks (16). A poly(*N*-(2-hydroxypropyl)methacrylamide) (PHPMA) network, crosslinked with DMHA, could be hydrolyzed at pH above 7 by undergoing a Lossen rearrangement (17), resulting in the formation of a polymer-bound carboxyl and amino group with concomitant release of carbon dioxide. The attempt of this study was to investigate the properties that would influence the swelling profile of IPN hydrogels. The relationship between the structure of individual networks and the properties of the IPN hydrogels has been evaluated.

To this end, Networks A and B were prepared separately, and homogeneous IPN hydrogels were prepared by a sequential process. Network A was prepared by the crosslinking of a reactive polymer precursor (copolymer of *N,N*-dimethylacrylamide (DMAA, to increase biocompatibility), acrylic acid (AA, pH-sensitive monomer), N-tert.butylacrylamide (BuAA, to improve mechanical properties), and *N*-methacryloylglycylglycine p-nitrophenyl ester (MA-GG-ONp, introduces reactive ester groups for crosslinking) with an aromatic azo group-containing diamine, *N,N'*-(ε-aminocaproyl)-4,4'diaminoazobenzene (NH_2-R-AZO-R-NH_2). Network B was prepared by crosslinking copolymerization of *N*-(2-hydroxypropyl)methacrylamide (HPMA) and the crosslinker DMHA. Modeling of network structure for both IPN and individual networks was accomplished using a statistical branching theory. The theoretical values and experimental data were compared and the impact of the composition of individual networks on the structure of IPNs was evaluated.

2.3 Materials and Methods

2.3.1 Chemicals

NH_2-R-AZO-R-NH_2 (18), HPMA (19), DMHA (16), and MA-GG-ONp (20) were synthesized as described previously. Solvents and reagents used for synthesis were purchased from Aldrich (Milwaukee, WI) or Sigma (St. Louis, MO) if not specified otherwise. Acrylic acid and *N*,*N*-dimethylacrylamide were distilled under reduced pressure. *N*-*tert*-Butylacrylamide was recrystallized from acetone.

2.3.2 Synthesis of Polymeric Precursors

The polymer precursors P1-P3 (Table 2.1) were synthesized (18) by free radical copolymerization of DMAA, AA, BuAA, and MA-GG-ONp in acetone at 50 °C for 24 h using 2,2'-azobisisobutyronitrile (AIBN) as the initiator. The stoichiometry of the comonomers in the feed was manipulated to prepare three copolymer compositions. Typically: DMAA (0.8723 g, 8.8 mmol, 44 mol%), AA (0.5765 g, 8.0 mmol, 40 mol%), BuAA (0.2544 g, 2.0 mmol, 10 mol%), MA-GG-ONp (0.3856 g, 1.2 mmol, 6 mol%), and AIBN (0.1 g, 0.61 mmol) were dissolved in acetone (20 ml), placed in an ampoule, purged with N_2 for 5 min, and sealed. After polymerization, the ampoule was cooled, opened, the precipitated copolymer filtered off, and washed with an excess of acetone. The copolymer was dissolved in MeOH and reprecipitated into diethyl ether/acetone (1/1 v/v). The yield of polymer was 750 mg (68.5 %).

Table 2.1. Synthesis of Polymeric Precursors

	AA (Mol %)	BuAA (Mol %)	DMAA (Mol %)	MA-GG-ONp (Mol %)	Moles of ONp in polymer (mol/g)	M_n	M_w
P1	40	10	47	3	1.68×10^{-4}	3.18×10^{4}	4.37×10^{4}
P2	40	10	46	4	2.48×10^{-4}	2.78×10^{4}	3.80×10^{4}
P3	40	10	44	6	4.62×10^{-4}	3.15×10^{4}	4.08×10^{4}

2.3.3. Synthesis of Aromatic Azo Bond-Containing Hydrogels (Network A)

Hydrogels (A1-A3; Table 2.2) were prepared by crosslinking of polymer precursors (P1-P3; Table 2.1) with NH_2-R-AZO-R-NH_2 as described previously (Scheme 2.1) (18). Briefly, NH_2-R-AZO-R-NH_2 (5.53 mg, 0.0127 mmol) was dissolved in DMSO (0.6 ml) to which trifluoroacetic acid (TFA) solution (mol ratio [TFA]: [NH_2] = 2 in DMSO, 50 µl) was added and mixed at room temperature (Solution A). In this solution (Solution A), a polymeric precursor (150 mg, 0.0253 mmol) was dissolved. The ratio of [ONp] in the polymeric precursor to [NH_2] in the crosslinking agent was 1:1. The final volume of the solution was increased to 1 ml with DMSO (final concentration of polymer precursor was 15 wt %). The crosslinking reaction was started by the addition of a methyl morpholine (MM) solution (mol ratio [MM]: [NH_2] = 4 in DMSO, 50 µl), and the mixture was thoroughly mixed with a vortex for 30 s. The resulting solution was then quickly transferred to a polymerization mold. The gel point was typically reached after about 1 h. Twenty-four hours later, the gel was retrieved and punched into disks (d = 0.7 cm; h = 0.17 cm). The disks were immersed in EtOH for 1 week to remove the unreacted compounds. The solvent was gradually changed to a 0.01 N HCl solution and stored until used.

2.3.4. Synthesis of Hydrolyzable Hydrogels (Network B)

The hydrolyzable hydrogels (H1-H3) were synthesized by free radical copolymerization of HPMA with DMHA at 50 °C for 24 h using AIBN as the initiator as previously described (Scheme 2.2) [18]. Typically, the monomers HPMA (300 mg, 2.095 mmol), crosslinker DMHA (11.3 mg, 0.067 mmol), and AIBN (11 mg, 0.067 mmol) as

Table 2.2. Composition of aromatic azo-bond containing hydrogel (Network A)

	Polymeric Precursor (mg)	Moles of ONp (mol)	Diamine (mg)	Diamine (mol)
A1	150	2.53×10^{-5}	5.53	1.27×10^{-5}
A2	150	3.72×10^{-5}	8.16	1.86×10^{-5}
A3	150	6.93×10^{-5}	15.20	3.47×10^{-5}

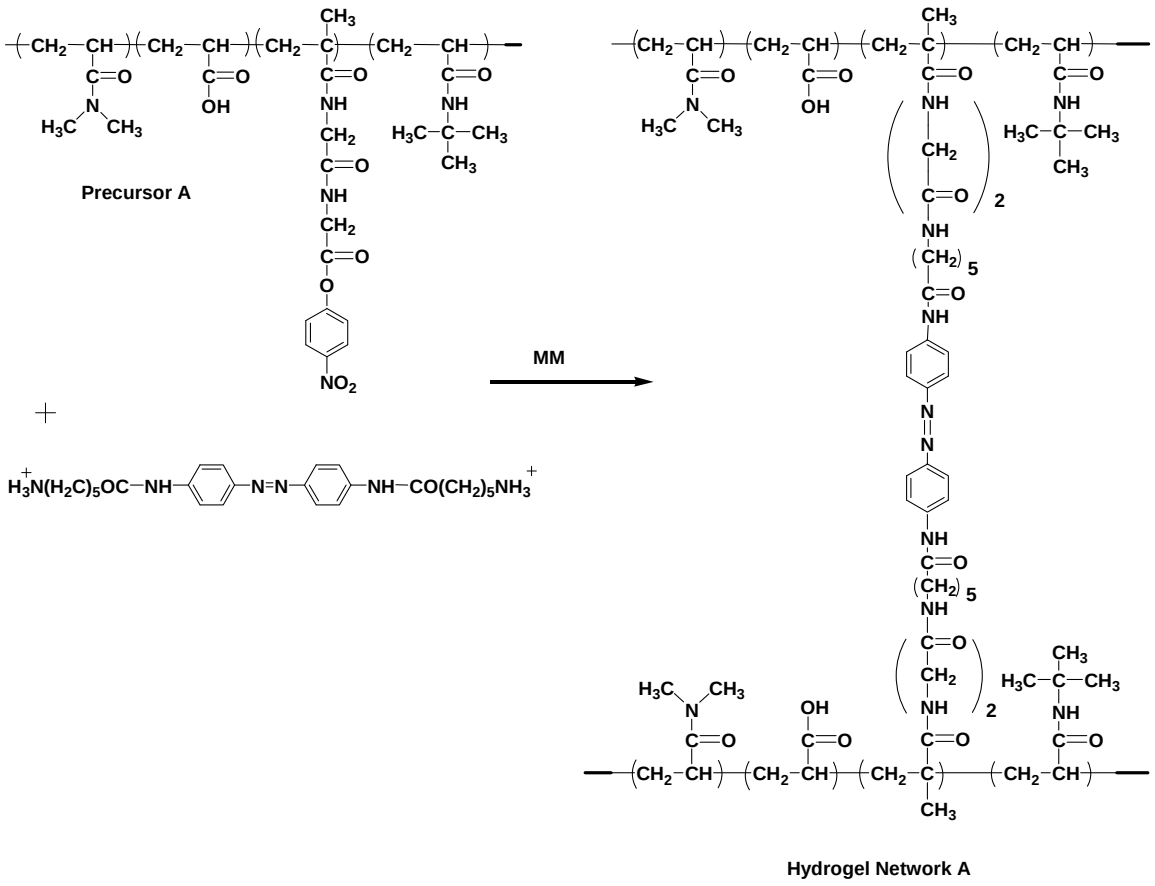

Scheme 2.1. Synthesis of Network A (aromatic azo bond-containing network).

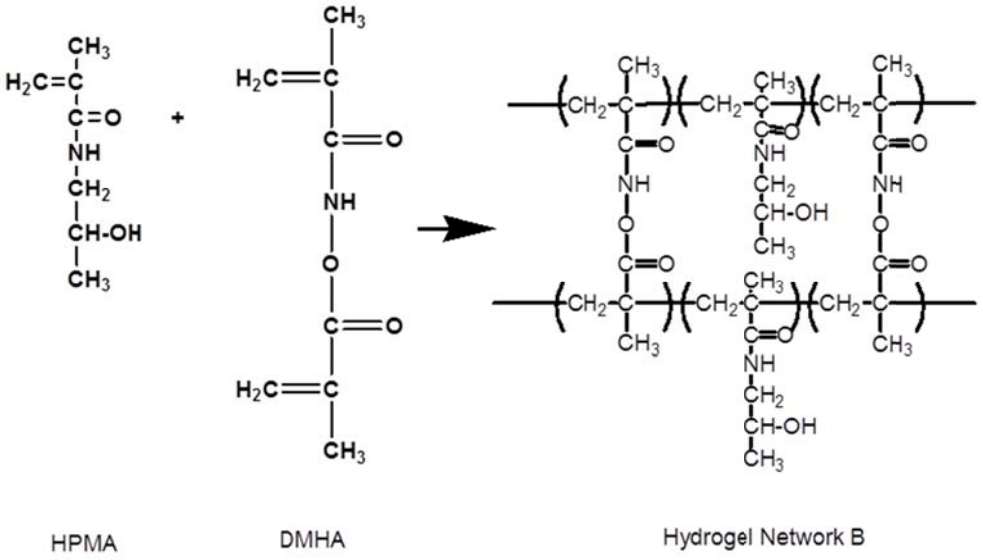

Scheme 2.2. Synthesis of Network B (hydrolyzable network).

initiator were dissolved in DMSO to yield a 30 wt % solution. The solution was transferred into a mold, purged with N_2 for 5 min, and sealed. The temperature of the mold was then increased to 50 ^{0}C to start the polymerization. After 24 h, the gels were retrieved and washed with EtOH and stored in 0.01 N HCl solutions (to prevent hydrolysis).

2.3.5. Synthesis of IPN Hydrogels (Network A and Network B)

The IPN hydrogels (IPN1-4) were prepared by a sequential (two-step) process (Scheme 2.3). Briefly, a DMSO solution (0.6 ml) containing HPMA (300 mg, 2.1 mmol), DMHA (11.3 mg, 0.067 mmol), AIBN (11 mg, 0.067 mmol), and NH_2-R-AZO-R-NH_2 (5.5 mg, 0.0126 mmol) was prepared and thoroughly mixed at room temperature to obtain a transparent solution. To this, TFA (0.0504 mmol, mol ratio [TFA]: [NH_2] = 2) solution (3.88 µl TFA in DMSO, 50 µl) was added and vortexed. Finally, the polymeric precursor (150 mg, [ONp] = 0.0252 mmol) was also added and dissolved. The ratio of [ONp] in the polymeric precursor to [NH_2] in the crosslinking agent was 1:1. A final volume of 1 ml was obtained with the addition of DMSO, and then followed by the addition of MM (0.10 mmol, mol ratio [MM]: [TFA] = 2, 11.08 µl MM in DMSO, 50 µl). The solution was then thoroughly mixed (vortexed ~ 30 s), transferred to a mold, purged with N_2 for 5 min, and sealed. During this (first) step, the mold was left unperturbed on the lab bench for the formation of the first network (Network A). The second step of the reaction involved transferring the mold to an oil bath at 50 ^{0}C. The mold was left at 50 ^{0}C for 24 h for the formation of the second network (Network B). Gels were removed

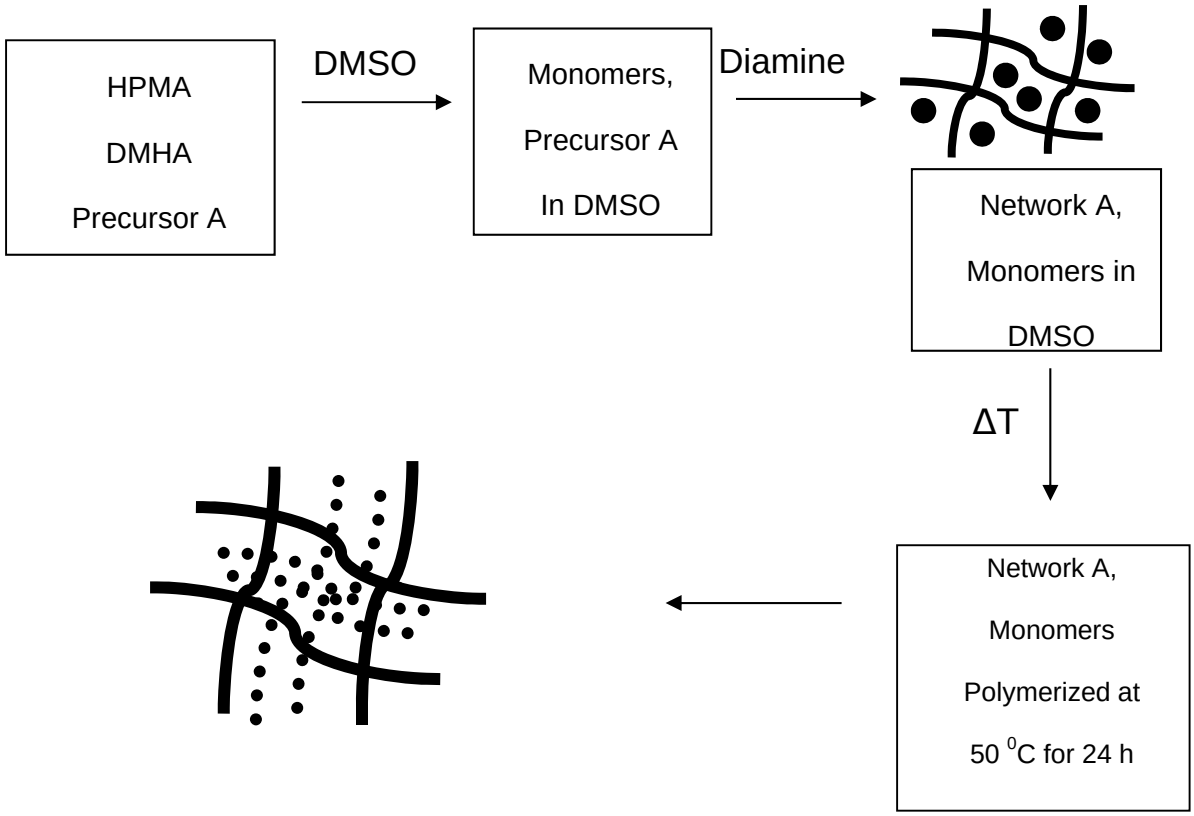

Scheme 2.3. Summarized steps for IPN hydrogel synthesis.

from the mold, cut in disks (d=0.7 cm), and washed using the same method previously described.

2.3.6. Swelling Kinetics

Swelling studies were performed at pH 7.4 (0.1 M phosphate buffer) at 37 ^{0}C. The ionic strength was adjusted with NaCl to 0.16. The swelling of the hydrogels (Network A, Network B, and IPN hydrogel) was measured as a function of time after an abrupt change in pH from 2 to 7.4 (to mimic the change in pH from the stomach to the small intestine). All measurements were done in triplicate. The swelling was expressed as a swelling ratio Q , where Q_t and Q_0 are the corresponding wet and dry weights of the gels, respectively.

$$Q = \frac{Q_t}{Q_0} \quad (1)$$

The dry weights of the hydrogels were measured to determine the amount of the soluble polymer fraction produced by hydrolysis (for the Network B and IPN hydrogels). Following hydrogel synthesis, the gels were washed for 1 week in EtOH and 1 % acetic acid (hydrolyzable bonds stable in this condition) and then subsequently dried to determine amount of soluble polymer fraction present for each time point. The swollen gels were also characterized by their value of ν_2 (volume fraction of the polymer in an equilibrium swollen gel) from the equation:

$$\nu_2 = \frac{\frac{m_1}{d_1}}{\frac{m_1}{d_1} + \frac{m_2}{d_2}} \quad (2)$$

where m_1 and d_1 are weight and density of the dry polymer, respectively (Network A = 1.22 g/cm^3, Network B (16,21) = 1.19 g/cm^3, IPN Network (average) = 1.205 g/cm^3), and m_2 and d_2 are the weight and density (1 g/cm^3) of solvent, respectively.

2.3.7 Characterization of the Mechanical Properties of the Hydrogels

The modulus of elasticity of the hydrogels was determined as a function of the uniaxial compression using a bench comparator (B. C. Ames Co. Waltham, MA) as described previously (22). The swelling and mechanical properties measurements were done in conjunction. Briefly, all gels were immersed in PBS buffer (0.1 M, pH 7.4) at 37 ^{0}C; the mechanical properties were measured by recording the equilibrium height of a given gel after applying a force. After measuring the deformation, the gels were allowed to relax to their original height before applying (increased) force again. The compression ratio λ ($\lambda = l/l_0$ where l and l_0 are compressed and initial heights, respectively) was measured for a known force F (N). For each particular time, 8 values of λ were determined by changing the F. The modulus of elasticity, G_0 (Pa), was calculated using the following equation (23).

$$\frac{F}{A} = -(G_0)(\lambda - \lambda^{-2}) \quad (3)$$

In the above equation, A is the cross-section of the swollen gel.

2.3.8. Structural Characterization of Hydrogel Networks

Network A was prepared by the reaction of reactive p-nitrophenyl ester groups (group X), located at side chain termini of the polymer precursor, with amino groups of the diamine (group Y) (24). Since the conversion of amine groups (Y) into amide bonds ($_{\gamma}$) is known, one can calculate the concentration of elastically active network chains (EANCs). There are several factors which will be assumed for the characterization of the network structure, like all functional groups having the same reactivity which is independent of conversion and also, intramolecular reactions are not considered. In characterizing the network, two cases will be considered: one corresponding to "relatively long" and commensurable (a) and the other one to "relatively short" (b) bridge connecting prepolymer chains (Scheme 2.4). "Relative" means the length (in equivalent units) of the bridge relative to the length of sequence between branch points (ONp monomer units) of the polymer precursor chain.

The crosslinking density was characterized as the concentration of elastically active network chains (EANCs), ν_e. This quantity can be obtained from the experimental modulus of elasticity using the branching theory. The branching theory used here is a statistical theory (Theory of Branching Processes) (25, 26). In the version used here, formation of elastically inactive loops is not considered and the values of ν_e are considered ideal. The basic distribution of building units in different reaction states is given by the probability generating function (pgf)

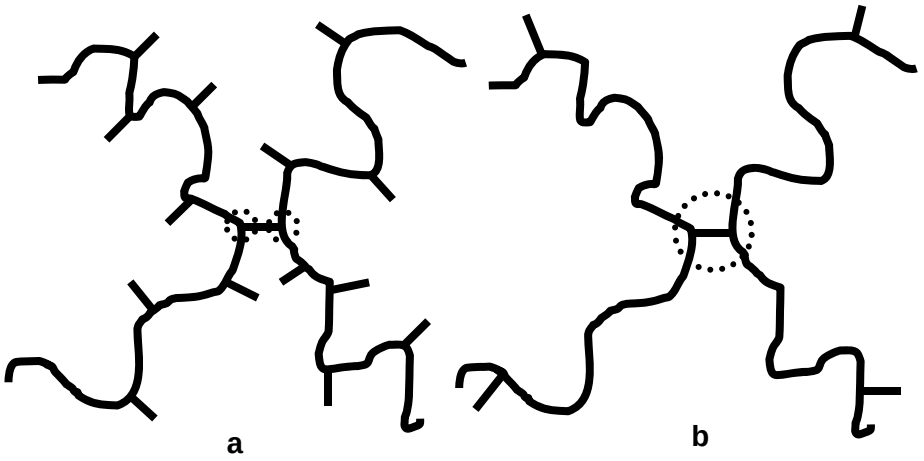

Scheme 2.4. Representation of (a) “relatively long” and (b) “relatively short” fused branch points.

$$F_0(z_X, z_Y) = n_Y(1-\alpha_Y+\alpha_Y z_X)^2 + n_X \frac{(1-q)\vartheta}{(1-q\vartheta)} \quad (4)$$

where α is conversion of NH_2 groups, and q are variables of the pgf [24] and

$$n_Y = 1 - n_X = \frac{2r_X}{2 + P_X x_X r_X}$$
$$r_X = \frac{P_X n_X x_X}{2n_Y}$$
$$\vartheta = 1 - x_X + x_X(1-\alpha_X+\alpha_X z_Y)$$

In these equations,

n_x, n_y are molar fractions of components X and Y, respectively

α_X, α_Y are conversion of groups X and Y

P_x is the number-average degree of polymerization of component X

x_x is the molar fraction of the active (ONp) monomer unit in the copolymer

The number-average molecular weight of a component unit is equal to

$$M_{0n} = n_X P_X M_{0X} + n_Y M_Y \quad (5)$$

M_{0X} and M_Y are molecular weights of polymer precursor and diamine, respectively.

The pgfs for the number of additional bonds issuing from units already connected by one of its reacted groups have the following forms

$$F_Y(z_X) = 1 - \alpha_Y + \alpha_Y z_X$$
$$F_X(z_Y) = \frac{(1-q)^2}{(1-q\vartheta)^2} \quad (6)$$

The extinction probabilities v_X and v_Y are obtained by solution of the equations

$$v_{\mathrm{Y}} = 1 - \alpha_{\mathrm{Y}} + \alpha_{\mathrm{Y}} v_{\mathrm{X}}$$

and

$$v_{\mathrm{X}} = \frac{(1-q)^2}{(1-q\vartheta_{\mathrm{v}})^2}$$

where

$$\vartheta_{\mathrm{v}} = 1 - x_{\mathrm{X}} + x_{\mathrm{X}}(1 - \alpha_{\mathrm{X}} + \alpha_{\mathrm{X}} v_{\mathrm{Y}}) \qquad (7)$$

The elastically active network chains are contributed only by component X because component Y is bifunctional and does not contain any branch point. The pgf $T_{\mathrm{X}}(z)$ expresses the distribution of X units with respect to the number of bonds with infinite continuation

$$T_{\mathrm{X}}(z) = \frac{(1-q)\vartheta_{\mathrm{inf}}(z)}{1-q\vartheta_{\mathrm{inf}}(z)} = \sum_{i=0}^{\infty} t_i z^i$$
$$\vartheta_{\mathrm{inf}}(z) = 1 - x_{\mathrm{X}} + x_{\mathrm{X}}(1 - \alpha_{\mathrm{X}} + \alpha_{\mathrm{X}}[v_{\mathrm{Y}} + (1 - v_{\mathrm{Y}})z]) \qquad (8)$$

The number of EANCs per component unit now depends on our choice (situations a or b) (Scheme 2.5).

In this situation (a), each inner elastically active branch point (having 2 paths to infinity) contributes by 3/2 to the number of EANCs, N_{e},

$$N_{\mathrm{e}} = (3/2) n_{\mathrm{X}} \sum_{i=3}^{\infty} (i-2) t_i \qquad (9)$$

The sum on the right-hand side can be expressed by values of the pgf T and its derivatives

$$N_{\mathrm{e}} = (3/2) n_{\mathrm{X}} (T_{\mathrm{X}}'(1) + 2T_{\mathrm{X}}(0) + T_{\mathrm{X}}'(0) - 2) \qquad (10)$$

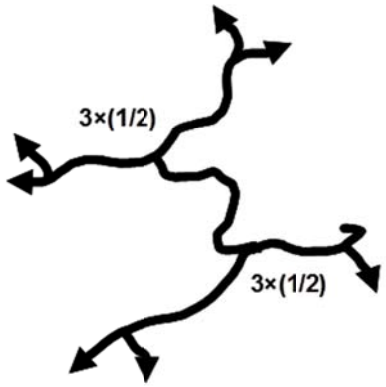

Scheme 2.5. Illustration of elastically active branch point (case (a)).

the concentration of EANCs is given by the equation

$$\nu_{\mathrm{e}} = N_{\mathrm{e}}\rho / M_{0\mathrm{n}} \qquad (11)$$

where ρ is specific gravity of the dry polymer.

For the relatively short bridge, never counted as an EANC, each inner elastically branch point contributes by 2×(1/2) to the number of EANCs. Each of the two outer branch points can contribute by ½ to N_{e}, if and only if they are coupled with an inner elastically active branch point of the adjoining chain (Scheme 2.6).

The number of outer branch points is equal to the sum of $2t_{\mathrm{i}}$ terms and the weighting factor ψ_{inn} is thus equal to

$$(N_{\mathrm{e}})_{\mathrm{cond}} = n_{\mathrm{X}}\left((2/2)\sum_{i=3}^{\infty}(i-2)t_i + (1/2)\psi_{\mathrm{inn}}\sum_{i=2}^{\infty}2t_i\right) = n_{\mathrm{X}}\left(\sum_{i=3}^{\infty}(i-2)t_i + \psi_{\mathrm{inn}}\sum_{i=2}^{\infty}t_i\right) =$$
$$= n_{\mathrm{X}}\left[T_{\mathrm{X}}^{'}(1) + 2T_{\mathrm{X}}(0) + T_{\mathrm{X}}^{'}(0) - 2 + \psi_{\mathrm{inn}}(1 - T_{\mathrm{X}}(0) - T_{\mathrm{X}}^{'}(0))\right] \qquad (12)$$

where

$$\psi_{\mathrm{inn}} = \frac{\sum_{i=3}^{\infty}(i-2)t_i}{\sum_{i=3}^{\infty}(i-2)t_i + \sum_{i=2}^{\infty}2t_i} = \frac{\sum_{i=3}^{\infty}(i-2)t_i}{\sum_{i=2}^{\infty}it_i} = \frac{T_{\mathrm{X}}^{'}(1) + 2T_{\mathrm{X}}(0) + T_{\mathrm{X}}^{'}(0) - 2}{T_{\mathrm{X}}^{'}(1) - T_{\mathrm{X}}^{'}(0)}$$

and the concentration of EANCs is equal to

$$(\nu_{\mathrm{e}})_{\mathrm{cond}} = (N_{\mathrm{e}})_{\mathrm{cond}}\rho / M_{0\mathrm{n}} \qquad (13)$$

In replacing the summations by values of the function $T_{\mathrm{X}}(z)$ and its derivatives, one should recollect that

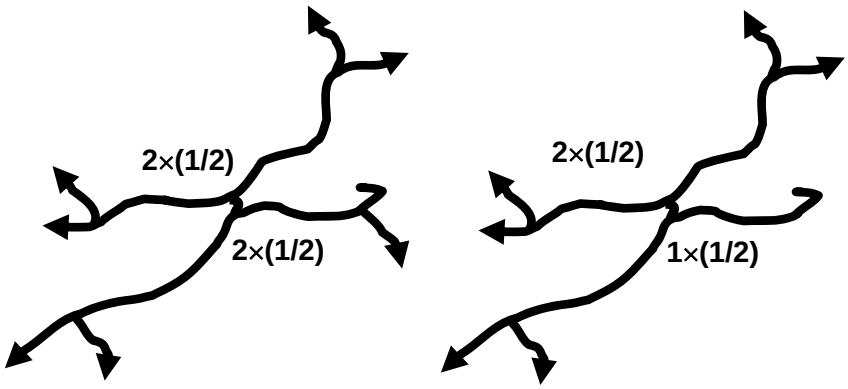

Scheme 2.6. Representation of fused branch points (case (b)). Branches with continuation to infinity are shown with an arrow; the finite branches do not have an arrow.

$$T_X(z=1)=\sum_{i=0}^{\infty} t_i = 1; \quad T_X(z=0)=t_0; \quad T_X'(z=0)=t_1; \quad T_X'(z=1)=\sum_{i=1}^{\infty} i t_i$$

The values of $T_X(z)$ are as follows

$$T_X(0)=\frac{(1-q)\vartheta_v}{1-q\vartheta_v}$$

$$\vartheta_v = 1 - x_X + x_X(1-\alpha_X+\alpha_X \nu_Y)$$

$$T_X'(0)=\frac{(1-q)\vartheta_{inf}'}{(1-q\vartheta_v)^2}$$

$$T_X'(1)=\frac{\vartheta_{inf}'}{(1-q)}$$

$$\vartheta_{inf}' = x_X \alpha_X (1-\nu_Y)$$

2.4. Results and Discussion

2.4.1. Structure and Properties of IPN Hydrogels

The properties of the novel IPN hydrogels were compared with the properties of individual networks. Using a crosslinking reaction of polymeric precursors, the synthesis of azo bond-containing pH-sensitive hydrogels (Network A) was synthesized based on previous work (18, 27). The hydrolyzable network (Network B), which contained polyHPMA as the backbone and DMHA as the crosslinking agent, was synthesized by free radical polymerization (16). The crosslinking agent of this network is stable under acidic conditions but undergoes Lossen rearrangement at neutral or mildly basic pH (17). We combined these two networks to form the IPN structure. Network formation conditions (amounts of crosslinker and wt % of monomers) of the hydrolyzable network were chosen from our preliminary work to ensure high conversion. The conversion of functional groups for the azo-containing network was approximately 85 % as determined

by measuring the soluble fraction after washing. The incomplete conversion of the azo-containing network is due the formation of network defects in the three-dimensional structure due to the presence of elastically inactive cycles (EIC) described previously (24).

2.4.2. Synthesis and Characterization of pH- Sensitive Network A

Hydrogels composed of azo crosslinks and pH- sensitive monomer units were synthesized by crosslinking of polymer precursors (18). Three different hydrogel networks with varying crosslinking density were synthesized (Table 2.3). The weight percent of all precursors and monomers in solution was approximately 15 %. The swelling (Fig. 2.1) and mechanical (Fig. 2.2) properties of these gels were determined. A rapid increase in the degree of swelling was observed upon change of the pH of the solution from an acidic to a basic environment. This rapid increase in swelling is a consequence of the ionization of the COOH groups, resulting mainly from the Donnan effect. Apparently, equilibrium was reached within a few hours of pH change (Fig. 2.1). Concomitantly with the swelling changes, a decrease in the modulus of elasticity occurred (Fig. 2.2), but it remained constant after equilibrium was reached.

The dependence of the concentration of the elastically active network chains (EANCs) was calculated using eqs. (11) and (13) (Fig. 2.3). The conversion of amine groups was measured; hence, the effective crosslink concentration (concentration of EANCs) for the given conversion can be calculated. Table 2.4 shows the composition of networks A and concentration of EANCs calculated from gel composition and conversion of amine groups (calc. ν_e) and experimental conversion, calculated from equilibrium modulus (exptl. ν_e). Since in "calc. ν_e", network defects arising from incomplete

Table 2.3. Composition and properties of Network A

	Precursor no-ave. funct. f_n	mol. fract. ONp x_X	ONp mol/g pol.	ideal ν_e mol/cm^3 (condensed bridges)	ideal ν_e mol/cm^3 (including all bridges)	calc. ν_e mol/cm^3 (condensed bridges)	calc. ν_e mol/cm^3 (including all bridges)
A1	6.5	0.014	1.63×10^{-4}	1.96×10^{-4}	2.94×10^{-4}	1.50×10^{-4}	1.93×10^{-4}
A2	9.4	0.021	2.35×10^{-4}	2.83×10^{-4}	4.25×10^{-4}	2.35×10^{-4}	3.20×10^{-4}
A3	16.8	0.037	4.20×10^{-4}	5.04×10^{-4}	7.56×10^{-4}	4.25×10^{-4}	5.80×10^{-4}

Table 2.3, continued

	conversion α_Y	exptl ν_e mol/cm^3	intermolec. conversion calcd. from exptl ν_e α_{inter}		intramolec. conversion α_{intra}		% bonds lost in elastically inactive cycles		equil. swelling in water φ_2
			cond.	all	cond	all	cond	all	
A1	0.975	1.45×10^{-4}	0.965	0.89	0.010	0.085	1.0	8.7	0.45
A2	0.982	1.49×10^{-4}	0.790	0.738	0.192	0.244	19.5	24.8	0.51
A3	0.979	2.40×10^{-4}	0.755	0.665	0.224	0.344	22.9	35.1	0.54

x_X is the molar fraction of branching units in the copolymer. Ideal ν_e was calculated for an ideal system without any network defect; calculated ν_e was obtained by application of branching theory for the experimental conversion of the amine groups, α_Y taking into account molecular weight of primary chains and functionality distribution; experimental conversion was calculated from the equilibrium modulus in compression. The values of intermolecular conversions were calculated from the equilibrium modulus using front factor A = 1 ("experimental ν_e"); the intramolecular conversion is equal to the difference between "calculated conversion" and that obtained from "experimental ν_e

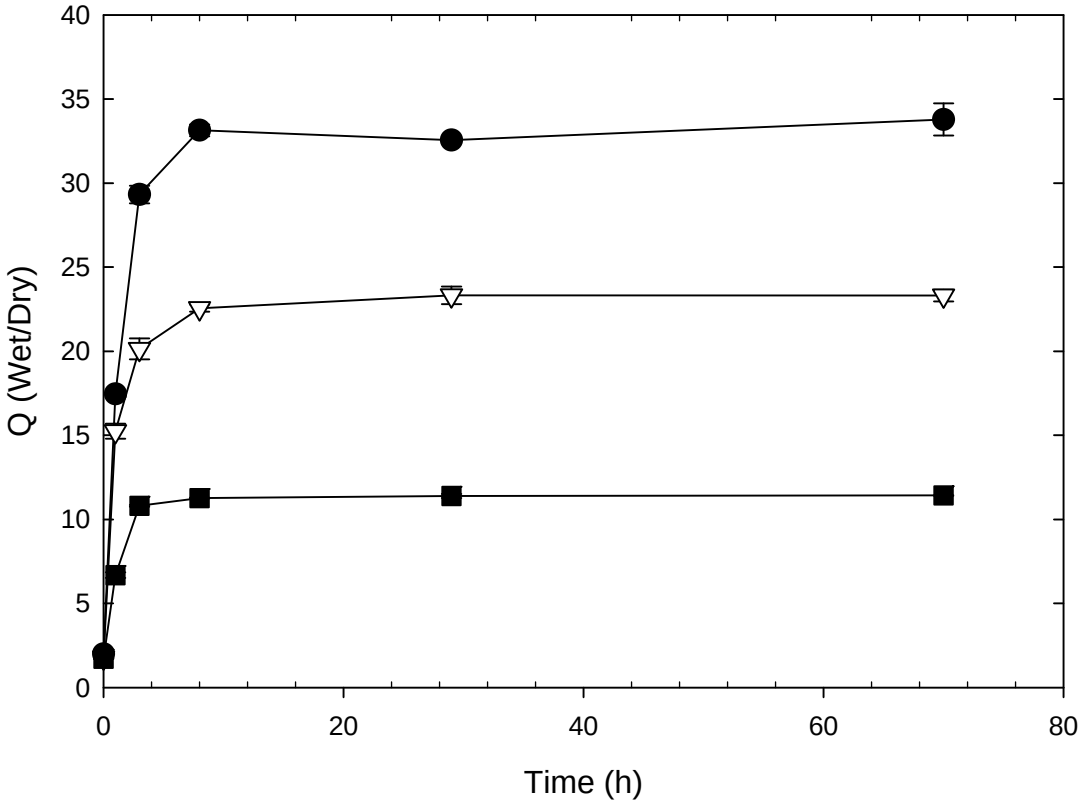

Figure 2.1. Swelling ratio Q (Q_t/Q_0) of aromatic azo bond-containing hydrogels (Network A) as a function of time after an abrupt change in pH (2.0 to 7.4). A1 (-●-); A2 (-∇-); A3 (-■-). Hydrogels equilibrated in an acidic solution (pH 2, 0.01 N HCl) were transferred to a vial containing 20 ml of PBS buffer solution (0.1 M, pH 7.4). At selected time intervals, the hydrogels were retrieved and weighed to determine the wet weight. Then, the hydrogels were washed with EtOH containing 1 % acetic acid for one week, dried in vacuo, and their dry weights were determined. For composition of hydrogels, see Table 2.2.

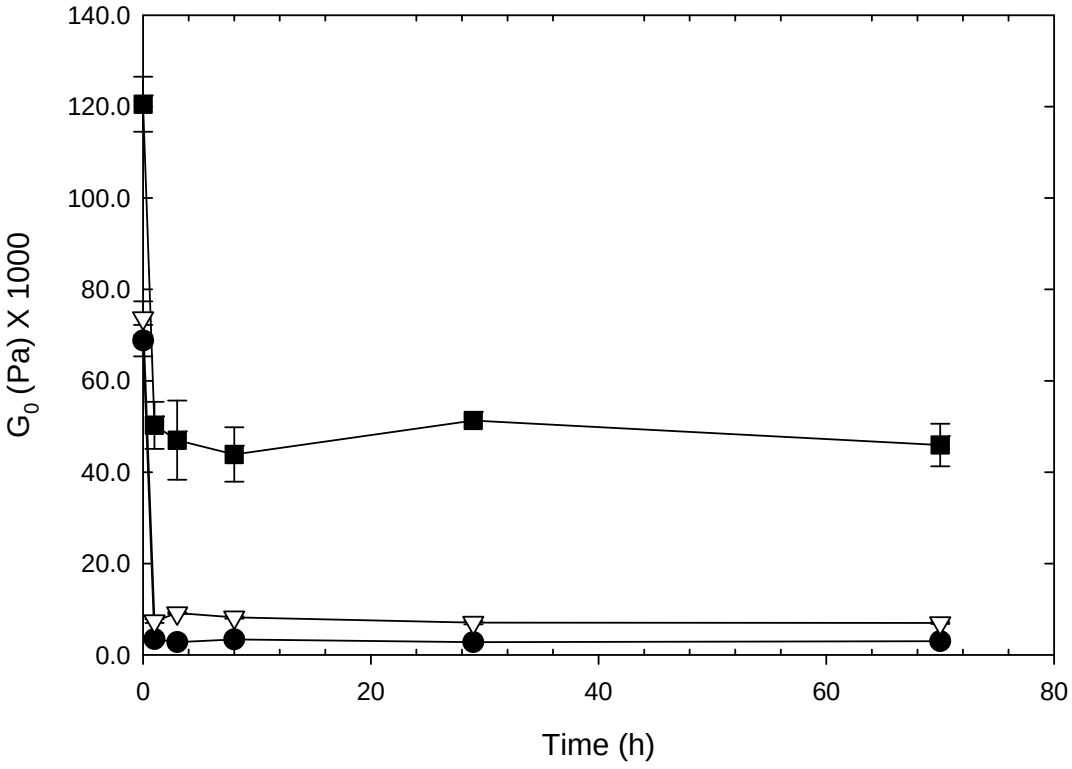

Figure 2.2. The modulus of elasticity in compression (G) of aromatic azo bond-containing hydrogels (Network A) as a function of time after an abrupt change in pH (2.0 to 7.4). A1 (-●-); A2 (-∇-); A3 (-■-). For composition of hydrogels, see Table 2.2.

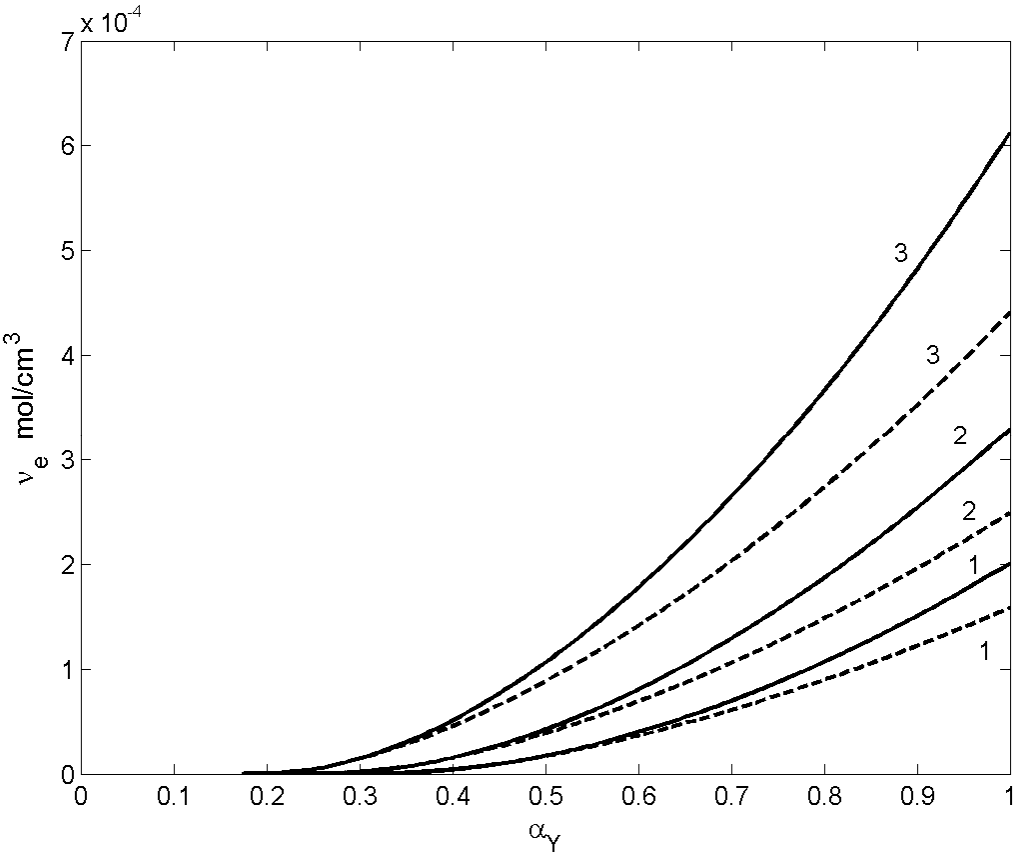

Figure 2.3. Dependence of the concentration of EANCs on conversion of amine groups (α_Y) for aromatic azo bond-containing hydrogels A1 (1), A2 (2), A3 (3) for long bridges (full lines) and condensed bridges (dashed lines) calculated from eqs. (11) and (13).

conversion and finite length of primary chains are taken into account, the differences in Number-average degree of polymerization of primary chains P_X =450, volume fraction of polymer during network formation ϕ_0 = 0.125 between "calc. ν_e", and "exptl. ν_e" are attributed to formation of elastically inactive cycles. Subsequent to the inspecting of Fig. 2.3 and Table 2.3, one could conclude that there is no apparent answer to the question of which theoretical model is better considering all branch points or fused branch points (relatively short bridge). The difference in concentration of EANCs amounts approximately to 30%. Since the "fused branch points" model offers for the weakest gel A1 practically no elastically inactive cycles, we think that the "all branch points" model is closer to reality. Generally, the results seem reasonable; the crosslinking efficiency varies between 90 and 65% or 99 - 76% ("fused branch points" model) which is for the step addition type of reaction but relatively high dilution a reasonable range. Also, the crosslinking efficiency decreasing with increase of crosslink density is to be expected.

2.4.3. Synthesis and Characterization of Hydrolyzable Network B

Three hydrolyzable networks with varying crosslinking density were synthesized (Table 2.4) by free radical crosslinking copolymerization. As expected, the wt% of monomers (dilution) during network formation played a critical role in the final conversion (28). A monomeric concentration of 30 wt% was needed to achieve close to complete conversion (as determined by measurement of the dry weight). Apparently, at lower monomer conversions, a large amount of the crosslinking agent incorporated into the network via one double bond only, or incorporated as elastically ineffective cycles (28). The swelling data (Fig. 2.4) shows that the crosslinking density influences the

Table 2.4. Composition of hydrolyzable hydrogels (Network B)

	HPMA (mol)	Mol %	DMHA (mol)	Mol %	Total Mol
H1	$2.095X10^{-3}$	97	$6.69X10^{-5}$	3	$2.23X10^{-3}$
H2	$2.095X10^{-3}$	96	$9.01X10^{-5}$	4	$2.25X10^{-3}$
H3	$2.095X10^{-3}$	95	$1.14X10^{-5}$	5	$2.28X10^{-3}$

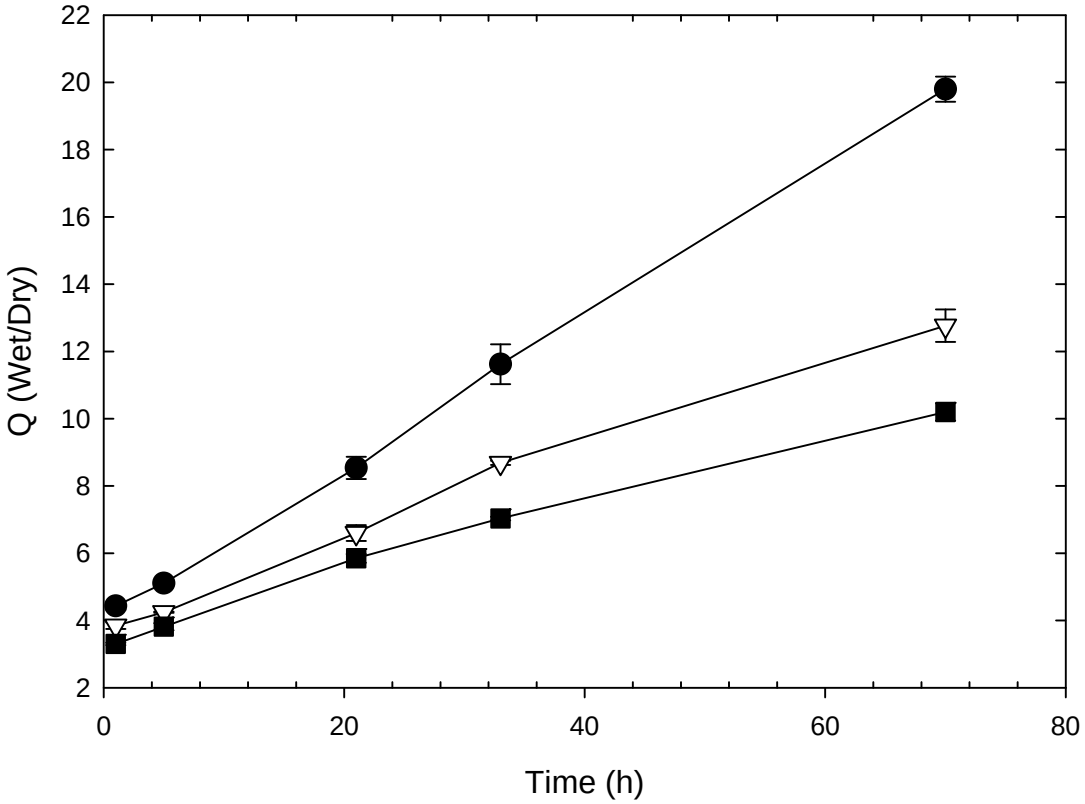

Figure 2.4. Changes of swelling ratio Q (Q_t/Q_0) of hydrolyzable hydrogels (Network B) as a function of time after an abrupt change in pH (2.0 to 7.4). H1 (-●-); H2 (-∇-); H3 (-■-). Hydrogels were pre-incubated in an acidic solution (pH 2, 0.01 N HCl), then transferred to a vial containing 20 ml of PBS buffer solution (0.1 M, pH 7.4). The hydrogels were retrieved at selected time intervals, weighed, washed with EtOH containing 1 % acetic acid for one week, dried in vacuo, and their dry weights measured. For composition of hydrogels, see Table 2.4.

degradation rate of the hydrogels as expected. The higher the crosslinking density, the slower the degradation rate and the lower the degree of swelling of the hydrogels (Fig. 2.4). It is important to note that as a result of the degradation process and corresponding swelling changes, the hydrogels were not at an equilibrium state at the time points evaluated. The decrease of the crosslinking density of the hydrogels with time resulted in a decrease of their moduli of elasticity (Fig. 2.5).

The divinyl monomer (DMHA) contains a hydrolyzable bond in its structure. Network B gels are less characterized than Network A gels in that the fraction of pendant double bonds is not known. Therefore, a comparison will be made between the ideal concentration of EANCs (all double bonds have reacted and all branch points contribute to the number of EANCs) and the "experimental" value of concentration of EANCs calculated from the equilibrium modulus. The crosslinking efficiency is given by the ratio of "experimental" to ideal concentration of EANCs. The results are summarized in Table 2.5.

It is clearly seen that the crosslinking efficiency is much lower than for the Network A despite the lower dilution of the polymerizing system B characterized by volume fraction of polymer during network formation ϕ_0. The difference in network formation mechanism is the main reason for this difference. It is well known (29, 30) that cyclization is very strong during the network formation mechanism with fast propagation and increases with increasing fraction of the polyunsaturated monomer.

2.4.4 Degradation of Hydrolyzable Network B

Network A does not contain hydrolyzable bonds, but the hydrogels are pH sensitive. Upon neutralization, the degree of swelling increases, but it does not change

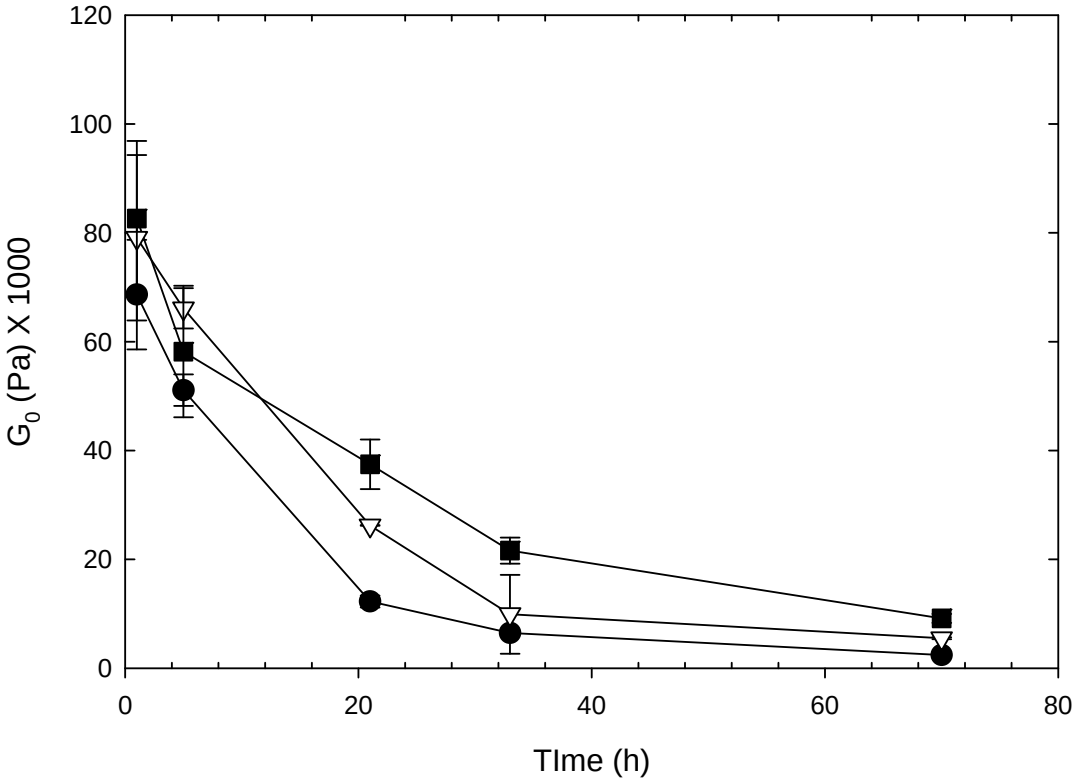

Figure 2.5. The modulus of elasticity (G) in compression of hydrolyzable hydrogels (Network B) as a function of the time of the network after an abrupt change in pH (2.0 to 7.4). H1 (-●-); H2 (-∇-); H3 (-■-). For composition of hydrogels, see Table 2.4.

Table 2.5. Composition and properties of Network type B

	vol. fract. polymer φ_2	crosslinker mol/g	ideal ν_e mol/cm^3 (condensed bridges)	ideal ν_e mol/cm^3 all branch points	G_{sw} kPa	exptl ν_e mol/cm^3	% cross-linker wasted all branch points
H1	0.190	2.08×10^{-4}	1.96×10^{-4}	2.94×10^{-4}	68.6	1.19×10^{-4}	60
H2	0.220	2.78×10^{-4}	2.83×10^{-4}	4.25×10^{-4}	79.1	1.28×10^{-4}	70
H3	0.260	3.47×10^{-4}	5.04×10^{-4}	7.56×10^{-4}	82.6	1.28×10^{-4}	83

Number-average degree of polymerization of primary chains P_X =420, volume fraction of polymer during network formation ϕ_0 = 0.27

Table 2.6. Increase of the equilibrium degree of swelling and decrease of equilibrium modulus of hydrolyzable gels upon cleavage of the hydrolyzable bond

	ϕ_2			G_{sw} kPa			experimental ν_e mol/cm^3		
Time (h)	H1	H2	H3	H1	H2	H3	H1	H2	H3
1.0	0.197	0.228	0.260	68.6	79.1	82.6	11.4×10^{-5}	12.5×10^{-5}	12.5×10^{-5}
5.0	0.170	0.206	0.230	51.1	66.1	58.2	8.98×10^{-5}	10.8×10^{-5}	9.17×10^{-5}
21.0	0.101	0.131	0.148	12.3	26.2	37.5	5.43×10^{-5}	4.98×10^{-5}	6.85×10^{-5}
33.0	0.073	0.099	0.122	6.47	9.91	21.6	1.50×10^{-5}	2.07×10^{-5}	4.20×10^{-5}
70.0	0.043	0.067	0.084	2.41	5.51	9.13	0.66×10^{-5}	1.31×10^{-5}	2.01×10^{-5}

with time. Also, the equilibrium modulus exhibits only random fluctuations. On the contrary, hydrolyzable Network B undergoes degradation and the concentration of EANCs decreases with increasing time of hydrolysis. The degree of swelling increases as a result of decrease of its crosslink density as well as appearance of hydrophilic groups. Thus, this degree of swelling increases and the modulus decreases (Table 2.6).

2.4.5. Characterization of IPN Hydrogels (Networks A+B)

The degradability of hydrogels depends strongly on the equilibrium degree of swelling (15). Hydrogels previously designed for colon-specific delivery possess a high degree of swelling at neutral pH due to the presence of ionizable monomer units in their structure (7,8,14,18,27). To control the rate of swelling of such hydrogels and achieve a more gradual swelling profile, we introduced a second hydrolyzable network. To this end, we synthesized four different IPN hydrogels, combining Network A and Network B. The first two gels (IPN1 and IPN2) were synthesized by manipulating the composition of Network B, whereas in hydrogels IPN3 and IPN4, the composition of Network A was changed (Table 2.7). The IPN hydrogels were characterized by determination of the time dependence of swelling, mechanical properties measurements, and the content of the soluble fraction (data not shown). A close to linear increase of the degree of swelling with time was observed for IPN structures after abrupt change of pH from 2 to 7.4, in contrast to the corresponding Network A (compare Figs. 2.1 and 2.6). Controlled time-dependent swelling can be achieved with these gels and the burst effect can be significantly reduced. The increase in the degree of swelling is not accompanied by a corresponding decrease of modulus (compare Figs. 2.6 and 2.7). The IPN networks are

Table 2.7. Composition of IPN hydrogels (Network A and B)

Name	Polymeric Precursor (mg)	Moles of ONp	Diamine (mol)	HPMA (mol %)	DMHA (mol %)	HPMA (mg)	DMHA (mg)
IPN1 (A2 + H1)	150	$3.72X10^{-5}$	$1.86X10^{-5}$	97	3	300	11.3
IPN2 (A2 + H3)	150	$3.72X10^{-5}$	$1.86X10^{-5}$	95	5	300	19.3
IPN3 (A1 + H1)	150	$2.53X10^{-5}$	$1.27X10^{-5}$	97	3	300	11.3
IPN4 (A3 + H1)	150	$6.93X10^{-5}$	$3.47X10^{-5}$	97	3	300	11.3

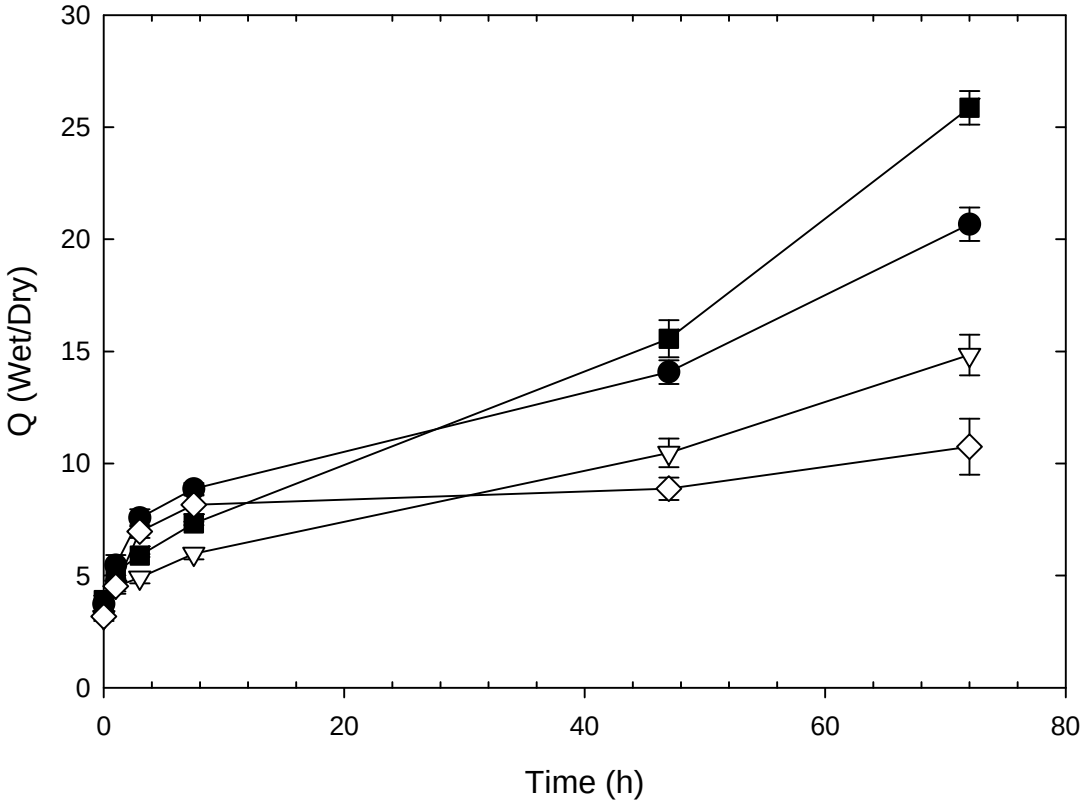

Fig. 2.6. Changes of swelling ratio Q (Q_t/Q_0) of IPN hydrogels as a function of time after an abrupt change in pH (2.0 to 7.4). IPN1 (-●-); IPN2 (-∇-); IPN3 (-■-), IPN4 (-◊-). The hydrogels were pre-incubated in an acidic solution (pH 2, 0.01 N HCl) and transferred to a vial containing 20 ml of PBS buffer solution (0.1 M, pH 7.4). The hydrogels were retrieved at selected time intervals, weighed, washed with EtOH containing 1 % acetic acid for one week, dried in vacuo, and their dry weights were measured. For composition of hydrogels, see Table 2.4.

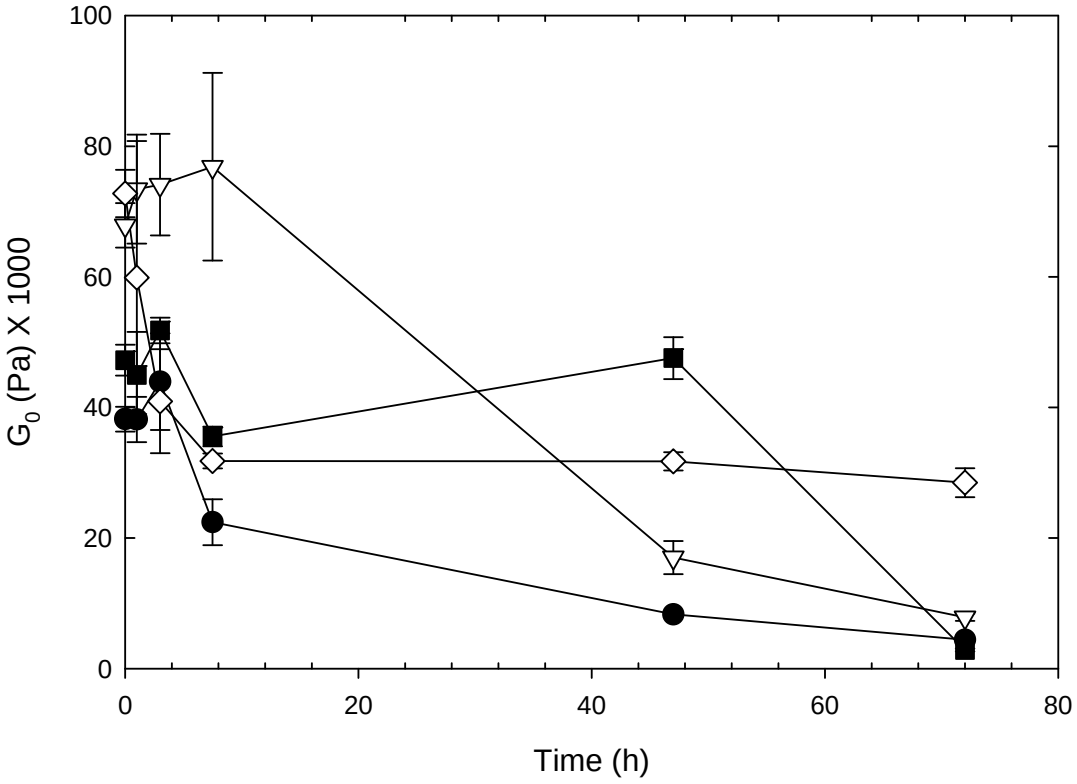

Figure 2.7. The modulus of elasticity (G) in compression of IPN hydrogels as a function of time after an abrupt change in pH (2.0 to 7.4). IPN1 (-●-); IPN2 (-∇-); IPN3 (-■-), IPN4 (-◊-). For composition of hydrogels, see Table 2.4.

homogeneous, showing no evidence of phase separation and network formation of Network A and Network B occurs at the same volume. This means that for both networks, the volume fraction at network formation effective in rubber elasticity is the same (the EANCs dimensions shrink by the same factor when solvent is removed). This is, however, not so when effect of dilution on network formation (cyclization) is considered. Then, the solvent as well as the other polymer are operative as diluents (ϕ_0^{NF}). As in the case of Network B, the experimental concentration of EANC's relative to ideal crosslinking density will be taken as measure of crosslinking efficiency, or wastage of crosslinking sites. The results are shown in Table 2.8.

The crosslinking efficiency for the IPNs is remarkably low. Higher dilution manifested by lower values of ϕ_0^{NF} compared to ϕ_0 for individual networks (Tables 2.5 and 2.6) and thus higher cyclization may be the main reason. However, it is not excluded that the residues of active groups of components of Network A (amine, ONp) affect the free radical polymerization by promoting chain transfer and thus a lower degree of polymerization of primary chains.

2.5. Conclusions

Novel IPN hydrogels were synthesized by a sequential process. They are composed of a pH-sensitive, aromatic azo group- containing network as one component (Network A), and a hydrolyzable network as the other component (Network B).

Network A was produced by crosslinking of a copolymer of *N*,*N*-dimethylacrylamide, acrylic acid, N-tert.butylacrylamide, and *N*-methacryloyl-

Table 2.8 Composition and properties of IPN networks

	ϕ_0^{NF}	ϕ_0^{NF}	ideal $(\nu_e)_A$ mol/cm^3 all branch p.	ideal $(\nu_e)_B$ mol/cm^3 all branch p.	ideal $(\nu_e)_{IPN}$ mol/cm^3 all branch p.
IPN1	0.132	0.259	4.24×10^{-4}	5.16×10^{-4}	4.85×10^{-4}
IPN2	0.132	0.266	4.24×10^{-4}	8.80×10^{-4}	7.14×10^{-4}
IPN3	0.128	0.259	2.94×10^{-4}	5.16×10^{-4}	4.43×10^{-4}
IPN4	0.138	0.259	6.30×10^{-4}	5.16×10^{-4}	5.99×10^{-4}

Table 2.8, continued

	ϕ_2	$(\phi_0)^{EL}$	G_e kPa	exptl.(ν_e) mol/cm^3	% groups wasted
IPN1	0.229	0.391	38.2	0.471×10^{-4}	90
IPN2	0.266	0.398	67.9	0.788×10^{-4}	89
IPN3	0.222	0.388	47.2	0.591×10^{-4}	87
IPN4	0.275	0.398	72.8	0.835×10^{-4}	86

ϕ_0^{EL} is volume fraction of polymer at network formation operative in rubber elasticity theories, $(\phi_0^{NF})_A$ and $(\phi_0^{NF})_B$ are volume fractions of polymer of component A and B, respectively, at network formation operative in network formation (the solvent and the other component are effective as diluents); ideal $(\nu_e)_A$ and ideal $(\nu_e)_B$ are contributions by gel A and B, respectively, to the ideal concentration of EANCs of the IPN and $(\nu_e)_{IPN}$ is the ideal concentration of EANCs.

glycylglycine p-nitrophenyl ester (polymer precursor) with an aromatic azo group-containing diamine ((*N*,*N*'-ε-aminocaproyl)-4,4'-diaminoazobenzene). Network B was formed by radical crosslinking copolymerization of *N*-(2-hydroxypropyl)methacrylamide with *N*,*O*-dimethacryloylhydroxylamine.

The crosslinking efficiency of radically polymerized Network B is much worse than that of step polyaddition Network A. For Network B, the efficiency goes down to 10-30%. The network formation mechanism assisted by dilution during polymerization is the main reason.

In the IPN gels, the crosslinking efficiency is even lower and approaches 10%. In addition to higher dilution, possible negative effect of other components on the free-radical polymerization is likely. Chain splitting and formation of ionizable groups during hydrolysis of the gel B is well documented by combined swelling and modulus measurements.

For IPN gels, it seems that formation of hydrophilic ionized groups is not accompanied by any major splitting of Network A chains. The dependence of swelling on pH and time indicate that the novel IPNs possess the ability to control the burst effect and have a potential to protect proteins from enzymatic degradation. It appears that they are suitable carriers for oral protein/peptide delivery.

2.6 Acknowledgements

The research was supported in part by NIH grant EB00251 (JK). We greatly appreciate the contribution made by Professor K. Dusek for this thesis chapter. The model describing the hydrogel networks was developed by Dr. Dusek. The synthesis and characterization of the network was carried out by Padmanabh Chivukula.

2.7 References

(1) Sakuma S, Hayashi M, and Akashi M. (2001) Design of nanoparticles composed of graft copolymers for oral peptide delivery. *Adv Drug Deliv Rev 47*, 21-37.

(2) Lee VHL, and Yamamoto A. (1990) Penetration and enzymatic barriers to peptide and protein absorption. *Adv Drug Deliv Rev 4*, 171-207.

(3) Ikesue K, Kopečková P, and Kopeček J. (1993) Degradation of proteins by guinea pig intestinal enzymes. *Int J Pharm 95*, 171-179.

(4) Lamprecht, A, Schafer U, and Lehr CM. (2001) Size-dependent bioadhesion of micro- and nanoparticulate carriers to the inflamed colonic mucosa. *Pharm Res 18*, 788-793.

(5) Muraoka M, Hu Z, Shimokawa T, Sekino S, Kurogoshi R, Kuboi Y, Yoshikawa Y, and Takada K. (1998) Evaluation of intestinal pressure-controlled colon delivery capsule containing caffeine as a model drug in human volunteers. *J Control Release 52*, 119-129.

(6) Rasmussen SN, Bondesen S, Hvidberg EF, Hansen SH, Binder V, Halskov S, and Flachs H. (1982) 5-aminosalicylic acid in a slow-release preparation: bioavailability, plasma level, and excretion in humans. *Gastroenterology 83*,1062-1070.

(7) Yeh PY, Berenson MM, Samowitz WS, Kopečková P, and Kopeček J. (1995) Site-specific drug delivery and penetration enhancement in the gastrointestinal tract. *J Control Release 36*,109-124.

(8) Brøndsted H, and Kopeček J. , (1992) pH Sensitive Hydrogels: Characteristics and Potential in Drug Delivery. In *Polyelectrolyte gels*, (Harland RS, and Prud'homme RK, Eds.) Washington, D.C.: American Chemical Society, 285-304.

(9) Akala EO, Kopečková P, and Kopeček J. (1998) Novel pH-sensitive hydrogels with adjustable swelling kinetics. *Biomaterials 19*,1037-1047.

(10) Klempner D, Sperling LH, and Utracki LA. (1991) *Interpenetrating Polymer Networks*, New York: American Chemical Society.

(11) Diez-Pena E, Quijada-Garido I, Frutos P, and Barrales-Rienda JM. (2002) Thermal properties of cross-linked poly(N-isopropylacrylamide) [P(N-iPAAm)], poly(methacrylic acid) [P(MAA)], their random copolymers [P(N-iPAAm-co-MAA)], and sequential interpenetrating polymer networks (IPNs). *Macromolecules 35*, 2667-2675.

(12) Zhang J, and Peppas NA. (2002) Morphology of poly(methacrylic acid)/poly(N-isopropyl acrylamide) interpenetrating polymeric networks. *J Biomater Sci Polym Ed 13*, 511-525.

(13) Ilavský M, Mamytbekov G, Hanyková L, and Dušek K. (2002) Phase transition in swollen gels 31. Swelling and mechanical behaviour of interpenetrating networks composed of poly(1-vinyl-2-pyrrolidone) and polyacrylamide in water/acetone mixtures. *Eur Polym J 38*,875-883.

(14) Yeh PY, Kopečková P, and Kopeček J. (1995) Degradability of hydrogels containing azoaromatic crosslinks. *Macromol Chem Phys 196*, 2183-2202.

(15) Ulbrich K, Strohalm J, and Kopeček J. (1982) Polymers containing enzymatically degradable bonds. VI. Hydrophilic gels cleavable by chymotrypsin. *Biomaterials 3*, 150-154.

(16) Ulbrich K, Šubr V, Seymour LW, and Duncan R. (1993) Novel biodegradable hydrogels prepared using the divinylic crosslinking agent N,O-dimethacryloylhydroxylamine. 1. Synthesis and characterization of rates of gel degradation, and rate of release of model drugs, in vitro and in vivo. *J Controlled Release 24*,181-190.

(17) Bauer L, and Exner O. (1974) Chemistry of hydroxamic acids and N-hydroxyimides. *Angew Chem Internatl Edit 13*, 374-384.

(18) Yeh PY, Kopečková P, and Kopeček J. (1994) Biodegradable and pH sensitive hydrogels: Synthesis by crosslinking of N,N-dimethylacrylamide copolymer precursors. *J Polym Sci Part A Polym Chem 32*,1627-1637.

(19) Kopeček J, and Bažilová H. (1973) Poly[N-(2-hydroxypropyl)methacrylamide]. 1. Radical polymerization and copolymerization. *Eur Polym J 9*, 7-14.

(20) Rejmanová P, Labský J, and Kopeček J. (1977) Aminolyses of monomeric and polymeric 4-nitrophenyl esters of methacryloylated amino acids. *Makromol Chem 178*, 2159-2168.

(21) Kopeček J, and Bažilová H. (1974) Poly[N-(2-hydroxypropyl)methacrylamide]. III. Crosslinking copolymerization. *Eur Polym J 10*, 465-470.

(22) Cluff EF, Gladding EK, and Pariser R. (1960) A new method for measuring the degree of crosslinking in elastomers. *J Polym Sci 45*, 341-345.

(23) Ulbrich K, Ilavský M, Dušek K, and Kopeček J. (1977) Preparation and properties of poly(N-ethylmethacrylamide) networks. *Eur Polym J 13*, 579-85.

(24) Wang D, Dušek K, Kopečková P, Dušková-Smrčková M, and Kopeček J. (2002) Novel aromatic azo-containing pH-sensitive hydrogels: Synthesis and characterization. *Macromolecules 35*, 7791-7803.

(25) Dušek K. (1978) Network formation in curing epoxy resins. *Adv Polym Sci 78*, 1-59.

(26) Dušek K, and Dušková-Smrčková M. (2000) Network structure formation during crosslinking of organic coating systems. *Progr Polym Sci 25*, 1215-1260.

(27) Ghandehari H, Kopečková P, Yeh PY, and Kopeček J. (1996) Biodegradable and pH sensitive hydrogels: Synthesis by a polymer - polymer reaction. *Macromol Chem Phys 197*, 965-980.

(28) Kopeček J, Jokl J, and Lim D. (1968) Mechanism of three-dimensional polymerization of glycol methacrylates (in German). *J Polym Sci C16*,3877-3889.

(29) Dušek K. (1982) Network formation by chain crosslinking (co)polymerization. Haward RN, editor. *Development in polymerization.*3. Barking: Applied Science Publishers. p. 143-206.

(30) Dušek K. (1998) Network formation involving polyfunctional polymer chains. Stepto RFT, editor. *Polymer networks. Principles of their formation, structure and properties.* London: Thompson Science, p. 64-92.

CHAPTER 3

SYNTHESIS AND CHARACTERIZATION OF *N*-(2-HYDROXYPROPYL) METHACRYLAMIDE COPOLYMER- CYCLIC NONAPEPTIDE CONJUGATES

3.1 Abstract

Three derivatives of the cyclic constrained nonapeptide (KPIEDRPME ; RPM), namely YWKPIEDRPME (RPM1), N-methacryloylglycylglycine-6-aminohexanoyl-8-amino-3,6-dioxaoctanoyl-8-amino-3,6-dioxaoctanoyl-8-amino-3,6-dioxaoctanoyl-YWKPIEDRPME (RPM2), and K(fluorescein)-KPIEDRPME (RPM3), were synthesized. RPM1 and RPM2 were incorporated into the water-soluble N-(2-hydroxypropyl)methacrylamide (HPMA) copolymer. HPMA copolymer-RPM1 conjugate was prepared by binding of RPM1 to an HPMA copolymer precursor via glycylglycine side-chains. The macromonomer RPM2 was copolymerized with HPMA and N-methacryloylaminopropyl fluorescein thiourea (MA-FITC) to produce an HPMA copolymer-RPM2 conjugate. Two narrow fractions of HPMA copolymer conjugates were obtained by preparative size-exclusion chromatography. The high molecular weight fractions, P(H)-RPM1-FITC and P(H)-RPM2-FITC, had a molecular weight of 100 kDa and 228 kDa, respectively; the low molecular weight fractions, P(L)-RPM1-FITC and P(L)-RPM2-FITC, were 30 kDa, and 41 kDa, respectively. The impact of the structure of

the HPMA copolymer-peptide conjugates on the biorecognition by poorly differentiated HT-29 colon carcinoma cells was investigated. The binding to and internalization by HT-29 cells were visualized by a radioiodination assay, flow cytometry, and confocal fluorescence microscopy. The free peptide RPM3 and HPMA copolymer-RPM1 and HPMA copolymer-RPM2 conjugates possessed low binding affinities; the K_d was in the 10^{-4} M range. However, flow cytometry data demonstrated clear shifts in fluorescence profiles when comparing control polymers, P(H)-FITC and P(L)-FITC, with corresponding HPMA copolymer conjugates containing peptides RPM1 or RPM2. A similar shift could be observed when comparing RPM3 with a nonspecific peptide (NSP, K(fluorescein)-KKHLGPQLE). Confocal fluorescence data clearly indicated a faster internalization of RPM3 when compared to a nonspecific sequence (NSP).

3.2 Introduction

Colon cancer still remains a common malignancy and this accounts for the second leading cause of cancer-related death in the United States (*1*). Recent advances in genomics and proteomics provided great insight into the key genetic alterations which occur in colorectal cancer (*2, 3*). Novel therapeutics can be developed to exploit cell surface markers over-expressed at these sites. To this end, we extensively study the use of water soluble *N*-(2-hydroxypropyl)methacrylamide (HPMA) copolymer as a targetable drug carrier (*4-10*). It has been shown that HPMA copolymers accumulate passively in solid tumors as a result of enhanced permeation and retention (EPR) effect (*11*), which leads to an altered biodistribution of polymer-bound drugs or diagnostics as compared to the free constituent. To further improve their therapeutic efficacy by enhanced cellular recognition, polymeric drug carriers can be conjugated to various cell-specific ligands,

such as peptides (*4, 5, 8, 12-14*), antibodies (*15, 16*), antibody fragments (*17, 18*), carbohydrates (*19*), and lectins (*20*). The ensuing change in their internalization mechanism from endocytosis to receptor-mediated endocytosis results in enhanced uptake of targeted conjugates.

Combinatorial peptide library techniques accelerated the identification of targeting peptides (*21-24*) and stimulated their use due to their ease of synthesis, low immunogenicity, and desirable pharmacokinetic properties. Recently, there has been considerable effort to develop peptides or proteins that can target colon cancers (*25-28*). Kelly et al. (*29*) used bacteriophage-derived libraries to select peptides binding to colon cancer cells. They used a subtraction method to distinguish between well-differentiated HCT116 and poorly differentiated HT29 colon carcinoma cells. Utilizing this method yielded peptides that displayed a consensus RPM motif, which mediated preferential binding to HT29 cells. A particular nonapeptide, CPIEDRPMC, was derived from a disulfide constrained CX_7C library and shown to bind specifically to poorly differentiated colon carcinoma cells (HT-29) (*29*).

Restraining the peptide backbone into a more defined conformation through cyclization is activity perused in synthetic peptide design (*30*). Conformational constrains may increase the probability of optimal peptide-receptor recognition, thereby increasing its binding affinities (*31*). However, disulfides can be reduced physiologically; hence, our strategy was to cyclize the peptide via an amide linkage (*32-34*). Specifically, a peptide (RPM) was designed that is cyclized via a side chain of lysine to a side chain of glutamic acid (KPIEDRPME) (*35, 36*). By introducing an amide

linkage, the targeting moiety, free or attached to a macromolecular conjugate, should be more stable *in vivo* than the disulfide analogue.

Peptides intrinsically suffer from low binding affinity partly due to disordered solution conformation (*24*); hence, to further enhance peptide targeting, multivalent interactions can be introduced by the use of biocompatible polymer carriers (*37-40*). Various bioactive peptides can be attached to the HPMA backbone to form HPMA copolymer-peptide conjugates, thereby containing multiple copies of peptides within a single polymer chain (*12, 41-43*).

Here, three RPM YWKPIEDRPME derivatives, (RPM1), *N*-methacryloylglycylglycine-8-amino-3,6-dioxaoctanoyl-8-amino-3,6-dioxaoctanoyl-8-amino-3,6-dioxaoctanoyl-YWKPIEDRPME (RPM2), and K(fluorescein)-KPIEDRPME (RPM3), containing the cyclic constrained nonapeptide (KPIEDRPME) were synthesized. HPMA copolymer-RPM1 conjugate was prepared by binding of RPM1 to an HPMA copolymer precursor via glycylglycine side chains. The macromonomer RPM2 was copolymerized with HPMA and *N*-methacryloylaminopropyl fluorescein thiourea (MA-FITC) to produce an HPMA copolymer-RPM2 conjugate. The effect of molecular weight and structure of HPMA copolymer conjugates on the biorecognition by poorly differentiated HT-29 colon carcinoma cells was investigated by determination of binding affinity, flow cytometry, and confocal fluorescence microscopy.

3.3 Materials and Methods

3.3.1 Materials

HPMA (*44*), *N*-methacryloylaminopropyl fluorescein thiourea (MA-FITC) (*45*), and *N*-methacroylglycylglycine thiazolidine-2-thione (MA-GG-TT) (*46*) were

synthesized as described previously. Solvents and reagents were of analytical grade and were used without further purification. They were purchased from Aldrich (Milwaukee, WI) or Sigma (St. Louis, MO) if not specified otherwise. 2-Chlorotrityl chloride resin, all N^{α}-Fmoc protected amino acids, PyBOP, and HOBt were purchased from Novabiochem (San Diego, CA); DMSO (99.9%) was purchased from EMD Chemicals (Gibbbstown, NJ); TFA, DMF, methanol, and piperidine were purchased from VWR and AIBN was from Soltech Ventures (Beverly, MA).

3.3.2. Peptide Synthesis

Peptides were synthesized using a solid-phase methodology and a manual Fmoc/tBu strategy on 2-chlorotrityl resin as described previously. Briefly, the peptides were prepared from the C-terminal by consecutive addition of protected amino acids (2.5 equiv.), PyBop (3 equiv.), and diisopropylethylamine (2.5 equiv.) to the first amino acid Fmoc-Glu(ODmab)-OH which was bound to 2-chlorotrityl resin. After the synthesis of the linear sequence, the peptide was cyclized. The cyclization (amide-bond formation) of the peptides was carried out via side-chain lysine and glutamic acid. These two amino acids were protected via a quasi-orthogonally-protected side-chain; namely, glutamic acid side-chain was protected via α-4-{N-[1-(4,4-dimethyl-2,6-dioxocyclohexylidene)-3-methylbutyl]amino}benzyl ester (ODmab)) and a lysine amino acid via N-ε-1-(4,4-dimethyl-2,6-dioxocyclohex-1-ylidene)-3-methylbutyl (ivDde); both these groups can be selectively removed with 2% v/v hydrazine in DMF solution. The cyclization step was carried out with PyBop (3 equiv.) in DMF for 24 h. After the desired peptide sequences were synthesized, the resulting dry resin-bound peptides were cleaved and side-chain deprotected using TFA/H_2O/ethanedithiol/triisopropylsilane (94.5:2.5:2.5:1) cocktail.

Crude peptides were purified by RP-HPLC (Agilent, 1100 Series with preparative Microsorb MV C18 column, 300 Å 5 μm, 250 × 22 mm, flow rate 8 mL · min^{-1}) employing a gradient from 2% to 90% B over 100 min, where buffer A was 0.1% TFA in water and buffer B 0.1% TFA in acetonitrile. The purity of the peptides was verified with analytical RP-HPLC. Peptide structures were ascertained by mass spectra determined by MALDI-TOF (Voyager-DE STR Biospectrometry Workstation, PerSeptive Biosystems). The synthesized peptides were derivatives of the cyclic nonapeptide RPM. Their structure is shown in Fig. 3.1.

The RPM sequence was extended at the *N*-terminus by the dipeptide YW (RPM1). This provided a way to quantitate the amount of peptide by UV spectrophotometry and an ^{125}I site at the tyrosine residue. MALDI-TOF MS for RPM1 (MH+) 1445.64, found 1445.77. The RPM1 structure was further extended by attaching three units of 8-amino-3,6-dioxaoctanoic acid at the N-terminus (RPM2). Finally, the peptide was capped with MA-Gly-Gly-OH monomer and then cyclized (Fig. 3.1). MALDI-TOF MS for RPM2: (M) KPIEDRPME 2063.29, found 2064.78. For the fluorescent labeled sequence, the RPM sequence was extended at the N-terminus by Fmoc-Lys-fluorescein (RPM3). First, *Fmoc-Lys-fluorescein* was prepared by reacting Fmoc-Lys-OH with an equimolar amount of 5(6)-carboxyfluorescein using PyBOP as coupling agent in DMF for 12 h. The product was purified using a preparative HPLC. The mass for Fmoc-Lys-fluorescein was verified via ESI MS: (MH+) 727, found 727.37.

During synthesis of RPM3, the lysine residue in position 2 and C-terminal glutamic acid (position 10) were orthogonally-protected via hindered Dde variant, ivDde. The cyclization (amide-bond formation) of the peptide via side-chain lysine and glutamic

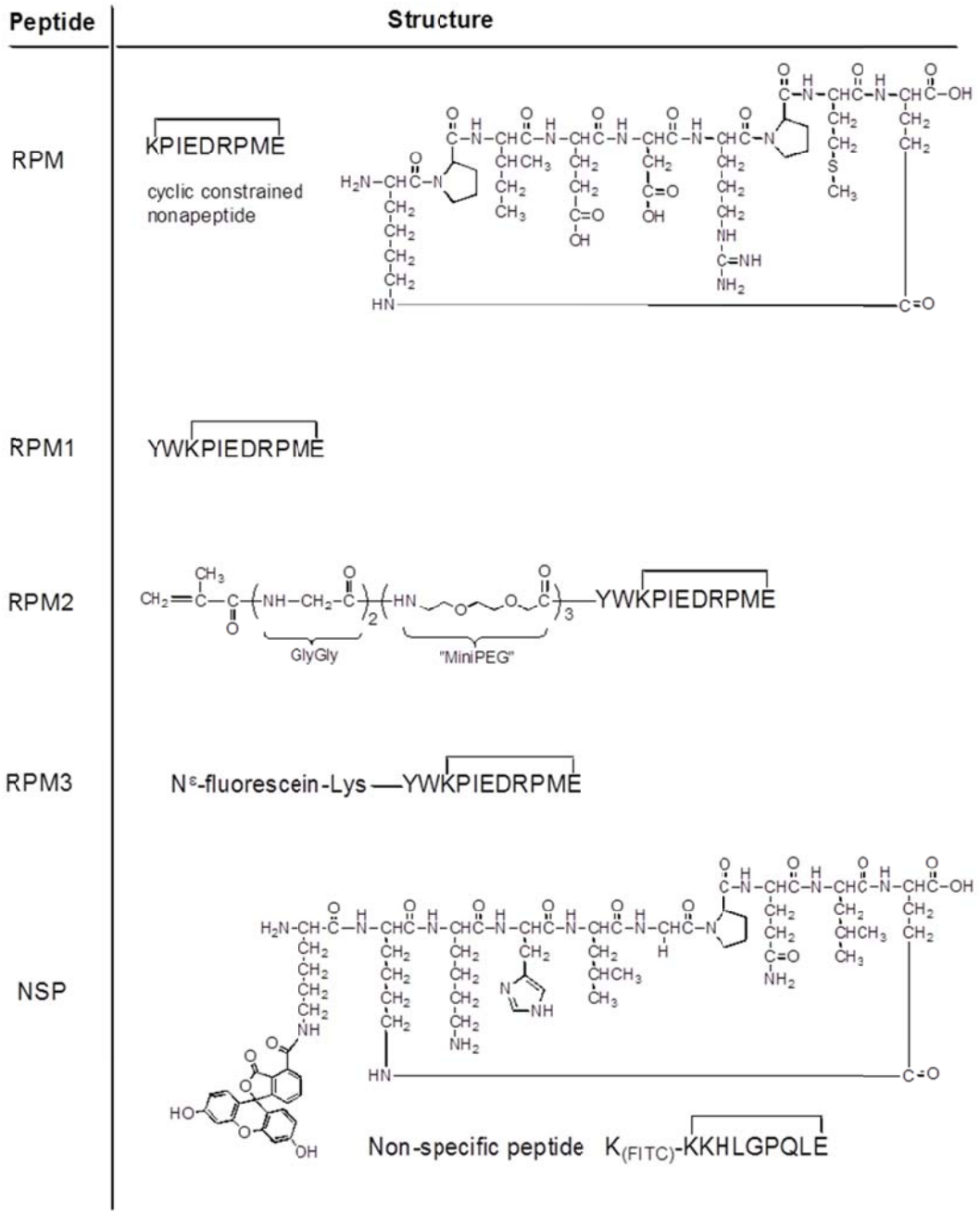

Figure 3.1. Structures of RPM, its derivatives, RPM1, RPM2, and RPM3, and of the non-specific peptide (NSP).

acid was carried out after removal of ivDde protection with 2% v/v hydrazine in DMF. The on-resin cyclization was carried out for 48 h using PyBOP, and HOBt as coupling agents. MALDI-TOF MS for RPM3: (MH+) K(fluorescein)-KKHLGPQLE 1583.73, found 1583.77. A control sequence (nonspecific peptide, (NSP)), (*29*), was also synthesized (Fig. 3.1). MALDI-TOF MS for NSP: (MH+) 1517.68, found 1517.74.

3.3.3 Synthesis of HPMA Copolymer – RPM1 Conjugate

The FITC labeled HPMA copolymer-RPM1 conjugate was synthesized in two steps (see structure in Fig. 3.2). First, an HPMA copolymer precursor containing reactive thiazolidine-2-thione groups was synthesized. In the second step, RPM1 was attached by polymeranalogous reaction.

The polymer precursors containing FITC and reactive thiazolidine-2-thione groups (*46*) in the side chains (P-FITC-TT, where P represents the polymeric backbone), were synthesized by free radical copolymerization of HPMA, MA-FITC, and MA-GG-TT in methanol at 50 °C for 24 h using 2,2'-azobisisobutyronitrile (AIBN) as the initiator. Briefly: HPMA (2 g, 14 mmol, 90.5 mol%), MA-FITC (0.169 g, 0.32 mmol, 2 mol%), MA-GG-TT (0.454 g, 1.2 mmol, 7.5 mol%), and AIBN (0.078 g, 0.48 mmol) were dissolved in methanol (10 mL), placed in an ampoule, purged with N_2 for 5 min, and sealed. After 24 h, the ampoule was cooled, opened, and the copolymer isolated by precipitation into an excess of diethyl ether/acetone (1/1 v/v). The yield of copolymer was 1.9 g (70 %). The TT content was 7.1 mol %, measured using UV spectrophotometry (305 nm, ε=10860 M^{-1} cm^{-1}, in methanol + 1 % acetic acid). Attachment of RPM1 to P-FITC-TT was performed in DMF at room temperature for 12 h with stirring (1:1 ratio of free peptide to the TT groups in precursor; [TT]:[NH_2] = 1:1;

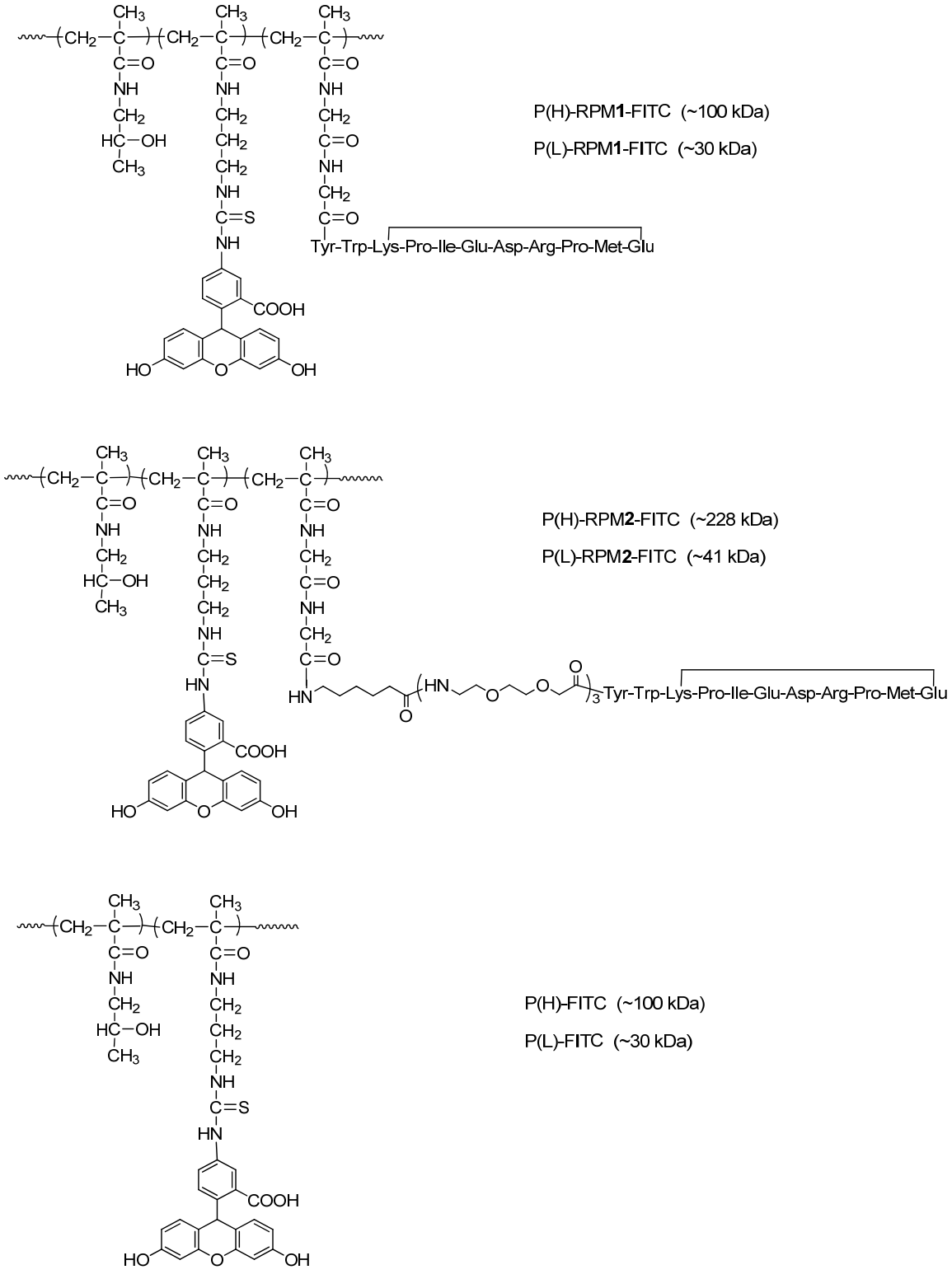

Figure 3.2. Structure of HPMA copolymer – RPM conjugates.

polymer concentration was 10 wt %). After the reaction, the volume of the reaction mixture was reduced in vacuo and the conjugate isolated by precipitation into an excess of acetone. The content of RPM1 in the polymeric conjugate was measured by UV-spectrophotometry (280 nm, ε = 6990 M^{-1} cm^{-1}, in PBS buffer (*47*)). This polymeric conjugate was fractionated into a low (P(L)-RPM1-FITC) and high (P(H)-RPM1-FITC) molecular weight portion and the content of RPM was 1 (30 Kd polymer) and 3.2 (100 Kd polymer) peptides per chain, respectively.

3.3.4 Synthesis of HPMA Copolymer – RPM2 Conjugate

HPMA copolymer-RPM2 conjugate, P-RPM2-FITC (Fig. 3.2), was synthesized by free radical copolymerization of HPMA, macromonomer RPM2, and MA-FITC. Typically: HPMA (40 mg, 0.28 mmol, 91 mol%), MA-FITC (3.26 mg, 0.0061 mmol, 2 mol%), macromonomer RPM2 (44.33 mg, 0.021 mmol, 7 mol%), and AIBN (0.75 mg, 0.0046 mmol) were dissolved in methanol (0.5 mL), placed in an ampoule, purged with N_2 for 5 min, and sealed. The polymerization proceeded at 50 ^{o}C for 24 h. Then, the ampule was cooled, opened, and the copolymer isolated by precipitation into an excess of diethyl ether/acetone (1/1 v/v). The yield of copolymer was 62 mg (~70 %). The content of peptide in the polymeric conjugate was measured by a UV-spectrophotometry (280 nm, ε = 6990 M^{-1} cm^{-1}, in PBS buffer (*47*)). This polymeric conjugate was also fractionated into a low (P(L)-RPM2-FITC) and high (P(H)-RPM2-FITC) molecular weight portion and the content of RPM was 3.5 (41 Kd) and 17 (228 Kd) peptides per chain, respectively.

3.3.5 Synthesis of Control Copolymer

FITC-labeled HPMA copolymer (without peptide), P-FITC (Fig. 3.2), was obtained by aminolysis of the side-chains of the polymer precursor P-FITC-TT. Typically: P-FITC-TT (200 mg) was dissolved in methanol (2 mL); to this solution, excess 1-aminopropan-2-ol was added and the reaction mixture stirred at r.t for 30 min. The hydrolyzed polymer reaction mixture was then run on a Sephadex™ LH-20 to separate the polymer and low molecular weight compounds. The copolymer fractions were concentrated under reduced pressure and precipitated into an excess of acetone.

3.3.6 Fractionation of Copolymers

To obtain narrow molecular weight fractions, polymer conjugates, P-RPM1-FITC, P-RPM2-FITC, and the control polymer, P-FITC, were applied on a preparative size exclusion Superose 6 (HR16/60) column. Fractions were collected using an automated fraction collector. Fractions from several runs were subsequently pooled into 4 separate collections. These were then dialyzed extensively against DI water and freeze-dried. The first and last ladder (corresponding to high and low molecular weight) was used for further experiments.

The molecular weight and molecular weight distribution of copolymers were measured on the ÄKTA FPLC system (GE Healthcare, formerly Amersham) equipped with UV and RI detectors using a Superose 6 HR10/30 column with PBS (pH 7.3) and PBS/acetonitrile (70/30) as the mobile phase. The average molecular weights were calculated using a calibration with polyHPMA fractions. The characterization of all HPMA copolymer conjugates is shown in Table 3.1.

Table 3.1. Characterization of HPMA copolymer-peptide conjugates

Conjugates	**Mw (kDa)**	**P[a]**	**Peptide / macromolecule**	**K_d[b] M x 10^{-6}**
P(H)-RPM1-FITC	100.5	1.25	3.2	912
P(L)-RPM1-FITC	30.5	1.14	1	601
P(H)-RPM2-FITC	228	1.1	17	575
P(L)-RPM2-FITC	41	1.2	3.5	416
P(H)-FITC (Control)	100.5	1.25	----	----
P(L)-FITC(Control)	32.8	1.22	----	----

[a] polydispersity (Mw/Mn); [b]K_d of free RPM3 = 555 μM

3.3.7 Cells

The human colorectal adenocarcinoma HT29 cell line was obtained from American Type Culture Collection (ATCC) (Manassas, VA). Cells were grown in McCoy's 5a medium supplemented with 10% FBS, 2 mM glutamine at 37 °C in 5% CO_2 and 95% humidified air. The cells were regularly subcultured to maintain a logarithmic phase of growth. Cells were plated into 96 well plates with an initial density of 3×10^5 cells/well. Experiments were initiated 24 h after plating of cells, unless otherwise stated. Cells were detached by applying trypsin-EDTA for 1 min.

3.3.8 Microscopy

For fluorescence microscopy, cells were grown on 35 mm glass bottom microwell dishes (MatTek, Ashland, MA). For all studies, 3×10^5 HT-29 cells were seeded on previously sterilized glass coverslips 24 h before incubation. Uptake studies were conducted by incubating cells with HPMA copolymer - peptide conjugates or free peptides for the desired time. The cells were then washed with DPBS after incubation, fixed with 3% paraformaldehyde for 20 min at room temperature, mounted with SlowFade Light antifade medium, and sealed. For all studies, the cells were imaged on an Olympus FluoView 1000 (Minneapolis, MN) confocal imaging system (60× oil objective) and an argon laser (FITC, excitation = 488 nm, emission = 505 nm long-pass filter). The settings for the confocal systems were adjusted so that control cells always yielded dark images. Image acquisitions and analyses were performed using FluoView software. The intensity of the laser beam and the photodetector sensitivity were kept constant in order to compare the relative fluorescence intensities between experiments.

3.3.9 Flow Cytometry

For flow cytometry, cells were grown on 12-well plates (seeded 24 h before incubation, 1×10^5 cells/well) and then uptake studies were conducted by incubating with polymeric conjugates or free peptide for selected time intervals. The cells were then washed three times with warm DPBS. The cells were then detached with trypsin-EDTA solution. Collected cells were incubated for 15 min with warm PBS/2% BSA. A FACScan (Becton Dickinson Biosciences, Mountain View, CA) equipped with a single 488 nm argon laser was used. After the flow cytometer was set for green (FL-1) and red (FL-2) fluorescence, the data were collected and analyzed with Cell Quest software (BD Biosciences) after appropriate gating.

3.3.10 Radiolabeling and Binding Experiments

The polymeric conjugates and free RPM peptide were labeled with ^{125}I using the Iodogen method. The conjugates or peptide (300 µl of a solution having a concentration equivalent to 1.0 mg/ml in PBS, pH 7.4), and 10 µl (0.5 mCi) of $Na^{125}I$ were mixed in an Iodogen tube. The reaction was left for 15 min while being periodically mixed. The unbound iodide was separated from the labeled conjugate by passing the reaction mixture over a Sephadex G-25 column, which had been pre-equilibrated with PBS and BSA. The labeled peptide or conjugates (specific activity 45-65 µCi/mg) were stored at 4 ^{0}C.

The antigen binding affinity constants (K_d) of the free and polymer-bound peptides were determined by radio-assay. Cells were plated in 96-well plates and grown for 24 h until 80-90 % confluence. One hour before the experiment, cells were switched from growth medium to DPBS, pH 7.4, and kept at 4 ^{0}C. Binding experiments were initiated by adding PBS solutions containing labeled free peptide or conjugates at various

concentrations (also chilled at 4 ^{0}C). Cells were incubated with the ligands for 1 h and then the unbound ligand was removed using an aspirator. Cells were solubilized with 200 μL of 1 N NaOH for 30 min and subsequently counted for radioactivity.

3.4 Results and Discussion

In HPMA copolymer - RPM conjugates, RPM was attached to the HPMA copolymer backbone via two spacers of different lengths (Fig. 3.2; Table 3.1), glycylglycyltyrosyltryptophan (P-RPM1-FITC) and 8-amino-3,6-dioxaoctanoyl-8-amino-3,6-dioxaoctanoyl-8-amino-3,6-dioxaoctanoyltyrosyltryptophan (P-RPM2-FITC). The peptides used in the preparation of conjugates were synthesized by solid phase peptide synthesis. The amide-bond cyclization between K and E was performed on peptide still attached to the beads. Two techniques were used for conjugate synthesis, namely polymeranalogous attachment of RPM1 to a HPMA copolymer precursor containing GG side-chains terminated in reactive TT groups (conjugate P-RPM1-FITC) and by copolymerization of macromonomer RPM2 with HPMA and MA-FITC. During the polymeranalogous attachment of RPM1 to HPMA copolymer precursor, there is a possibility of Arg side-chain reactivity. However, there was no broadening of the SEC profile after the reaction was detected (when compared to the profile before the reaction). To avoid this problem, the monomeric form of the peptide (RPM2) was synthesized and incorporated into the HPMA copolymer conjugate by copolymerization.

The HPMA copolymer conjugates were fractionated on a preparative Superpose 6 (HR16/60) column. Two fractions, a high molecular weight sample and a low molecular weight sample, were isolated and used in the experiments. On Fig. 3.3, the molecular weight profiles of high molecular weight HPMA copolymer – RPM1 conjugate, P(H)-

RPM1-FITC (100 kDa) and of the low molecular weight HPMA copolymer – RPM1 conjugate, P(L)-RPM1-FITC (30 kDa) are shown.

To evaluate the biorecognition of the RPM structure by HT-29 cells, the internalization of RPM3 and NSP was studied by confocal fluorescence microscopy (Fig. 3.4a,b). Images of HT-29 cells (taken after 3 h of incubation) show that the non-specific sequence (NSP) had very marginal uptake (Fig. 3.4a), whereas cells incubated with the RPM3 peptide exhibited punctuate fluorescence (Fig. 3.4b), consistent with the internalization by receptor-mediated endocytosis. These results are consistent with data by Kelly et al. (*29*) regarding the specificity of RPM peptide toward HT29 cells. Similar results were obtained by flow cytometry; the shift of the profile of HT-29 cells incubated with the RPM3 peptide was considerably larger than that of the nonspecific NPS sequence (Fig. 3.4c).

The uptake of HPMA copolymer – RPM1 conjugate and of the control FITC-labeled HPMA copolymer by HT-29 cells was evaluated by confocal fluorescence microscopy after 3 h incubation at 37 °C (Fig. 3.5). Interestingly, the internalization of high molecular weight (100 kDa) conjugates, P(H)-FITC (Fig. 3.5B) and P(H)-RPM1-FITC (Fig. 3.5C), appeared to be lower than the internalization of low molecular weight (approx. 30 kDa) conjugates, P(L)-FITC (Fig. 3.5D) and P(L)-RPM1-FITC (Fig. 3.5E). Comparison of images 5D and 5E seems to indicate a more enhanced internalization of the RPM-targeted conjugate P(L)-RPM1-FITC than that of the control copolymer, P(L)-FITC. Flow cytometry data (Fig. 3.6) distinguished the conjugates only based on molecular weight. Low molecular weight conjugates (Fig. 3.6A), P(L)-FITC and P(L)-

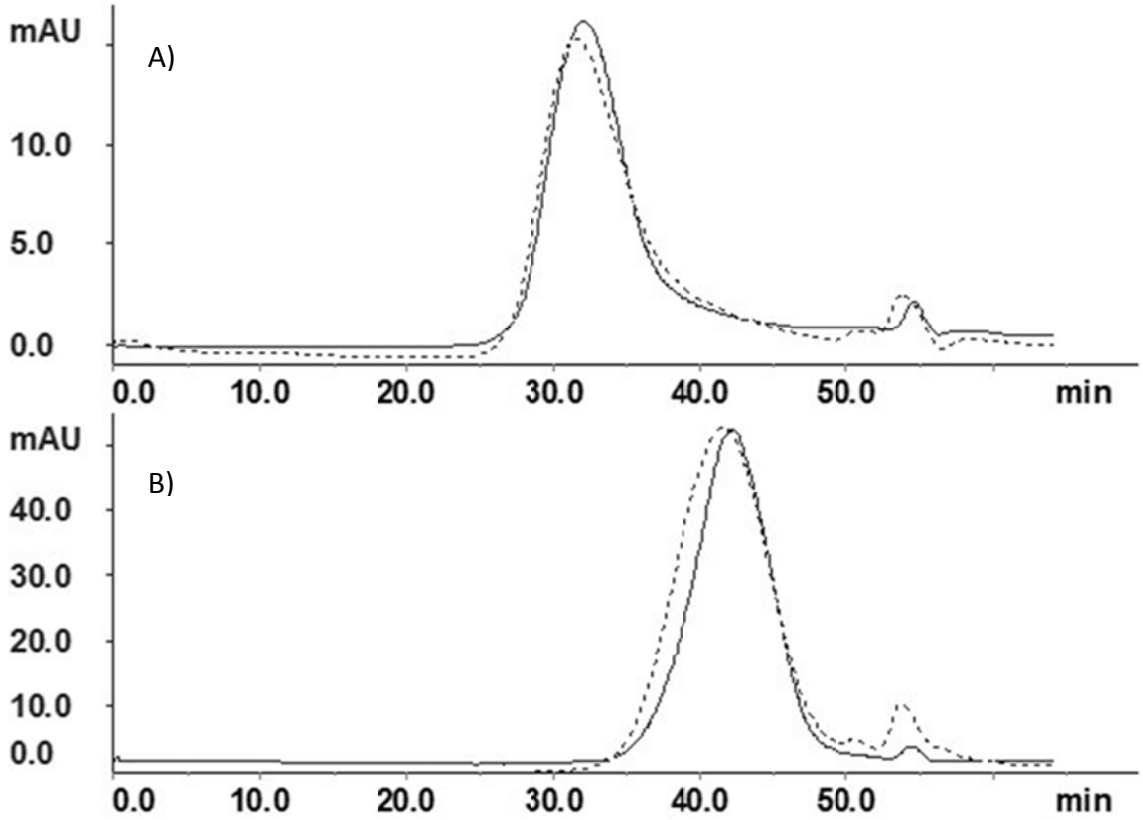

Figure 3.3. Molecular weight distribution profiles of HPMA copolymer - RPM conjugates as determined by size-exclusion chromatography (SEC). (A) P(H)-FITC (---) and P(H)-RPM1-FITC **(▬);** (B) P(L)-FITC (---) and P(L)-RPM1-FITC **(▬)**.

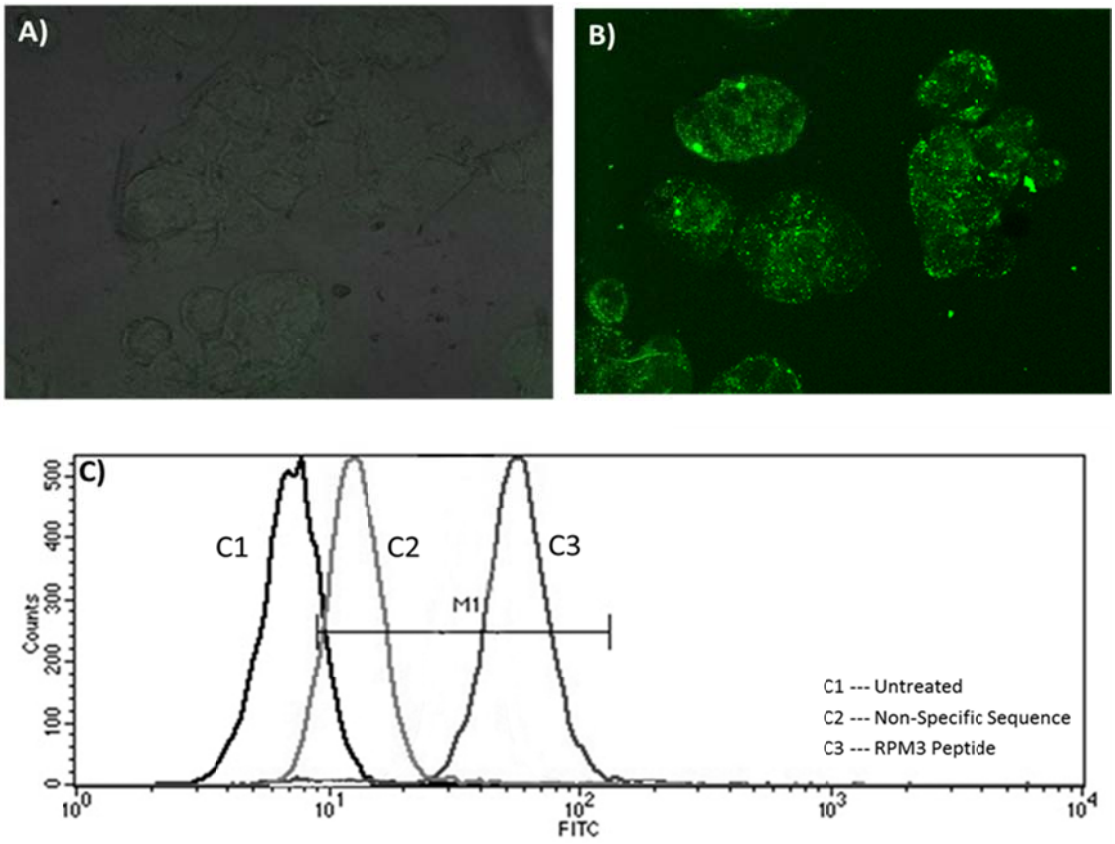

Figure 3.4. Confocal fluorescence images (60x oil) and flow cytometry profiles of HT-29 cells incubated with RPM3 or nonspecific peptide (NSP). (A) 20 μM NSP fixed after 3 h incubation; (B) 20 μM RPM3 fixed after 3 h incubation; (C) Flow cytometry profile of RPM3 and NSP after 3 h incubation.

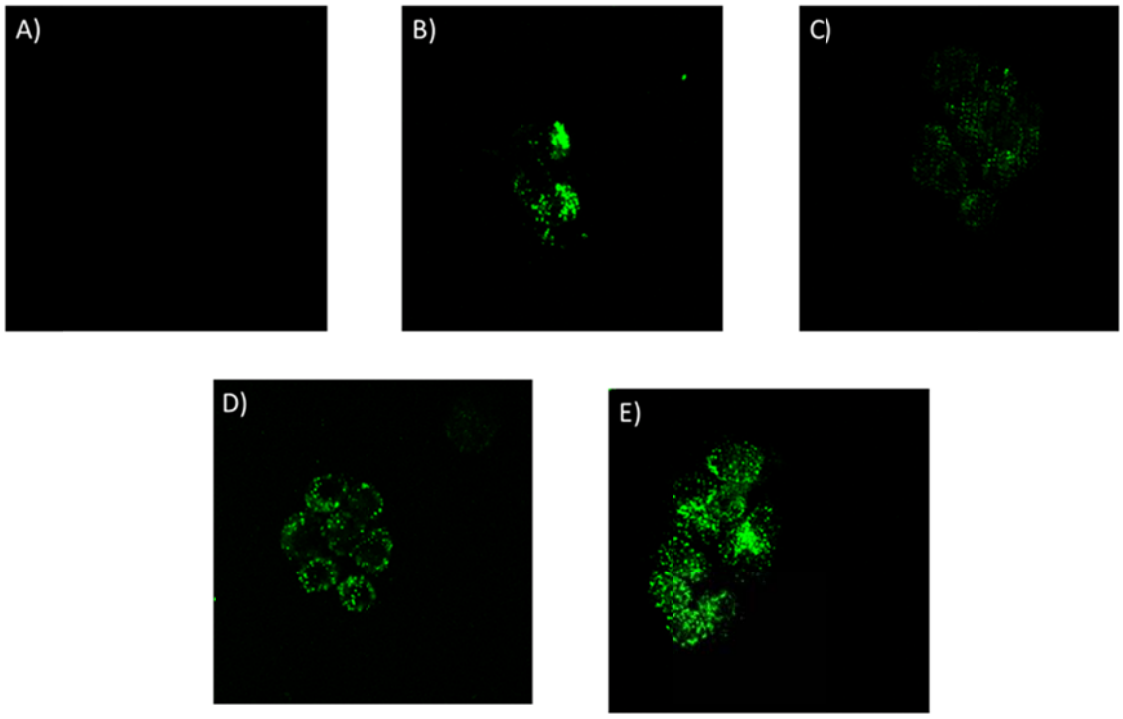

Figure 3.5. Confocal fluorescence images (60x oil) profiles of HT-29 cells incubated with fluorescently labeled HPMA copolymer conjugates. (A) Untreated cells; (B) P(H)-FITC; (C) P(H)-RPM1-FITC; (D) P(L)-FITC; (E) P(L)-RPM1-FITC.

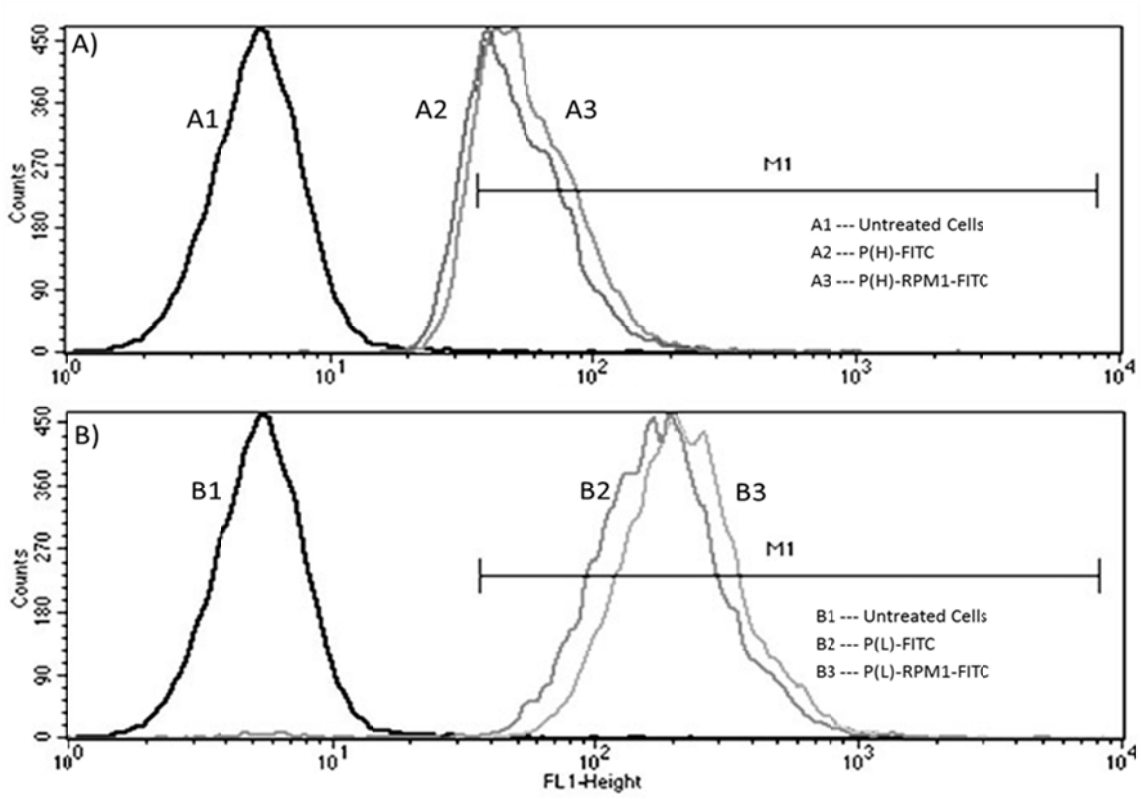

Figure 3.6. Flow cytometry profiles of HT-29 cells incubated with HPMA copolymer-RPM conjugates for 3 h at 37 ° C. (A) P(H)-FITC and P(H)-RPM1-FITC; (B) P(L)-FITC and P(L)-RPM1-FITC

RPM1-FITC, were internalized faster than high molecular weight conjugates (Fig. 3.6B), P(H)-FITC and P(H)-RPM1-FITC (Fig. 3.6B).

One important factor in the biorecognition of polymer conjugates is the spacer length between the polymer backbone and the recognition (targeting) moiety (*41*). To test the impact of spacer length on biorecognition, a longer spacer, 8-amino-3,6-dioxaoctanoyl-8-amino-3,6-dioxaoctanoyl-8-amino-3,6-dioxaoctanoyltyrosyltryptophan, was introduced between the HPMA copolymer and RPM moiety (conjugate P-RPM2-FITC). As mentioned above, the synthesis of P-RPM2-FITC was carried out in a one-step process by copolymerization of HPMA, MA-FITC, and macromonomer RPM2. This copolymer was also fractionated and two fractions, namely a high molecular weight (228 kDa) sample, P(H)-RPM2-FITC, and a low molecular weight (41 kDa) sample, P(L)-RPM2-FITC, were prepared (Table 3.1). Flow cytometry data (Fig. 3.7) revealed that introduction of the longer spacer resulted in a clear distinction between RPM containing conjugates, P(H)-RPM2-FITC and P(L)-RPM2-FITC, and control polymers, P(H)-FITC and P(L)-FITC. For both, high molecular weight and low molecular weight conjugates, the RPM-containing conjugate produced a larger shift of the flow cytometry profile than the corresponding control polymer (without RPM). It is interesting to note that the shift of the flow cytometry profile appeared to be larger for the low molecular weight conjugate. The decreased biorecognition of the high molecular weight conjugate might be the consequence of the conformation of the macromolecule in solution. Apparently, the RPM peptide is less accessible in the high molecular weight conjugate. The intramolecular interactions of peptide-terminated side chains may lead to the formation of unimolecular micelles with biorecognition units inside and hydrophilic groups on the

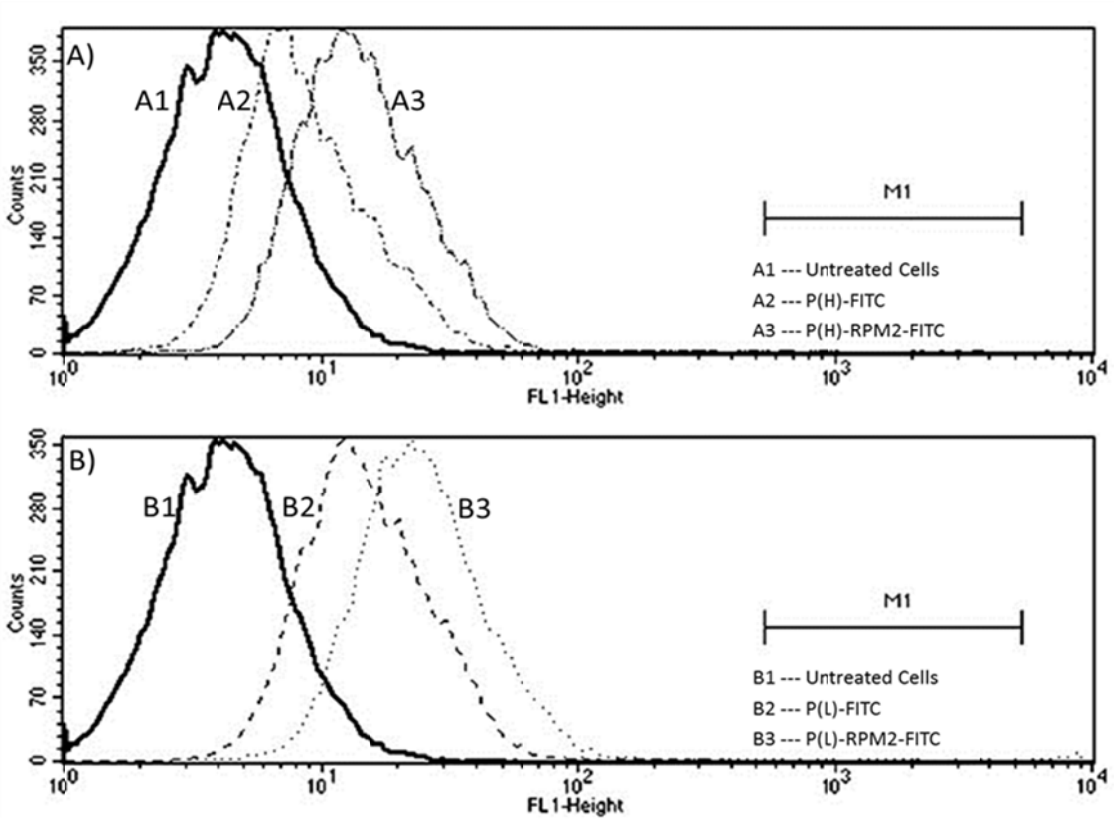

Figure 3.7. Flow cytometry profiles of HT-29 cells incubated with HPMA polymer-RPM conjugates for 3 h at 37 $^{\circ}$ C. (A) P(H)-FITC and P(H)-RPM2-FITC; (B) P(L)-FITC and P(L)-RPM2-FITC.

outside. Formation of unimolecular micelles in HPMA copolymer conjugates was observed previously (*48*). The results discussed above indicated that the binding constant of RPM to HT-29 cells would be modest. To quantitatively characterize the interaction of free and HPMA copolymer-bound RPM, a radioiodination assay, using cell monolayers, was employed and dissociation constants determined. The free peptide (RPM3) and HPMA copolymer – RPM conjugates were incubated with chilled cells (4 ^{0}C) for 1 h in PBS buffer. The dissociation constants (Table 3.1) were calculated using SigmaPlot by fitting the binding data to a one-site saturation ligand binding equation. The dissociation constants of free and HPMA copolymer-bound peptides were of the same order (10^{-4} M^{-1}). The results corroborated internalization and flow cytometry data. Binding of low molecular weight conjugates was enhanced when compared to high molecular weight ones. The highest binding was observed for the P(L)-RPM2-FITC conjugate. Several factors may contribute to enhanced binding of this conjugate: length of spacer, number of RPT moieties per macromolecule, and conformation of the macromolecule in solution. These data evidently showed the need of balancing the physical as well as biological components to achieve optimal cellular biorecognition.

In summary, these results showed that water-soluble polymers (like HPMA copolymers) can be used for facile attachment of targeting moieties and therapeutics. Additionally, the RPM peptide possesses a potential as a targeting moiety to deliver therapeutics specifically to colon cancer cells. It was demonstrated that the spacer length between the polymer backbone and the RPM peptide plays an important role in biorecognition. Optimizing the physicochemical properties of the copolymers is crucial in achieving favorable biorecognition (*49*). One pathway to follow is the modification of

RPM structure, by systemically altering the nonessential amino acids (*50*), to improve biorecognition. Currently, the receptor-binding site for this peptide is unknown; further experiments are essential to identify the receptor and its density on cellular surface. This would permit us to design conjugates, which could benefit from multivalent binding to the cellular surface

3.5 References

(1) Jemal, A., Siegel, R., Ward, E., Murray, T., Xu, J., and Thun, M. J. (2007) Cancer Statistics, 2007 *CA Cancer J Clin 57*, 43-66.

(2) Sjoblom, T., Jones, S., Wood, L. D., Parsons, D. W., Lin, J., Barber, T. D., Mandelker, D., Leary, R. J., Ptak, J., Silliman, N., Szabo, S., Buckhaults, P., Farrell, C., Meeh, P., Markowitz, S. D., Willis, J., Dawson, D., Willson, J. K., Gazdar, A. F., Hartigan, J., Wu, L., Liu, C., Parmigiani, G., Park, B. H., Bachman, K. E., Papadopoulos, N., Vogelstein, B., Kinzler, K. W., and Velculescu, V. E. (2006) The consensus coding sequences of human breast and colorectal cancers. *Science 314*, 268-274.

(3) McDonald, S. A., Preston, S. L., Lovell, M. J., Wright, N. A., and Jankowski, J. A. (2006) Mechanisms of disease: from stem cells to colorectal cancer. *Nat Clin Pract Gastroenterol Hepatol 3*, 267-274.

(4) Ding, H., Prodinger, W. M., and Kopeček, J. (2006) Two-step fluorescence screening of CD21-binding peptides with one-bead one-compound library and investigation of binding properties of N-(2-hydroxypropyl)methacrylamide copolymer-peptide conjugates. *Biomacromolecules 7*, 3037-3046.

(5) Ding, H., Prodinger, W. M., and Kopeček, J. (2006) Identification of CD21-binding peptides with phage display and investigation of binding properties of HPMA copolymer-peptide conjugates. *Bioconjug Chem 17*, 514-523.

(6) David, A., Kopečková, P., Minko, T., Rubinstein, A., and Kopeček, J. (2004) Design of a multivalent galactoside ligand for selective targeting of HPMA copolymer-doxorubicin conjugates to human colon cancer cells. *Eur J Cancer 40*, 148-157.

(7) Wang, D., Miller, S., Sima, M., Kopečková, P., and Kopeček, J. (2003) Synthesis and evaluation of water-soluble polymeric bone-targeted drug delivery systems. *Bioconjug Chem 14*, 853-859.

(8) Tang, A., Kopečková, P., and Kopeček, J. (2003) Binding and cytotoxicity of HPMA copolymer conjugates to lymphocytes mediated by receptor-binding epitopes. *Pharm Res 20*, 360-367.

(9) Omelyanenko, V., Kopečková, P., Prakash, R. K., Ebert, C. D., and Kopeček, J. (1999) Biorecognition of HPMA copolymer-adriamycin conjugates by lymphocytes mediated by synthetic receptor binding epitopes. *Pharm Res 16*, 1010-1019.

(10) Jelinkova, M., Strohalm, J., Plocova, D., Subr, V., St'astny, M., Ulbrich, K., and Rihova, B. (1998) Targeting of human and mouse T-lymphocytes by monoclonal

antibody-HPMA copolymer-doxorubicin conjugates directed against different T-cell surface antigens. *J Control Release 52*, 253-270.

(11) Shiah, J. G., Dvorak, M., Kopečková, P., Sun, Y., Peterson, C. M., and Kopeček, J. (2001) Biodistribution and antitumour efficacy of long-circulating N-(2-hydroxypropyl)methacrylamide copolymer-doxorubicin conjugates in nude mice. *Eur J Cancer 37*, 131-139.

(12) Mitra, A., Nan, A., Papadimitriou, J. C., Ghandehari, H., and Line, B. R. (2006) Polymer-peptide conjugates for angiogenesis targeted tumor radiotherapy. *Nucl Med Biol 33*, 43-52.

(13) Kawamura, K., Oishi, J., Sakakihara, S., Niidome, T., and Katayama, Y. (2006) Intracellular signal-responsive artificial gene regulation. *J Drug Target 14*, 456-464.

(14) Chau, Y., Padera, R. F., Dang, N. M., and Langer, R. (2006) Antitumor efficacy of a novel polymer-peptide-drug conjugate in human tumor xenograft models. *Int J Cancer 118*, 1519-1526.

(15) Omelyanenko, V., Kopečková, P., Gentry, C., Shiah, J. G., and Kopeček, J. (1996) HPMA copolymer-anticancer drug-OV-TL16 antibody conjugates. 1. influence of the method of synthesis on the binding affinity to OVCAR-3 ovarian carcinoma cells in vitro. *Journal of Drug Targeting 3*, 357-373.

(16) Shiah, J., Sun, Y., Kopečková, P., Peterson, C. M., Straight, R. C., and Kopeček, J. (2001) Combination chemotherapy and photodynamic therapy of targetable N-(2-hydroxypropyl)methacrylamide copolymer-doxorubicin/mesochlorin e(6)-OV- TL 16 antibody immunoconjugates. *Journal of Controlled Release 74*, 249-253.

(17) Lu, Z. R., Kopečková, P., and Kopeček, J. (1999) Polymerizable Fab' Antibody Fragments for Targeting of Anticancer Drugs. *Nature Biotechnology 17*, 1101-1104.

(18) Lu, Z. R., Shiah, J. G., Kopečková, P., and Kopeček, J. (2003) Polymerizable Fab' antibody fragment targeted photodynamic cancer therapy in nude mice. *S.T.P. Pharma Sci 13*, 69-75.

(19) Rathi, R. C., Kopečková, P., Rihova, B., and Kopeček, J. (1991) N-(2-Hydroxypropyl)methacrylamide Copolymers Containing Pendant Saccharide Moieties. Synthesis and Bioadhesive Properties. *Journal of Polymer Science, Part A: Polymer Chemistry 29*, 1895-1902.

(20) Wroblewski, S., Berenson, M., Kopečková, P., and Kopeček, J. (2001) Potential of lectin-N-(2-hydroxypropyl)methacrylamide copolymer-drug conjugates for the treatment of pre-cancerous conditions. *Journal of Controlled Release 74*, 283-293.

(21) Liu, R., Enstrom, A. M., and Lam, K. S. (2003) Combinatorial peptide library methods for immunobiology research. *Exp Hematol 31*, 11-30.

(22) Kumaresan, P. R., Natarajan, A., Song, A., Wang, X., Liu, R., DeNardo, G., DeNardo, S., and Lam, K. S. (2007) Development of tissue plasminogen activator specific "on demand cleavable" (odc) linkers for radioimmunotherapy by screening one-bead-one-compound combinatorial peptide libraries. *Bioconjug Chem 18*, 175-182.

(23) Landon, L. A., and Deutscher, S. L. (2003) Combinatorial discovery of tumor targeting peptides using phage display. *J Cell Biochem 90*, 509-517.

(24) Williams, W. V., Kieber-Emmons, T., VonFeldt, J., Greene, M. I., and Weiner, D. B. (1991) Design of bioactive peptides based on antibody hypervariable region structures. Development of conformationally constrained and dimeric peptides with enhanced affinity. *J Biol Chem 266*, 5182-5190.

(25) Kelly, K., Alencar, H., Funovics, M., Mahmood, U., and Weissleder, R. (2004) Detection of Invasive Colon Cancer Using a Novel, Targeted, Library-Derived Fluorescent Peptide. *Cancer Res 64*, 6247-6251.

(26) Reubi, J. C., Laderach, U., Waser, B., Gebbers, J. O., Robberecht, P., and Laissue, J. A. (2000) Vasoactive intestinal peptide/pituitary adenylate cyclase-activating peptide receptor subtypes in human tumors and their tissues of origin. *Cancer Res 60*, 3105-3112.

(27) Rasmussen, U. B., Schreiber, V., Schultz, H., Mischler, F., and Schughart, K. (2002) Tumor cell-targeting by phage-displayed peptides. *Cancer Gene Ther 9*, 606-612.

(28) Moody, T. W., Mantey, S. A., Pradhan, T. K., Schumann, M., Nakagawa, T., Martinez, A., Fuselier, J., Coy, D. H., and Jensen, R. T. (2004) Development of high affinity camptothecin-bombesin conjugates that have targeted cytotoxicity for bombesin receptor-containing tumor cells. *J Biol Chem 279*, 23580-23589.

(29) Kelly, K. A., and Jones, D. A. (2003) Isolation of a colon tumor specific binding peptide using phage display selection. *Neoplasia 5*, 437-444.

(30) Davies, J. S. (2003) The cyclization of peptides and depsipeptides. *J Pept Sci 9*, 471-501.

(31) Cudic, M. W., J. D. Otvos, L. Jr. (2000) Convenient synthesis of a head-to-tail cyclic peptide containing an expanded ring. *Tetrahedron Lett 41*, 4527-4531.

(32) Joly, J. C., and Swartz, J. R. (1997) In vitro and in vivo redox states of the Escherichia coli periplasmic oxidoreductases DsbA and DsbC. *Biochemistry 36*, 10067-10072.

(33) Letvin, N. L., Goldmacher, V. S., Ritz, J., Yetz, J. M., Schlossman, S. F., and Lambert, J. M. (1986) In vivo administration of lymphocyte-specific monoclonal antibodies in nonhuman primates. In vivo stability of disulfide-linked immunotoxin conjugates. *J Clin Invest 77*, 977-984.

(34) Rietsch, A., and Beckwith, J. (1998) The genetics of disulfide bond metabolism. *Annu Rev Genet 32*, 163-184.

(35) Li, P., Roller, P. P., and Xu, J. (2002) Current Synthetic Approaches to Peptide and Peptidomimetic Cyclization. *Curr Org Chem 6*, 411-440.

(36) Kofod-Hansen, M., Peschke, B., and Thogersen, H. (2002) Head-to-backbone cyclization of peptides on solid support by nucleophilic aromatic substitution. *J Org Chem 67*, 1227-1232.

(37) Wolfenden, M. L., and Cloninger, M. J. (2006) Carbohydrate-functionalized dendrimers to investigate the predictable tunability of multivalent interactions. *Bioconjug Chem 17*, 958-966.

(38) Wolfenden, M. L., and Cloninger, M. J. (2005) Mannose/glucose-functionalized dendrimers to investigate the predictable tunability of multivalent interactions. *J Am Chem Soc 127*, 12168-12179.

(39) Banaszak Holl, M. M., Leroueil, P., Hong, S., Baker, J. R., Jr., Orr, B. G., DiMaggio, S., and Kelly, C. (2007) in *PMSE Preprints* pp 323-324.

(40) Nan, A., Ghandehari, H., Hebert, C., Siavash, H., Nikitakis, N., Reynolds, M., and Sauk, J. J. (2005) Water-soluble polymers for targeted drug delivery to human squamous carcinoma of head and neck. *J Drug Target 13*, 189-197.

(41) Ding, H., Prodinger, W. M., and Kopeček, J. (2006) Two-step fluorescence screening of CD21-binding peptides with one-bead one-compound library and investigation of binding properties of N-(2-hydroxypropyl)methacrylamide copolymer-peptide conjugates. *Biomacromolecules 7*, 3037-3046.

(42) Ding, H., Prodinger, W. M., and Kopeček, J. (2006) Identification of CD21-binding peptides with phage display and investigation of binding properties of HPMA copolymer-peptide conjugates. *Bioconjug Chem 17*, 514-523.

(43) Tang, A., Kopečková, P., and Kopeček, J. (2003) Binding and cytotoxicity of HPMA copolymer conjugates to lymphocytes mediated by receptor-binding epitopes. *Pharm Res 20*, 360-367.

(44) Kopeček, J., and Bazilova, H. (1973) Poly[N-(2-Hydroxypropyl)methacrylamide]. 1. Radical Polymerization and Copolymerization. *Eur Polymer J 9*, 7-14.

(45) Omelyanenko, V., Kopečková, P., Gentry, C., and Kopeček, J. (1998) Targetable HPMA copolymer-adriamycin conjugates. Recognition, internalization, and subcellular fate. *J Control Release 53*, 25-37.

(46) Subr, V., and Ulbrich, K. (2006) Synthesis and properties of new N-(2-hydroxypropyl)-methacrylamide copolymers containing thiazolidine-2-thione reactive groups. *Reactive & Functional Polymers 66*, 1525-1538.

(47) Pace, C. N., Vajdos, F., Fee, L., Grimsley, G., and Gray, T. (1995) How to measure and predict the molar absorption coefficient of a protein. *Protein Sci 4*, 2411-2423.

(48) Shiah, J. G., Konak, C., Spikes, J. D., and Kopeček, J. (1997) Solution and photoproperties of N-(2-hydroxypropyl)methacrylamide copolymer meso-chlorin e(6) conjugates. *J Phys Chem B 101*, 6803-6809.

(49) Rejman, J., Oberle, V., Zuhorn, I. S., and Hoekstra, D. (2004) Size-dependent internalization of particles via the pathways of clathrin- and caveolae-mediated endocytosis. *Biochem J 377*, 159-169.

(50) Peng, L., Liu, R., Marik, J., Wang, X., Takada, Y., and Lam, K. S. (2006) Combinatorial chemistry identifies high-affinity peptidomimetics against alpha4beta1 integrin for in vivo tumor imaging. *Nat Chem Biol 2*, 381-389.

CHAPTER 4

IN VIVO EVALUATION OF NOVEL COLON CANCER TARGETED HPMA-9-AMINOCAMPTOTHECIN CONJUGATES TREATED LOCALLY AND SYSTEMICALLY

4.1. Abstract

Two novel, linear polymeric systems were designed for systemic delivery, one containing a biorecognizable sequence and the other without. This polymeric system was compared to a polymer designed for local delivery. The former system P-GFLG-9-AC was a carrier composed of N-(2-hydroxypropyl)methacrylamide (HPMA) copolymer, 9-aminocamptothecin (9-AC), and with or without a biorecognizable cyclic nonapeptide. The anticancer drug 9-AC was attached via a spacer consisting of a lysosomally degradable linker, namely an oligopeptide spacer glycylphenylalanylleucylglycyl (GFLG) and a self-eliminating 4-aminobenzyl alcohol structure. In the latter system, a copolymer of HPMA and 9-aminocamptothecin bound via an aromatic azo bond (P-AZO-9AC) and a self-elimination spacer was synthesized. Therapeutic efficiency of a systemic versus local approach was evaluated in vivo using a noninvasive bioluminescence imaging tumor model. To this end, six groups were compared: a) untreated, b) free drug (oral), c) P-AZO-9-AC (oral), d) P-GFLG-9-AC (i.v.), e) P-GFLF-9-AC-minPEG-PRM (i.v.), f) combination of P-GFLG-9AC (i.v) and P-AZO-9-AC

(oral). Mice treated with the polymer conjugates containing 9-AC or free drug had significantly longer tumor growth delay compared to untreated controls. Polymer conjugates given parenteral performed slightly better than the conjugates given orally. No significant difference in the therapeutic effects among the targeted or untargeted conjugates was observed.

4.2. Introduction

Colon cancer is the second leading cause of cancer-related death in the United States (*1*). Its death rate has not significantly changed over the past 20 years in spite of surgical procedures that have vastly improved in the same period (*2*). This is likely due to the late stage at which CRC is diagnosed, and the intrinsically high, nonspecific toxicity from which conventional chemotherapeutic treatments suffer (*3, 4*). Due to failure and limitation of current therapies, the development of novel approaches for the treatment of colon cancer is currently under intense investigation (*5, 6*).

The mainstay of treatment for metastatic or recurrent colorectal cancer is chemotherapy. For many years, 5-fluorouracil (5-FU), has been the main treatment option; however, modest efficacy has been observed. Recently, several new chemotherapeutic agents, including capecitabine, oxaliplatin, and various derivatives of camptothecin have become available. Camptothecin (CPT), discovered in the 1960s (*7*) and later identified as an unequivocal inhibitor of topoisomerase I (*8, 9*), is a naturally occurring alkaloid. During Phase I and Phase II clinical trials, it showed strong antitumor activity among patients with gastrointestinal cancers, though it caused severe side effects, with the most severe being myelosupression and haemorrhagic cystitis. By examining the

structure activity relationships of camptothecins, various analogs have been developed that increase its solubility and reduce its side effects (*10*). One analog that demonstrated superior topo I inhibitory activity than its parent compound or two other clinically approved derivatives (topotecan or irinotecan) was 9-aminocamptothecin (9-AC) (IDEC-132) (*11*). However, 9-AC- has a major drawback related to dose limiting toxicity, which ultimately resulted in discontinuation of Phase II studies (*12, 13*).

The use of hydrophilic polymers as drug delivery vehicles is well accepted and they have dramatically changed the way we diagnose and treat patients. Polymeric carriers based on *N*-(2-hydroxypropyl)methacrylamide (HPMA) have been extensively studied (*14-17*). Drugs incorporated in polymeric carriers have various advantages (when compared to low-molecular weight drugs), including long-lasting circulation in the bloodstream, decreased nonspecific toxicity of the conjugated drug, increased solubility of hydrophobic compounds, and decreased immunogenicity of the targeting moiety (*18, 19*).

Strategies of incorporating 9-aminocamptothecin within polymeric carriers have dramatically reduced the nonspecific toxicity of the parent drug (*20-22*). A wide array of orally bioavailable colon-specific delivery systems incorporating 9-AC have been designed and synthesized previously (*23-27*). This approach has utilized the drug bound to a copolymer of HPMA via an aromatic azo bond and a self-elimination spacer (*28-30*). After selectively targeting the macromolecule to the colon, the unmodified drug can be released at the site of action (*31*). Using this strategy, Gao et al. (*28*) have shown a dramatic improvement in the pharmacokinetic profile with a substantially higher local concentration of the drug in vivo.

However, it is prudent to utilize a systemic therapy approach for the treatment of metastatic colorectal cancer. Macromolecules afford the advantage of nonspecific accumulation inside solid tumors. This phenomenon is due to the so-called Enhanced Permeability and Retention (EPR) effect (*32*). However, the drawback of conventional polymeric delivery systems relates to the slow rate of internalization after passive targeting to tumor tissue through the endocytic pathway. Hence, there is an immense interest in designing a new generation of molecularly targeted therapeutics through tumor-specific mAbs or ligands that bind to receptors that are present on tumor cells. Development of these systems can potentially lead to a higher local concentration and enhance tumor cytotoxicity as compared to their untargeted counterpart. Furthermore, targeted therapeutics may change the mechanism of cell entry from fluid phase pinocytosis to receptor-mediated endocytosis. The latter mode of entry results in a faster rate of internalization when compared to fluid phase (nontargeted systems) uptake (*33*) and is thus more efficient. Numerous antibodies (*34, 35*) and peptides (*36-40*) have been developed to target colon cancer. The most interesting targeting agent for colorectal cancers is based on peptide sequences. Combinatorial peptide library techniques have accelerated the identification of targeting peptides and stimulated their application due to their ease of synthesis, low immunogenicity, and desirable pharmacokinetic properties. Two of the most promising sequences found in literature are the HEWSYLAPYPWF (*39*) sequence targeted to WiDr cells and the nonapeptide, CPIEDRPMC, derived from a disulfide constrained CX_7C library and shown to bind specifically to poorly differentiated colon carcinoma cells (HT-29) (*36*).

Kelly et al. (*36*) used bacteriophage-derived libraries to select peptides binding to colon cancer cells. They used a subtraction method to distinguish between well-differentiated HCT116 and poorly differentiated HT29 colon carcinoma cells. This method yielded peptides that displayed a consensus RPM motif, which mediated preferential binding to HT29 cells. This peptide sequence was then further modified to carry an imaging agent for real-time endoscopic tumor detection in a murine model (*41*). The modified peptide had a 24 min blood half life and tumoral accumulation was 6.9% of injected dose/g, approximately 7-fold higher than a scrambled control peptide. They also observed orthotopic colonic tumors (HT29) that were readily detectable by fluorescence endoscopy even when tumors were submucosal.

In the present study, two novel linear polymeric-systems were designed, one for systemic and the other for local delivery. The former system P-GFLG-9-AC was a carrier composed of N-(2-hydroxypropyl)methacrylamide (HPMA) copolymer, 9-aminocamptothecin (9-AC), and biorecognizable cyclic nonapeptide. The anticancer drug 9-AC was attached via a spacer consisting of a lysosomal degradable linker, namely an oligopeptide spacer glycylphenylalanylleucylglycyl (GFLG) and a self-eliminating 4-aminobenzyl alcohol structure (MA-GFLF-ABA-9-AC). The nonapeptide was incorporated into the polymeric backbone via N-methacryloylglycylglycine-6-aminohexanoyl-8-amino-3,6-dioxaoctanoyl-8-amino-3,6-dioxaoctanoyl-8-amino-3,6-dioxaoctanoyl- YWKPIEDRPME (miniPEG-RPM) linker. In the latter system, a copolymer of HPMA and 9-aminocamptothecin bound via an aromatic azo bond (P-AZO-9AC) and a self-elimination spacer was synthesized. Therapeutic efficiency of a

systemic versus local approach was evaluated *in vivo* using a noninvasive orthotopic tumor model.

4.3. Materials and Methods

4.3.1. Chemicals

9-Aminocamptothecin was a generous gift from the National Cancer Institute. 9-*N*-{4-[4-(N-methacryloyl-N′-oxymethylcarbonyl-propyldiamino)-3-chlorophenyl-azo] benzylmethoxycarbonyl}aminocamptothecin (*29*), HPMA (*42*), and MA-GFLG-OH (*43*) were synthesized as described previously. Solvents and reagents used for synthesis were purchased from Aldrich (Milwaukee, WI) or Sigma (St. Louis, MO) if not specified otherwise.

4.3.2. Synthesis MA-GFLG-ABA

MA-GFLG-OH (1 g, 2.17 mmol) was dissolved in 5 ml dichloromethane (DCM), to which were added 4-Aminobenzyl alcohol (0.267 g, 2.17mmol) and *N*,*N*′-dicyclohexylcarbodiimide (0.477g, 2.17 mmol). This solution was stirred at r.t overnight. The solvent was concentrated under vacuum and dicyclohexylurea (DCU) removed by filtration. The product was purified using a preparative HPLC. The mass for *N*-methacryloylglycylphenylalanylleucylglycyl aminobenzyl alcohol (MA-GFLG-ABA) was verified via MALDI-TOF MS: (MH+) 565, found 565.76, and TLC showed one spot in ethyl acetate:hexane (1:1).

4.3.3. Synthesis MA-GFLG-ABA-9AC

9-AC (0.05 mg, 0.14 mmol), dissolved in 15 ml methylene chloride, was mixed with 1 ml of 20% phosgene solution in toluene and stirred for 2 h at r.t. The excess

phosgene and solvent were removed under vacuum. The residue was dissolved in 15 ml DCM, MA-GFLG-ABA (0.078 g, 0.14 mmol) and potassium carbonate (0.039 g, 0.28 mmol) were added, and stirred for 48 h at r.t. After evaporation of the solvent, the MA-GFLG-ABA-9AC (Fig. 4.1) was purified by preparative HPLC. The mass was verified via MALDI-TOF MS: (MH+) 955, found 978.76 (Na+ peak). The target compound was also verified via TLC using ethyl acetate:hexane (1:1) as mobile phase.

4.3.4. Peptide Synthesis

Peptides were synthesized using a solid-phase methodology and a manual Fmoc/tBu strategy on 2-chlorotrityl resin as described previously (*44*). Briefly, the peptides were prepared from the C-terminal by consecutive addition of protected amino acids (2.5 equiv.), benzotriazol-1-yl-oxytripyrrolidinophosphonium hexafluorophosphate (PyBop) (3 equiv.), and diisopropylethylamine (2.5 equiv.) to the first amino acid Fmoc-Glu(ODmab)-OH which was bound to 2-chlorotrityl resin. After the synthesis of the linear sequence N-methacryloylglycylglycine-6-aminohexanoyl-8-amino-3,6-dioxaoctanoyl-8-amino-3,6-dioxaoctanoyl-8-amino-3,6-dioxaoctanoyl-YWKPIEDRPME, the peptide was cyclized (Fig. 4.2). The cyclization (amide-bond formation) of the peptides was carried out via side-chains of lysine and glutamic acid. These two amino acids were protected via a quasi-orthogonally-protected side-chain, namely glutamic acid, that was protected via α-4-{N-[1-(4,4-dimethyl-2,6-dioxocyclohexylidene)-3-methylbutyl]amino}benzyl ester (ODmab)) and lysine via N-ε-1-(4,4-dimethyl-2,6-dioxocyclohex-1-ylidene)-3-methylbutyl (ivDde); both these groups can be selectively removed with 2% v/v hydrazine in DMF solution. The cyclization step

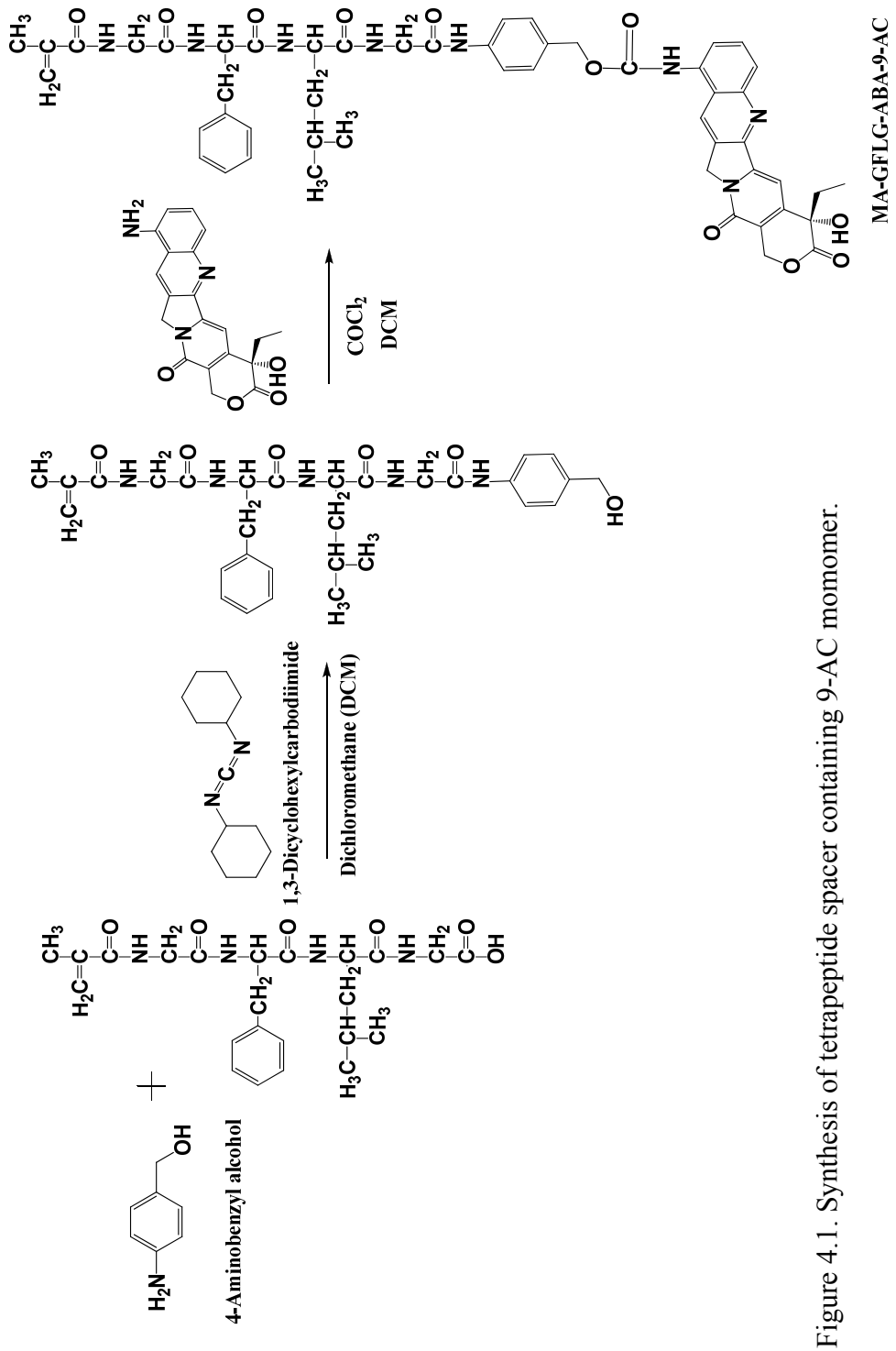

Figure 4.1. Synthesis of tetrapeptide spacer containing 9-AC momomer.

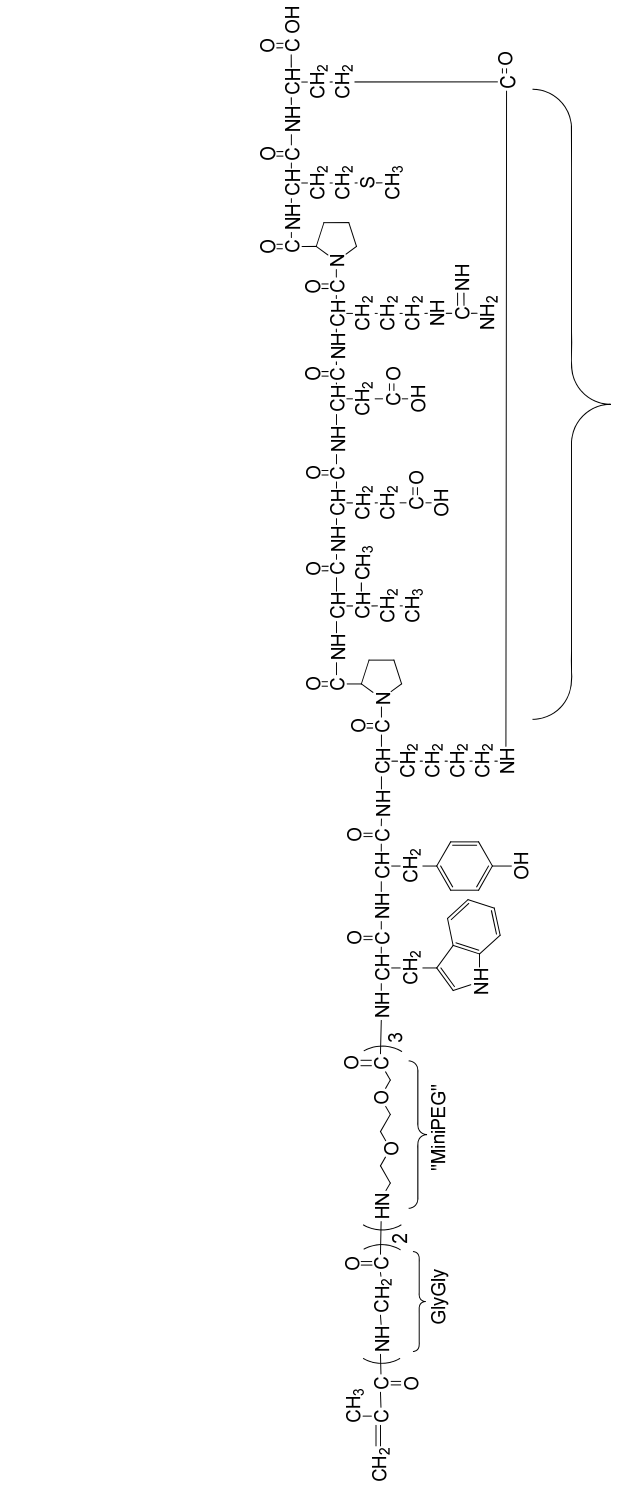

Figure 4.2. Structure of MA-MiniPEG-RPM

was carried out with PyBop (3 equiv.) in DMF for 24 h. After the desired peptide sequences were synthesized, the resulting dry resin-bound peptides were cleaved and side-chain deprotected using a TFA/H_2O/ethanedithiol/triisopropylsilane (94.5:2.5:2.5:1) cocktail. Crude peptides were purified by RP-HPLC (Agilent, 1100 Series with preparative Microsorb MV C18 column, 300 Å 5 μm, 250 × 22 mm, flow rate 8 mL · min^{-1}) employing a gradient from 2% to 90% B over 100 min, where buffer A was 0.1% TFA in water and buffer B 0.1% TFA in acetonitrile. The purity of the peptides was verified with analytical RP-HPLC. Peptide structures were ascertained by mass spectra determined by MALDI-TOF (Voyager-DE STR Biospectrometry Workstation, PerSeptive Biosystems).

4.3.5. Synthesis of a HPMA Copolymer GFLG–9AC Conjugate

HPMA copolymer-9AC conjugate, P-9AC, was synthesized by free radical copolymerization of HPMA and MA-GFLG-ABA-9AC. Typically: HPMA (100 mg, 0.7 mmol, 98 mol%), MA-GFLG-ABA-9AC (13.6 mg, 0.014 mmol, 2 mol%), and AIBN (3.5 mg, 0.021 mmol) were dissolved in methanol (0.5 mL), placed in an ampoule, purged with N_2 for 5 min, and sealed. The polymerization proceeded at 50 ^{o}C for 24 h. Then, the ampoule was cooled, opened, and the copolymer isolated by precipitation into an excess of diethyl ether/acetone (1/1 v/v). The yield of copolymer was 80 mg (~70 %). The content of 9-AC in the polymeric conjugate was measured by UV-spectrophotometry (360 nm, ε = 12000 M^{-1} cm^{-1}, in MeOH) (Fig. 4.3B).

4.3.6. Synthesis of HPMA Copolymer GFLG–9AC-RPM Conjugate

HPMA copolymer-9AC conjugate, P-9AC-RPM, was synthesized by free radical copolymerization of HPMA, MA-GFLG-ABA-9AC, and RPM macromonomer. Typically: HPMA (100 mg, 0.7 mmol, 96 mol%), MA-GFLG-ABA-9AC (13.9 mg, 0.0145 mmol, 2 mol%), RPM macromonomer (30 mg, 0.0145 mmol, 2 mol%), and AIBN (3.6 mg, 0.022 mmol) were dissolved in methanol (0.5 mL), placed in an ampoule, purged with N_2 for 5 min, and sealed. The polymerization proceeded at 50 ^{o}C for 24 h. Then, the ampoule was cooled, opened, and the copolymer isolated by precipitation into an excess of diethyl ether/acetone (1/1 v/v). The yield of copolymer was 100 mg (~70 %). The content of drug (9-AC) and peptide in the polymeric conjugate was measured by UV-spectrophotometry (9-AC: 360 nm, $\varepsilon = 12000\ M^{-1}\ cm^{-1}$, in MeOH, peptide: 280 nm, $\varepsilon = 6990\ M^{-1}\ cm^{-1}$, in PBS buffer) (Fig. 4.3C) (Table 4.1).

4.3.7. Synthesis of HPMA Copolymer AZO-9AC Conjugate

HPMA copolymer-9AC conjugate, P-9AC-RPM, was synthesized by free radical copolymerization of HPMA and MA-AZO-9AC. Typically: HPMA (100 mg, 0.7 mmol, 96 mol%), MA-AZO-9AC (12.09 mg, 0.0145 mmol, 2 mol%), and AIBN (3.6 mg, 0.022 mmol) were dissolved in methanol (0.5 mL), placed in an ampoule, purged with N_2 for 5 min, and sealed. The polymerization proceeded at 50 ^{o}C for 24 h. Then, the ampoule was cooled, opened, and the copolymer isolated by precipitation into an excess of diethyl ether/acetone (1/1 v/v). The yield of copolymer was 100 mg (~70 %). The content of

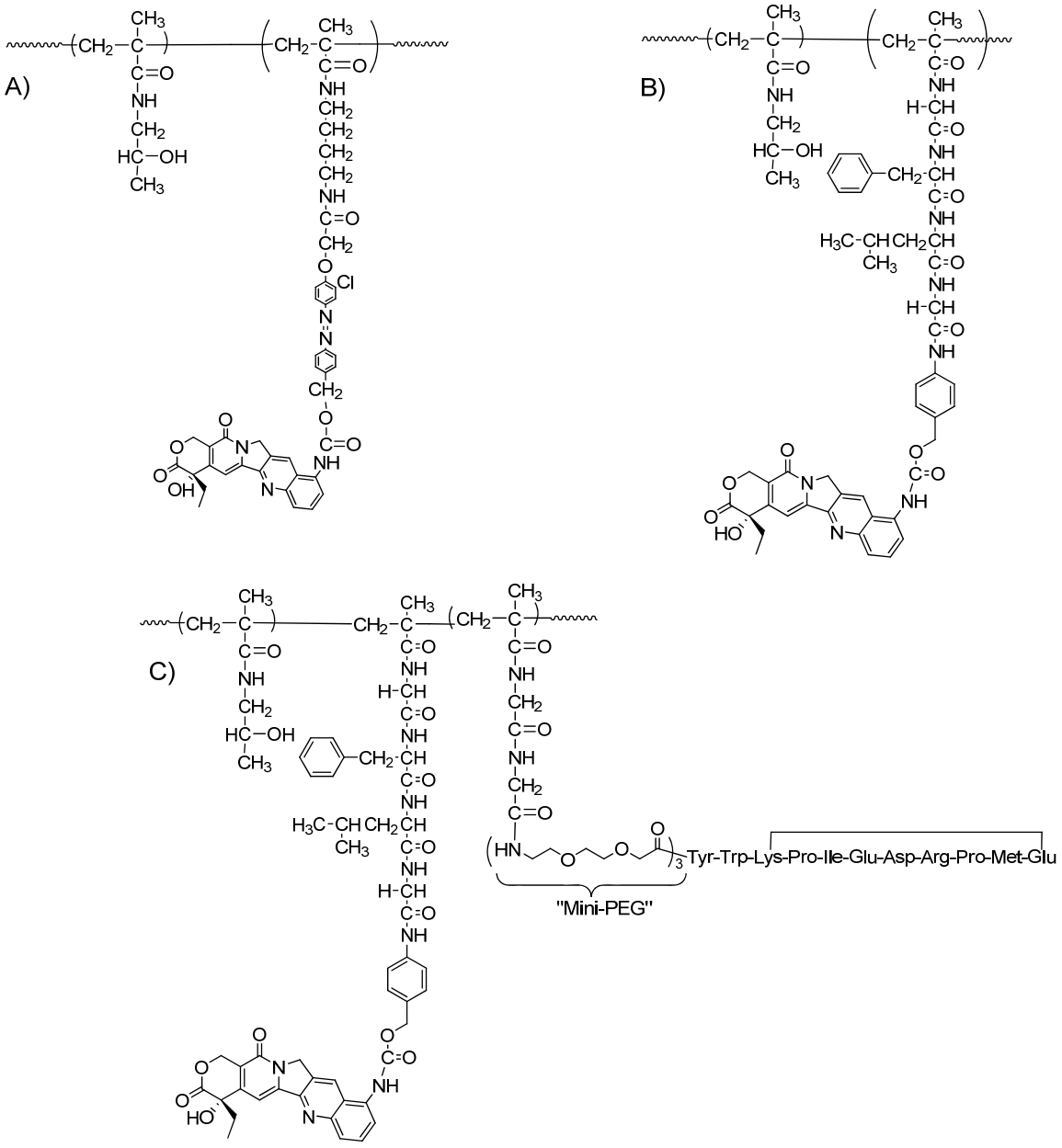

Figure 4.3. A) HPMA–AZO-9AC Copolymer, B) HPMA-GFLG–9AC Conjugate, C) HPMA-GFLG–9AC-RPM Conjugate.

Table 4.1. Characterization of HPMA copolymers

Conjugates	Mw[a] (kDa)	P[b]	Peptide / macromolecule	9-AC content mol . g^{-1}	9-AC Wt %
P-GFLF-9AC	34	1.5	---	$1.48x10^{-4}$	16.48
P-GFLG-9AC-RPM	30	1.4	2	$4.32x10^{-5}$	4.30
P-AZO-9AC	28	1.9	---	$2.11x10^{-5}$	1.82

[a]Determined by SEC using the AKTA FPLC system (Pharmacia) on Superose 6 columns calibrated with PHPMA samples; [b] polydispersity (Mw/Mn); [c]Determined by UV spectrophotometry in methanol.

drug (9-AC) and peptide in the polymeric conjugate was measured by UV-spectrophotometry (9-AC: 360 nm, ε = 12000 M^{-1} cm^{-1}, in MeOH) (Fig. 4.3A) (Table 4.1).

4.3.8. Animals

Female nu/nu mice, 15–19 g bodyweight, were purchased from Charles River (Wilmington, MA) and kept in a typical laboratory environment: five per cage with an air filter cover under light (12 h light/dark cycle) and temperature control (22±1 °C). All animals received care in compliance with the "Principles of Laboratory Animal Care" and "Guide for the Care and Use of Laboratory Animals". Experiments followed an approved protocol from the University of Utah Institutional Animal Care and Use Committee.

4.3.9. Cells

The human colorectal adenocarcinoma HT29 cell line was obtained from American Type Culture Collection (ATCC) (Manassas, VA). Cells were grown in McCoy's 5a medium supplemented with 10% FBS, 2 mM glutamine at 37 °C in 5% CO_2 and 95% humidified air. The cells were regularly subcultured to maintain a logarithmic phase of growth.

4.3.10. HT-29 Orthotropic Tumor Model

Female nu/nu mice (5-6 weeks of age, 15 – 17 gm in weight) were used for the evaluation. The mice were purchased from Charles River (Wilmington, MA). The technique for cell implantation has been described previously by Cowen et al. (*45*). The brief procedure is as follows: Mice were anesthetized with ketamine, and the abdomen

was prepared for sterile surgery. A small abdominal incision was made, and the cecum was exteriorized and isolated on sterile gauze. A suspension of luciferase-expressing HT-29 cells (2 X 10^6 cell/100 µl/mouse) containing 0.5 mg of "matrigel" basement membrane matrix (Matrigel, Becton Dickinson Bioscience, MA) were injected into the cecal wall from the serosal side with a 28-gauge needle. After injection, the cecum was returned to the abdominal cavity and the incision in the abdominal wall sealed using the tissue adhesive. Orthotopic tumors usually developed within 1 week after the transplantation.

4.3.11. In Vivo Imaging

Five minutes prior to imaging, mice were anaesthetized with ketamine (100 mg/kg intraperitoneally) and xylazine (10 mg/kg intraperitoneally), and an aqueous solution of luciferin (150 mg/kg intraperitoneally) (Xenogen, Alameda, CA). Animals were placed into the light-tight chamber of the CCD camera system (IVIS 100, Xenogen), and a grayscale body surface reference image (digital photograph) was taken under weak illumination. After switching off the light source, photons emitted from luciferase expressing cells within the animal body and transmitted through the tissue were quantified over a 1 min period using the software program "Living Image" (Xenogen) as an overlay on Igor (Wavemetrics, Seattle, WA). For anatomical localization, a pseudocolor image representing light intensity (blue, least intense; red, most intense) was generated in "Living Image" and superimposed over the grayscale reference image.

4.3.12. Antitumor Activity

The HPMA copolymer–9-AC conjugates (P-AZO-9AC, P-GFLG-9AC, P-GFLF-9AC-miniPEG-RPM) were dissolved in saline, whereas free 9-AC was dissolved in dimethyl acetamide (DMA), and then mixed with diluents containing 51% polyethylene glycol (PEG) 400, and 49% 0.01M phosphoric acid . The final solution consisted of 6% DMA, 48% PEG 400, and 46% 0.01 M phosphoric acid (*46*). For oral or intravenous (IV) injection administration, three doses (2 mg/kg 9-AC equivalent on each of days 1, 5 and 9) of free drug or polymeric conjugates were administered (*47*). Tumor volume and body weight were measured weekly for 5 weeks. Tumor growth inhibition (%T/C) was used to determine antitumor effectiveness.

4.4. Results and Discussions

Two novel, linear polymeric systems were designed for systemic delivery, one containing a biorecognizable sequence and the other without. This polymeric system was compared to a polymer designed for local delivery. The former system P-GFLG-9-AC was a carrier composed of N-(2-hydroxypropyl)methacrylamide (HPMA) copolymer, 9-aminocamptothecin (9-AC), and biorecognizable cyclic nonapeptide. The anticancer drug 9-AC was attached via a spacer consisting of a lysosomally degradable linker, namely an oligopeptide spacer glycylphenylalanylleucylglycyl (GFLG) and a self-eliminating 4-aminobenzyl alcohol structure. The nonapeptide was incorporated into the polymeric backbone via N-methacryloylglycylglycine-6-aminohexanoyl-8-amino-3,6-dioxaoctanoyl-8-amino-3,6-dioxaoctanoyl-8-amino-3,6-dioxaoctanoyl- YWKPIEDRPME (miniPEG-RPM) linker. The peptides used in the preparation of conjugates were

synthesized by solid phase peptide synthesis. The amide-bond cyclization between K and E was performed on peptide still attached to the beads. The novel targeted and untargeted conjugates were synthesized, by copolymerization of HPMA, MA-GFLG-9AC, and with or without macromonomer RPM, respectively. In the latter system, a copolymer of HPMA and 9-aminocamptothecin bound via an aromatic azo bond (P-AZO-9AC) and a self-elimination spacer was synthesized. This copolymer was also synthesized by free radical polymerization of HPMA and MA-AZO-9AC.

The HPMA copolymer conjugates were purified on a Sephadex LH20 column to remove any unreacted monomers. The molecular weights distributions were characterized by using an analytical Superose 6 (HR16/60) column (Table 4.1).

Design of an animal model of colorectal cancer that can be used to track tumor progression noninvasively is very important in the development and evaluation of novel therapeutics. The result presented demonstrates the remarkable sensitivity of bioluminescence-based imaging strategies and the ability to quantitatively measure tumor burden over the entire spectrum of disease. This approach has several advantages over conventional tumor models. First, the sensitivity of cell detection in vivo is surprisingly high. Only 5 days after tumor injection, a strong signal can be detected, with progressive increase in signal intensity with increase in tumor size. Second, since cells can be detected deep with the tissue, tumor cell trafficking and metastasis could be visualized. Using this technology, it is possible to study early stages of tumor development long before any clinical signs of disease are evident as well as the efficiency of therapeutic interventions in minimal disease stages.

In these initial experiments, the tranduced cell line HT-29-*luc* was implanted into female nu/nu animals as proof of principle. Initial studies showed that therapeutic efficiency of the polymer conjugates could be visualized noninvasively. The effect of 9-AC and 9-AC conjugates, P-AZO-9AC, P-GFLG-9AC, and P-GFLF-9AC-RPM, were studied. A drug dose of 2 mg/kg 9-AC equivalent on each of days 1, 5, and 9 was used based on previously published results from Conover et al. (*47*).

Antitumor effect of HPMA-9AC conjugates was assessed in orthotopic tumor model using bioluminescence imaging. A retroviral transduction system was used for the delivery of a luciferase gene into HT-29 cells. This yielded a transduced cells line that showed positive expression of luciferase (Fig. 4.4). These cells ($2x10^6$ cell/mice) were then injected into the cecal wall of female nu/nu mice from the serosal side, which allowed the noninvasive visualization of tumor progression (Fig. 4.5). Only 60 % of the mice injected with cell-generated tumors. Repetitive imaging of individual mice showed that the cell growth followed an exponential growth. The tumor distribution pattern of one representative control animal shows tumor metastatic infiltration (Fig. 4.6).

Mice that generated tumors were randomly divided into six groups (n=6): a) untreated, b) free drug (oral), c) P-AZO-9-AC (oral), d) P-GFLG-9-AC (i.v.), e) P-GFLF-9-AC-minPEG-PRM (i.v.), f) combination of P-GFLG-9-AC (i.v) and P-AZO-9-AC (oral). As expected, animals within a control group that received no treatment showed a continuous increase in their tumor signal (Fig. 4.7A). In contrast, treatment groups (n=6) resulted in a substantial reduction in tumor within 20 days. This was followed by a relapse 2 to 3 weeks after treatment and exponential growth of the tumor over the

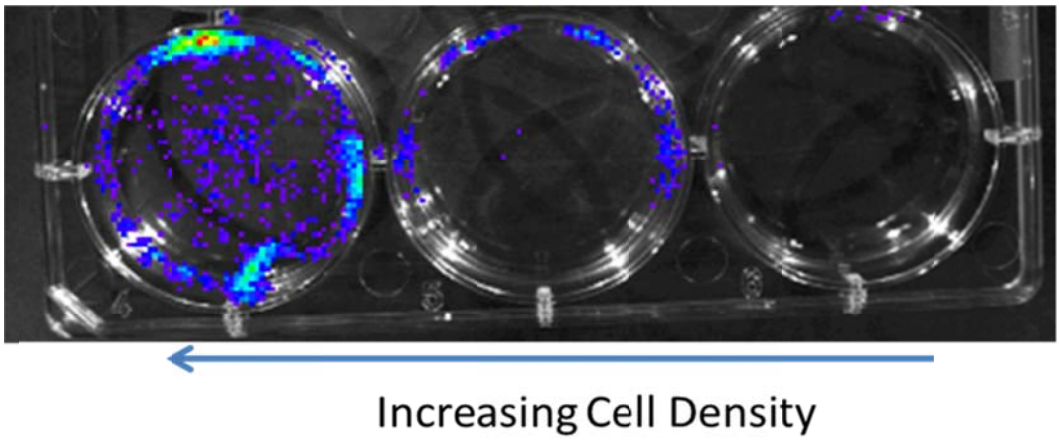

Figure 4.4. Positive expression of HT-29 transfected with luciferase gene, imaged using a CCD camera system (IVIS, Xenogen).

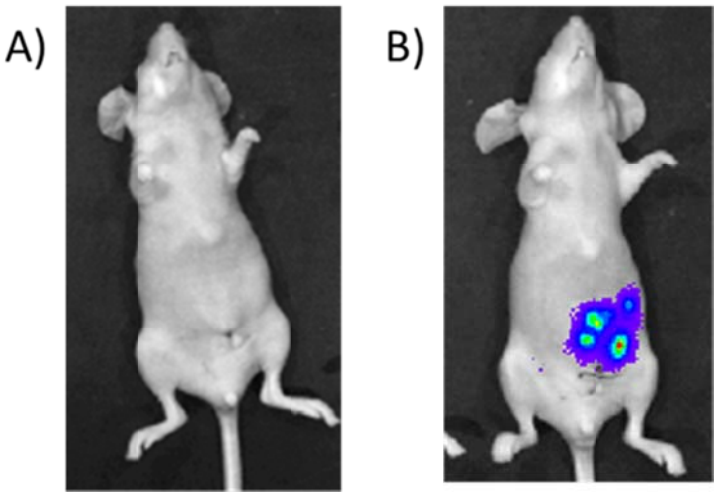

Figure 4.5. $2x10^6$ HT-29 cells injected into the cecal wall. Five days after injection, a bioluminescent signal was detectable from the mouse. A) Mouse that did not generate tumors. B) Strong signal from positive mice.

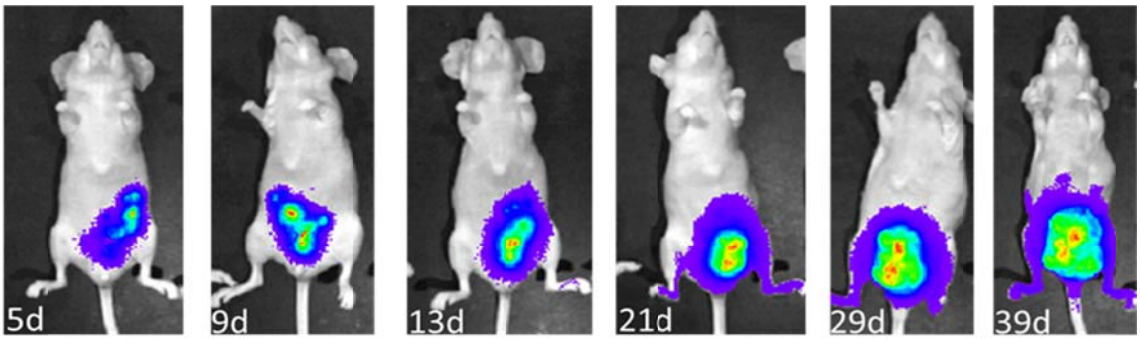

Figure 4.6. Tumor distribution pattern of one representative control mouse, Day 5, 9, 13, 21, 29, and 39 after injection of tumor into cecal wall.

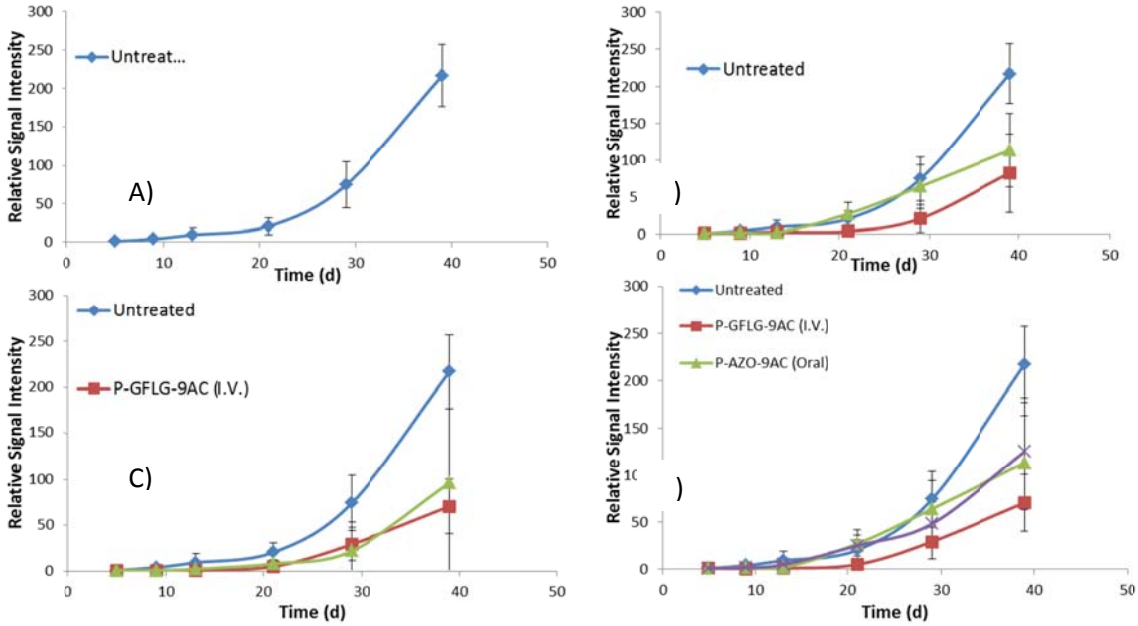

Figure 4.7. Tumor regression in response to chemotherapy. A) Growth of untreated mice, B) comparison of oral delivery systems, C) comparison of targeted and untargeted conjugates given systemically, D) comparison between systemic, oral delivery, and combination delivery.

remaining observation time of 5 weeks (Fig. 4.7B-D). Polymer conjugates given systemically performed slightly better than the conjugates given orally (Fig. 4.76D). However, there was no difference in the therapeutic effects among the targeted or untargeted conjugates (Fig. 4.7C).

While all delivery systems improved survival of animals with tumors, no cures were obtained. This model can be used for future experiments with dose escalation and biodistribution studies to obtain more insight into the delivery systems used.

In conclusion, bioluminescence-based imaging strategies are a powerful tool to study tumor progression. This noninvasive, highly sensitive, and quantitative approach is ideally suited for evaluation of novel drug delivery systems. Further evaluation using both systemic and local approach is warranted to obtain conclusive results regarding the benefit of either system. Finally, dose escalation studies can be performed to optimize the therapeutic dose.

4.5 References

(1) Jemal, A., Siegel, R., Ward, E., Murray, T., Xu, J., and Thun, M. J. (2007) Cancer Statistics, 2007 *CA Cancer J Clin 57*, 43-66.

(2) Nicum, S., Midgley, R., and Kerr, D. J. (2003) Colorectal cancer. *Acta Oncol 42*, 263-275.

(3) Nicum, S., Midgley, R., and Kerr, D. J. (2000) Chemotherapy for colorectal cancer. *J R Soc Med 93*, 416-419.

(4) Xiong, H. Q., and Ajani, J. A. (2004) Treatment of colorectal cancer metastasis: the role of chemotherapy. *Cancer Metastasis Rev 23*, 145-163.

(5) Benson, A. B., 3rd. (2006) New approaches to the adjuvant therapy of colon cancer. *Oncologist 11*, 973-980.

(6) Rosen, L. S., Bilchik, A. J., Beart, R. W., Jr., Benson, A. B., 3rd, Chang, K. J., Compton, C. C., Grothey, A., Haller, D. G., Ko, C. Y., Lynch, P. M., Nelson, H., Stamos, M. J., Turner, R. R., and Willett, C. G. (2007) New approaches to assessing and treating early-stage colon and rectal cancer: summary statement from 2007 Santa Monica Conference. *Clin Cancer Res 13*, 6853s-6856s.

(7) Wall, M. E. W., M.C. Cook, C.E. Palmer, K.H. McPhail, A.I. Sim, G.A. (1966) Plant antitumor agents. I. The isolation and structure of camptothecin, a novel alkaloidal leukemia and tumor inhibitor from camptotheca acuminate. *J. Am. Chem. Soc 88*, 3888-3890.

(8) Hsiang, Y. H., Hertzberg, R., Hecht, S., and Liu, L. F. (1985) Camptothecin induces protein-linked DNA breaks via mammalian DNA topoisomerase I. *J Biol Chem 260*, 14873-14878.

(9) Hsiang, Y. H., and Liu, L. F. (1988) Identification of mammalian DNA topoisomerase I as an intracellular target of the anticancer drug camptothecin. *Cancer Res 48*, 1722-1726.

(10) Ulukan, H., and Swaan, P. W. (2002) Camptothecins: a review of their chemotherapeutic potential. *Drugs 62*, 2039-2057.

(11) Kingsbury, W. D., Boehm, J. C., Jakas, D. R., Holden, K. G., Hecht, S. M., Gallagher, G., Caranfa, M. J., McCabe, F. L., Faucette, L. F., Johnson, R. K., and et al. (1991) Synthesis of water-soluble (aminoalkyl)camptothecin analogues: inhibition of topoisomerase I and antitumor activity. *J Med Chem 34*, 98-107.

(12) Takimoto, C. H., Dahut, W., Marino, M. T., Nakashima, H., Liang, M. D., Harold, N., Lieberman, R., Arbuck, S. G., Band, R. A., Chen, A. P., Hamilton, J. M., Cantilena, L. R., Allegra, C. J., and Grem, J. L. (1997) Pharmacodynamics and pharmacokinetics of a 72-hour infusion of 9-aminocamptothecin in adult cancer patients. *J Clin Oncol 15*, 1492-1501.

(13) Dahut, W., Harold, N., Takimoto, C., Allegra, C., Chen, A., Hamilton, J. M., Arbuck, S., Sorensen, M., Grollman, F., Nakashima, H., Lieberman, R., Liang, M., Corse, W., and Grem, J. (1996) Phase I and pharmacologic study of 9-aminocamptothecin given by 72-hour infusion in adult cancer patients. *J Clin Oncol 14*, 1236-1244.

(14) Pan, H., Liu, J., Dong, Y., Sima, M., Kopečková, P., Brandi, M. L., and Kopeček, J. (2008) Release of Prostaglandin E(1) from N-(2-Hydroxypropyl)methacrylamide Copolymer Conjugates by Bone Cells. *Macromol Biosci*.

(15) Cuchelkar, V., Kopečková, P., and Kopeček, J. (2008) Synthesis and Biological Evaluation of Disulfide-Linked HPMA Copolymer-Mesochlorin e(6) Conjugates. *Macromol Biosci*, 375-383.

(16) Hongrapipat, J., Kopečková, P., Prakongpan, S., and Kopeček, J. (2008) Enhanced antitumor activity of combinations of free and HPMA copolymer-bound drugs. *Int J Pharm 351*, 259-270.

(17) Wang, D., Sima, M., Mosley, R. L., Davda, J. P., Tietze, N., Miller, S. C., Gwilt, P. R., Kopečková, P., and Kopeček, J. (2006) Pharmacokinetic and biodistribution studies of a bone-targeting drug delivery system based on N-(2-hydroxypropyl)methacrylamide copolymers. *Mol Pharm 3*, 717-725.

(18) Rihova, B., Ulbrich, K., Kopeček, J., and Mancal, P. (1983) Immunogenicity of N-(2-hydroxypropyl)-methacrylamide copolymers--potential hapten or drug carriers. *Folia Microbiol (Praha) 28*, 217-227.

(19) Rihova, B., Bilej, M., Vetvicka, V., Ulbrich, K., Strohalm, J., Kopeček, J., and Duncan, R. (1989) Biocompatibility of N-(2-hydroxypropyl) methacrylamide copolymers containing adriamycin. Immunogenicity, and effect on haematopoietic stem cells in bone marrow in vivo and mouse splenocytes and human peripheral blood lymphocytes in vitro. *Biomaterials 10*, 335-342.

(20) de Jonge, M. J., Punt, C. J., Gelderblom, A. H., Loos, W. J., van Beurden, V., Planting, A. S., van der Burg, M. E., van Maanen, L. W., Dallaire, B. K., Verweij, J., Wagener, D. J., and Sparreboom, A. (1999) Phase I and pharmacologic study of oral (PEG-1000) 9-aminocamptothecin in adult patients with solid tumors. *J Clin Oncol 17*, 2219-2226.

(21) Morgan, M. T., Nakanishi, Y., Kroll, D. J., Griset, A. P., Carnahan, M. A., Wathier, M., Oberlies, N. H., Manikumar, G., Wani, M. C., and Grinstaff, M. W. (2006) Dendrimer-encapsulated camptothecins: increased solubility, cellular uptake, and cellular retention affords enhanced anticancer activity in vitro. *Cancer Res 66*, 11913-11921.

(22) Kehrer, D. F., Soepenberg, O., Loos, W. J., Verweij, J., and Sparreboom, A. (2001) Modulation of camptothecin analogs in the treatment of cancer: a review. *Anticancer Drugs 12*, 89-105.

(23) Gao, S. Q., Lu, Z. R., Kopeckova, P., and Kopecek, J. (2007) Biodistribution and pharmacokinetics of colon-specific HPMA copolymer--9-aminocamptothecin conjugate in mice. *J Control Release 117*, 179-185.

(24) Gao, S. Q., Lu, Z. R., Petri, B., Kopeckova, P., and Kopecek, J. (2006) Colon-specific 9-aminocamptothecin-HPMA copolymer conjugates containing a 1,6-elimination spacer. *J Control Release 110*, 323-331.

(25) Lu, Z. R., Shiah, J. G., Sakuma, S., Kopeckova, P., and Kopecek, J. (2002) Design of novel bioconjugates for targeted drug delivery. *J Control Release 78*, 165-173.

(26) Gao, S. Q., Sun, Y., Kopeckova, P., Peterson, C. M., and Kopecek, J. (2008) Pharmacokinetic modeling of absorption behavior of 9-aminocamptothecin (9-AC) released from colon-specific HPMA copolymer-9-AC conjugate in rats. *Pharm Res 25*, 218-226.

(27) Sakuma, S., Lu, Z. R., Kopeckova, P., and Kopecek, J. (2001) Biorecognizable HPMA copolymer-drug conjugates for colon-specific delivery of 9-aminocamptothecin. *J Control Release 75*, 365-379.

(28) Gao, S. Q., Lu, Z. R., Kopečková, P., and Kopeček, J. (2007) Biodistribution and pharmacokinetics of colon-specific HPMA copolymer--9-aminocamptothecin conjugate in mice. *J Control Release 117*, 179-185.

(29) Gao, S. Q., Lu, Z. R., Petri, B., Kopečková, P., and Kopeček, J. (2006) Colon-specific 9-aminocamptothecin-HPMA copolymer conjugates containing a 1,6-elimination spacer. *J Control Release 110*, 323-331.

(30) Gao, S. Q., Sun, Y., Kopečková, P., Peterson, C. M., and Kopeček, J. (2008) Pharmacokinetic modeling of absorption behavior of 9-aminocamptothecin (9-AC) released from colon-specific HPMA copolymer-9-AC conjugate in rats. *Pharm Res 25*, 218-226.

(31) Sakuma, S., Lu, Z. R., Kopečková, P., and Kopeček, J. (2001) Biorecognizable HPMA copolymer-drug conjugates for colon-specific delivery of 9-aminocamptothecin. *J Control Release 75*, 365-379.

(32) Matsumura, Y., and Maeda, H. (1986) A new concept for macromolecular therapeutics in cancer chemotherapy: mechanism of tumoritropic accumulation of proteins and the antitumor agent smancs. *Cancer Res 46*, 6387-6392.

(33) Omelyanenko, V., Kopečková, P., Gentry, C., and Kopeček, J. (1998) Targetable HPMA copolymer-adriamycin conjugates. Recognition, internalization, and subcellular fate. *J Control Release 53*, 25-37.

(34) Roovers, R. C., van der Linden, E., de Bruine, A. P., Arends, J. W., and Hoogenboom, H. R. (2001) Identification of colon tumor-associated antigens by phage antibody selections on primary colorectal carcinoma. *Eur J Cancer 37*, 542-549.

(35) Welt, S., Divgi, C. R., Scott, A. M., Garin-Chesa, P., Finn, R. D., Graham, M., Carswell, E. A., Cohen, A., Larson, S. M., and Old, L. J. (1994) Antibody targeting in metastatic colon cancer: a phase I study of monoclonal antibody F19 against a cell-surface protein of reactive tumor stromal fibroblasts. *J Clin Oncol 12*, 1193-1203.

(36) Kelly, K. A., and Jones, D. A. (2003) Isolation of a colon tumor specific binding peptide using phage display selection. *Neoplasia 5*, 437-444.

(37) Laburthe, M., Rousset, M., Chevalier, G., Boissard, C., Dupont, C., Zweibaum, A., and Rosselin, G. (1980) Vasoactive intestinal peptide control of cyclic adenosine 3':5'-monophosphate levels in seven human colorectal adenocarcinoma cell lines in culture. *Cancer Res 40*, 2529-2533.

(38) Pallela, V. R., Thakur, M. L., Chakder, S., and Rattan, S. (1999) 99mTc-labeled vasoactive intestinal peptide receptor agonist: functional studies. *J Nucl Med 40*, 352-360.

(39) Rasmussen, U. B., Schreiber, V., Schultz, H., Mischler, F., and Schughart, K. (2002) Tumor cell-targeting by phage-displayed peptides. *Cancer Gene Ther 9*, 606-612.

(40) Hsiung, P. L., Hardy, J., Friedland, S., Soetikno, R., Du, C. B., Wu, A. P., Sahbaie, P., Crawford, J. M., Lowe, A. W., Contag, C. H., and Wang, T. D. (2008) Detection of colonic dysplasia in vivo using a targeted heptapeptide and confocal microendoscopy. *Nat Med 14*, 454-458.

(41) Kelly, K., Alencar, H., Funovics, M., Mahmood, U., and Weissleder, R. (2004) Detection of invasive colon cancer using a novel, targeted, library-derived fluorescent peptide. *Cancer Res 64*, 6247-6251.

(42) Kopeček, J., and Bazilova, H. (1973) Poly[N-(2-Hydroxypropyl)methacrylamide]. 1. Radical Polymerization and Copolymerization. *Eur Polym J 9*, 7-14.

(43) Rejmanová, P., Pohl, J., Baudys, M., Kostka, V., and Kopeček, J. (1983) Polymers Containing Enzymatically Degradable Bonds. 8. Degradation of Oligopeptide Sequences in N-(2-Hydroxypropyl)methacrylamide Copolymers by Bovine Spleen Cathepsin B. *Makromol. Chem 184*, 2009-2020.

(44) Pechar, M., Kopeckova, P., Joss, L., and Kopecek, J. (2002) Associative diblock copolymers of poly(ethylene glycol) and coiled-coil peptides. *Macromolecular Bioscience 2*, 199-206.

(45) Cowen, S. E., Bibby, M. C., and Double, J. A. (1995) Characterisation of the vasculature within a murine adenocarcinoma growing in different sites to evaluate the potential of vascular therapies. *Acta Oncol 34*, 357-360.

(46) Mani, S., Iyer, L., Janisch, L., Wang, X., Fleming, G. F., Schilsky, R. L., and Ratain, M. J. (1998) Phase I clinical and pharmacokinetic study of oral 9-aminocamptothecin (NSC-603071). *Cancer Chemother Pharmacol 42*, 84-87.

(47) Conover, C. D., Greenwald, R. B., Pendri, A., Gilbert, C. W., and Shum, K. L. (1998) Camptothecin delivery systems: enhanced efficacy and tumor accumulation of camptothecin following its conjugation to polyethylene glycol via a glycine linker. *Cancer Chemother Pharmacol 42*, 407-414.

CHAPTER 5

CONCLUSIONS AND FUTURE WORK

5.1. Specific Aim 1. Design and Synthesis of Novel Interpenetrating Network (IPN) Hydrogels for Colon-Specific Drug Delivery

To investigate the structure - property relationship of interpenetrating network (IPN) hydrogels suitable as colon-specific drug delivery systems, we have synthesized and evaluated the properties of IPN hydrogels composed from pH-sensitive, aromatic azo group-containing hydrogels as the first component, and a hydrolyzable network as the second. Interpenetrating network (IPN) hydrogels composed of pH-sensitive, aromatic azo group-containing hydrogels as one of its components (Network A), and a hydrolyzable network as the other were synthesized (Network B) and were prepared by a sequential process. The properties of IPNs with the aim of identification of structures suitable as colon-specific drug delivery systems were investigated.

The first network was formed by crosslinking of a reactive polymer precursor (copolymer of *N*,*N*-dimethylacrylamide, acrylic acid, N-tert.butylacrylamide, and *N*-methacryloyl-glycylglycine p-nitrophenyl ester) with an aromatic azo group-containing diamine ((*N*,*N*'-ε-aminocaproyl)-4,4'-diaminoazobenzene). The second network was formed by radical crosslinking copolymerization of *N*-(2-hydroxypropyl)methacrylamide with N,O-dimethacryloylhydroxylamine. Hydrogels synthesized in this manner were

homogeneous and showed no evidence of phase separation. The composition of the hydrogels was manipulated to determine the influence of hydrogel composition on the equilibrium degree of swelling, modulus of elasticity in compression, and on the rate of degradation of Network B. To mimic the conditions in the gastrointestinal tract, properties of the hydrogels were evaluated after abrupt change of pH from pH 2.0 to pH 7.4. The analysis of IPN structure revealed that crosslinking efficiency of radically polymerized Network B (10-30%) was lower than that of step polyaddition Network A. In the IPN gels, the crosslinking efficiency was even lower and was close to 10%. Factors contributing to the low crosslinking efficiency of IPN include higher dilution at network formation and possible negative effect of the components of Network A on radical polymerization of Network B. The major advantage of IPN hydrogels, when compared to traditional pH-sensitive networks, is the linear swelling profile following abrupt change of pH from 2 to 7.4. This indicates the potential of IPNs as carriers for oral drug delivery.

5.2. Specific Aim 2. Design and Evaluation of a Targeted HPMA-Copolymer

Targeting is one of the primary considerations in designing a specific and efficient drug delivery system. Here, a colon cancer-specific targeted polymeric drug delivery carrier was developed by conjugating a cyclic constrained nonapeptide into the water-soluble N-(2-hydroxypropyl)methacrylamide (HPMA) copolymer. HPMA copolymer-RPM1 conjugate was prepared by binding of RPM1 to an HPMA copolymer precursor via glycylglycine side-chains. The macromonomer RPM2 was copolymerized with

HPMA and N-methacryloylaminopropyl fluorescein thiourea (MA-FITC) to produce an HPMA copolymer-RPM2 conjugate.

The impact of the structure of the HPMA copolymer-peptide conjugates on the biorecognition by poorly differentiated HT-29 colon carcinoma cells was investigated. The binding to and internalization by HT-29 cells were visualized by a radioiodination assay, flow cytometry, and confocal fluorescence microscopy. The free peptide RPM3 and HPMA copolymer-RPM1 and HPMA copolymer-RPM2 conjugates possessed low binding affinities; the K_d was in the 10^{-4} M range. However, flow cytometry data demonstrated clear shifts in fluorescence profiles when comparing control polymers, P(H)-FITC and P(L)-FITC, with corresponding HPMA copolymer conjugates containing peptides RPM1 or RPM2. Confocal fluorescence data clearly indicated a faster internalization of RPM3 when compared to a nonspecific sequence (NSP).

5.3. Specific Aim 3. In Vivo Evaluation of Novel Colon Cancer Targeted HPMA-9-Aminocamptothecin

A major challenge in cancer chemotherapy is the selective delivery of small molecule anticancer agents to tumor cells. Water-soluble polymer-drug conjugates exhibit good water solubility, increased halflife, and potent antitumor effects. By localizing the drug at the desired site of action, macromolecular therapeutics have improved efficacy and enhanced safety at lower doses. In this study, two novel, linear polymeric-systems were designed, one for systemic and the other for local delivery. The former system was a carrier composed of N-(2-hydroxypropyl)methacrylamide (HPMA) copolymer, 9-aminocamptothecin (9-AC), and biorecognizable cyclic nonapeptide. The anticancer drug 9-AC was attached via a spacer consisting of a lysosomal degradable

linker, namely an oligopeptide spacer glycylphenylalanylleucylglycyl (GFLG) and a self-eliminating 4-aminobenzyl alcohol structure. In the latter system, a copolymer of HPMA and 9-aminocamptothecin bound via an aromatic azo bond and a self-elimination spacer was synthesized.

Since small molecule drugs and macromolecular drugs enter cells by different pathways, multidrug resistance (MDR) can be minimized. Therapeutic efficiency of a systemic versus local approach was also evaluated *in vivo* using a noninvasive bioluminescence imaging tumor model. To this end, six groups were compared: a) untreated, b) free drug (oral), c) P-AZO-9-AC (oral), d) P-GFLG-9-AC (i.v.), e) P-GFLF-9-AC-minPEG-RPM (i.v.), f) combination of P-GFLG-9-AC (i.v) and P-AZO-9-AC (oral). Mice treated with the polymer conjugates containing 9-AC or free drug had significantly longer tumor growth delay compared to untreated controls. Polymer conjugates given systemically performed slightly better than the conjugates given orally. However, there was no difference in the therapeutic effects among the targeted or untargeted conjugates.

5.4. Future Work

Studies outlined in this thesis tried to investigate novel drug delivery strategies to reduce the nonspecific toxicities of conventional chemotherapeutics. Optimization of the binding affinity and due to the recent advances in cancer biology, selecting new targets can potentially increase the specificity of the delivery systems. Hence, the future work described below discusses the next generation of targeted therapeutics.

5.4.1. Optimization of RPM Peptide Sequence

High-affinity and high-specificity peptide can be potentially derived from the cyclic constrained nonapeptide, KPIEDRPME, by optimizing the sequence of the non-essential amino acids present (*1*). The first and last amino acids of this sequence are required for the cyclization process, and the RPM motif is essential for the biorecognition. Hence, the four amino acids flanking the RPM sequence can be altered to select peptides with a superior binding affinity. A combinatorial approach can be very advantageous in deriving novel sequences using a biased library (*2, 3*).

5.4.3. In Vivo Studies

The data for the preliminary in vivo experiments can be used to design two additional experiments. First, a dose escalation study can be performed to optimize the therapeutic regiment. Second, biodistribution studies can be used to determine the efficacy of the targeted HPMA conjugates to localize preferentially within the solid tumor.

5.4.2. Selective Targeting of Cancer Stem Cells

Conventional targeted therapies have been designed largely to target receptors that are overexpressed on the majority of tumor cells. While these therapies target and kill differentiated tumor cells, they spare a subset of population termed cancer stem cells (CSCs). Current advances in cancer stem cell biology suggest this subset of cells has the capacity to initiate tumors and possess therapeutic resistance (*4, 5*). This leads to the failure of current therapeutics to cure most cancer.

Al-Hajj et al. (*6*) was one of the first groups to identify cancer stem cells in solid tumors. Since then, numerous markers have been identified in a variety of tumors (Table

5.1). Hence, novel therapeutic agents can be designed to target this subset of population. Markers like CD44 and CD133+ (activated leukocyte cell adhesion molecule) are differentially expressed markers on the colon cancer stem cell (*7, 8*). Hence, antibodies or novel peptide targets to these cells can potentially increase the cure rate for CRC.

Table 5.1 List of Tumor Stem Cell Markers

Cancer/tumor type	Markers	Reference
Breast	CD44+CD24−/low, CK+, Hedgehog components	(*9-11*)
Prostate	c-myc, beta-catenin, CD44(+), D133(+), ABCG2, Androgen receptor, CD44+/alpha2beta1hi	(*12-16*)
Colorectal	EpCAM, CD44, CD166	(*7, 8, 17*)
Melanomas	CD20+	(*18*)

5.5 Reference

(1) Peng, L., Liu, R., Marik, J., Wang, X., Takada, Y., and Lam, K. S. (2006) Combinatorial chemistry identifies high-affinity peptidomimetics against alpha4beta1 integrin for in vivo tumor imaging. *Nat Chem Biol 2*, 381-389.

(2) Lam, K. S., Lehman, A. L., Song, A., Doan, N., Enstrom, A. M., Maxwell, J., and Liu, R. (2003) Synthesis and screening of "one-bead one-compound" combinatorial peptide libraries. *Methods Enzymol 369*, 298-322.

(3) Hsiung, P. L., Hardy, J., Friedland, S., Soetikno, R., Du, C. B., Wu, A. P., Sahbaie, P., Crawford, J. M., Lowe, A. W., Contag, C. H., and Wang, T. D. (2008) Detection of colonic dysplasia in vivo using a targeted heptapeptide and confocal microendoscopy. *Nat Med 14*, 454-458.

(4) Hirschmann-Jax, C., Foster, A. E., Wulf, G. G., Nuchtern, J. G., Jax, T. W., Gobel, U., Goodell, M. A., and Brenner, M. K. (2004) A distinct "side population" of cells with high drug efflux capacity in human tumor cells. *Proc Natl Acad Sci U S A 101*, 14228-14233.

(5) Szotek, P. P., Pieretti-Vanmarcke, R., Masiakos, P. T., Dinulescu, D. M., Connolly, D., Foster, R., Dombkowski, D., Preffer, F., Maclaughlin, D. T., and Donahoe, P. K. (2006) Ovarian cancer side population defines cells with stem cell-like characteristics and Mullerian Inhibiting Substance responsiveness. *Proc Natl Acad Sci U S A 103*, 11154-11159.

(6) Al-Hajj, M., Wicha, M. S., Benito-Hernandez, A., Morrison, S. J., and Clarke, M. F. (2003) Prospective identification of tumorigenic breast cancer cells. *Proc Natl Acad Sci U S A 100*, 3983-3988.

(7) Dalerba, P., Dylla, S. J., Park, I. K., Liu, R., Wang, X., Cho, R. W., Hoey, T., Gurney, A., Huang, E. H., Simeone, D. M., Shelton, A. A., Parmiani, G., Castelli, C., and Clarke, M. F. (2007) Phenotypic characterization of human colorectal cancer stem cells. *Proc Natl Acad Sci U S A 104*, 10158-10163.

(8) Ricci-Vitiani, L., Lombardi, D. G., Pilozzi, E., Biffoni, M., Todaro, M., Peschle, C., and De Maria, R. (2007) Identification and expansion of human colon-cancer-initiating cells. *Nature 445*, 111-115.

(9) Liu, S., Dontu, G., Mantle, I. D., Patel, S., Ahn, N. S., Jackson, K. W., Suri, P., and Wicha, M. S. (2006) Hedgehog signaling and Bmi-1 regulate self-renewal of normal and malignant human mammary stem cells. *Cancer Res 66*, 6063-6071.

(10) Donnenberg, V. S., Landreneau, R. J., and Donnenberg, A. D. (2007) Tumorigenic stem and progenitor cells: implications for the therapeutic index of anti-cancer agents. *J Control Release 122*, 385-391.

(11) Dontu, G., Liu, S., and Wicha, M. S. (2005) Stem cells in mammary development and carcinogenesis: implications for prevention and treatment. *Stem Cell Rev 1*, 207-213.

(12) Heffron, C. C., Gallagher, M. F., Guenther, S., Sherlock, J., Henfrey, R., Martin, C., Sheils, O., and O'Leary, J. J. (2007) Global mRNA analysis to determine a transcriptome profile of cancer stemness in a mouse model. *Anticancer Res 27*, 1319-1324.

(13) Collins, A. T., and Maitland, N. J. (2006) Prostate cancer stem cells. *Eur J Cancer 42*, 1213-1218.

(14) Collins, A. T., Berry, P. A., Hyde, C., Stower, M. J., and Maitland, N. J. (2005) Prospective identification of tumorigenic prostate cancer stem cells. *Cancer Res 65*, 10946-10951.

(15) Shepherd, C. J., Rizzo, S., Ledaki, I., Davies, M., Brewer, D., Attard, G., de Bono, J., and Hudson, D. L. (2008) Expression profiling of CD133(+) and CD133(-) epithelial cells from human prostate. *Prostate*.

(16) Rizzo, S., Attard, G., and Hudson, D. L. (2005) Prostate epithelial stem cells. *Cell Prolif 38*, 363-374.

(17) O'Brien, C. A., Pollett, A., Gallinger, S., and Dick, J. E. (2007) A human colon cancer cell capable of initiating tumour growth in immunodeficient mice. *Nature 445*, 106-110.

(18) Fang, D., Nguyen, T. K., Leishear, K., Finko, R., Kulp, A. N., Hotz, S., Van Belle, P. A., Xu, X., Elder, D. E., and Herlyn, M. (2005) A tumorigenic subpopulation with stem cell properties in melanomas. *Cancer Res 65*, 9328-9337.